Operation of Microbial Electrolysis Cells for Methane Production

Danilo Pérez

A thesis submitted to

Auckland University of Technology

In fulfilment of the requirements for the degree of

Doctor of Philosophy

2021

Supervisors:

Prof. Tek Lie, Auckland University of Technology

Prof. Cameron Weber, University of Auckland

Abstract

Microbial electrolysis cells (MECs) are capable of enhancing naturally occurring methanogenesis, achieving efficient small-scale methane production from a range of organic matter feedstock when a low voltage is applied. This capacity increase is relevant considering the role of biogas in the decarbonisation of the economy, beyond large-scale projects with economies of scale advantages.

Significant performance improvements have been achieved through fundamental research to understand microbiology dynamics and molecular mechanisms. Additionally, extensive material testing and design development have contributed to the understanding of the underlying phenomena and individual factors' effects.

However, the variety of designs and operating conditions make the results hard to compare, and scaling up comparisons difficult, creating a body of knowledge fragmented and isolated from large scale industrial applications.

It is intended here to fill those gaps, providing information regarding the individual and combined influences of alternative designs over MECs' performance. This study focuses particularly on the influence and interaction of different anode-to-cathode relative surface area; and operational parameters such as hydraulic retention time (HRT), organic load, voltage, and hydrogen injection, over the performance of MECs from an energy-storage solution perspective.

The data necessary for the discussion was obtained via sets of bio-electrochemical cultures, systematically organised as Placket-Burmann, and a complete factorial design of experiments. This allows a direct comparison of results, to identify the most influential factors and interactions that affect the overall performance. The cultures were carried out on 1L MECs with connections provided for both inlet and outlet of synthetic wastewater, H_2/biogas and electrical connections for the carbon felt electrodes, using a total cell potential strategy for imposing the voltage.

It was found that the organic load, voltage, and favouring the cathodic surface have a positive influence on methane production. Applying a voltage enhances the overall performance, with a positive correlation for both MPR and MCR when the applied voltage surpasses 600 mV. MEC B appears to be consistently more efficient than MEC A, regardless of the organic load and despite its smaller electrode surface area. A higher organic load increases methane production but reduces the efficiency of the overall process. 33% energy storage efficiency was achieved by MEC B when imposing 1000 mV, and 10 days of HRT.

The empirical methane production rate and reference values from the literature were used to simulate the integration of MECs into household and industrial scenarios in terms of energy and mass balance. These results highlighted the feasibility of a household-scale integration, despite the carbon supply limitation. Conversely, for the industrial scenario, the current reaction rate

achievable limits the contribution, although it would offset the extra energy cost required to operate a carbon capture and storage plant that reduces the CO_2 emission up to 90% of a power plant, thus, *hydrogenotrophic methanogenesis* engagement appear crucial to converting greater amounts of vented CO_2.

It is expected that the results obtained in this study, especially the contour plot produced, help to operationalise the knowledge regarding MECs' performance relationship with operational parameters, and contributes to the technology development.

Acknowledgments

As a member of the STEM community, I adhere to those recognizing science and engineering as tools for improving quality of life, not solving technical issues. This allows me to understand that “experts” are not the only ones who deserve to express themselves when it comes to building society, appreciating the role that all contributions play within the big scheme of things.

This work aims to contribute to society respecting that vision, and couldn’t have been done without the emotional support of my people, nor without my supervisors' professor Tek Lie, and professor Cameron Weber help and guidance, and all the AUT staff that at some point contributed to making this happen.

I particularly thank that wide and diverse group of Chilean citizens that gathered in 1925 to discuss a new constitution. The truncated constitution defining education as the tool for economic self-support while providing the capacity to understand life, truth, and beauty.

Abbreviation list

A:C	Anode-to-cathode surface area ratio
AEM	Anion Exchange Membrane
AD	Anaerobic Digestion
BG_{CH4}	Biogas Methane Content in $\%_{CH4}$
°C	Celsius Degree
CCS	Carbon Capture and Storage
CDCS	Charge-Discharge Control System
CEM	Cation Exchange Membrane
COD	Chemical Oxygen Demand
CS	Central Storage
CFs	Cell Yield in $g_C\ g_{Cell}^{-1}$
CF_{CO2}	Yield CO2/x in $g_{CO2}\ g_{OD}^{-1}$
CF_{CH4}	Yield CH4/x in $g_{CH4}\ g_{OD}^{-1}$
CFS	Carbon in Biomass in $g_C\ g_{Cell}^{-1}$
C_u	Specific cost of energy used for charging the storage
CSTR	Continuously Stirred Tank Reactor
d	day
DE	Destruction Efficiency in %
DIET	Direct Interspecies Electron Transfer
DoD	Depth of Discharge in %
D	Diffusion coefficient in $cm^2\ s^{-1}$
Dt	Doubling Time in units of time
EET	Extracellular Electron Transfer
Eff_{ww}	Treatment efficiency in %
ES	Energy Storage
F	Faraday Constant in Farad

g	Acceleration of gravity (9.81 m s^{-2}),
h	Differential head in m
hf	Feedstock Heating
hl	Heat losses
HRT	Hydraulic Retention Time in day
H_{2g}	Hydrogen Concentration in the gaseous phase in mol L^{-1}
H_{2L},	Hydrogen Concentration in the liquid phase in mol L^{-1}
H	Hour
I	Current in A
$I_{density}$	Current density in A m^{-3}
K_La	Gas transfer coefficient in d^{-1}
K_S	Constant of Saturation (substrate concentration to achieve $\mu_m/_2$)
L	litre
MEC	Microbial Electrolysis Cell
MCF_{ww}	Correction factor in % to CH4
M_{CO2}	Carbon dioxide mass in kg
M_{CH4}	Methane mass in kg
MCR	Methane Conversion Rate in g_{CH4} $kgCOD^{-1}$
MPR	Methane Production Rate in mL_{CH4} $L_{reactor}^{-1}$ h^{-1}
mL	millilitre
OD	Oxygen demand in mg_{COD} L^{-1}
OCP	Open Circuit Potential
ORL	Organic Load in g L^{-1} d^{-1}
Ph	Hydraulic power in KW
PTS	Power transformation System
PV	Photovoltaic
q	Flow capacity in m^3 h^{-1}
Q_{ww}	Flow rate in L day^{-1}

R	Fixed Annual cost of storage facility
r_t	transfer rate between gas and liquid in $L_{H2}\ L^{-1}_{reactor}\ d^{-1}$
S	limiting substrate concentration
SAM	System Advice Model
StD	Standard Deviation
V	Voltage in V
WW	Wastewater
Z_S	Annual cost of a storage facility
δ	Diffusion Layer Thickness
μ	Specific Growth Rate in h^{-1}
μ_m	Maximum Specific Growth Rate in h^{-1}
η_C	Number of charge-discharge cycles during a year
ρ	Fluid density in kg m^{-3}
a	Model Constant

Table of Contents

List of Figures

List of Tables

Attestation of Authorship

"I hereby declare that this submission is my own work and that, to the best of my knowledge and belief, it contains no material previously published or written by another person (except where explicitly defined in the acknowledgements), nor material which to a substantial extent has been submitted for the award of any other degree or diploma of a university or other institution of higher learning."

Danilo Pérez

Co-Authored Works

This thesis contains data published as jointly research papers, based in the original work of Danilo. All authors were involved at every stage of the research, nevertheless the focus of each one was:

Danilo Pérez: Conceptualization, Methodology, Investigation and Writing – Original Draft.

Cameron Weber: Validation, Writing – Review & Editing.

Tek Lie: Resources, Supervision and Writing – Review & Editing.

Perez, D., Lie, T.T., Weber, C.C., 2020. Relative electrode size and organic load effects on the energy storage efficiency of microbial electrolysis cells. Bioresour. Technol. Reports 11, 100518. https://doi.org/10.1016/j.biteb.2020.100518

Perez, D., Weber, C., Lie, T., 2021. Operationalization of a microbial electrolysis cell : The interaction of the primary factors for energy storage efficiency. Bioresour. Technol. 326, 1–10. https://doi.org/10.1016/j.biortech.2021.124788

Chapter 1 Introduction

1.1 Structure of the thesis

This thesis is structured in 7 chapters. The first chapter is the introduction which presents the background of the study; describes the rationale and the significance of research conducted; and provides an overview of the structure of this thesis.

Chapter 2 is a literature review that provides a brief overview of the historical development of microbial electrolysis cells (MEC), identifying the main components and their most relevant features. The review is then extended to the overall operation of MECs and how the design and operation of the system will affect the overall performance. The chapter finishes describing the project aims, providing an overview of the goals and research questions guiding this work.

A description of the materials and methods used during the work is provided in Chapter 3. Particular care is taken to describe the design of the MEC device used in this work, and the sampling and analysis used to monitor its operation and performance. Finally, the key performance indicators used to assess the different outcomes of the imposed conditions are presented.

Chapter 4 describes the process of setting up and starting up the operation of the laboratory prototypes, including discussions regarding improvements necessary to achieve the final design used to obtain the results discussed in the next sections.

Chapters 5 and 6 present the design of experiments, results, and discussions of the experiments carried out in the laboratory. Chapter 5 focuses on the effect of relevant operational parameters such as the organic load, relative electrode size, and hydrogen injection on the overall performance of the systems. Chapter 6 aims to provide an integrative vision of the results, using a factorial design of experiments to organise and analyse the results. These chapters also include the description of experiments not initially considered in the design of experiments, but they were designed and performed to confirm or complement hypothesis and observations from the execution of the planned experiments, drawing special attention, or corresponding to a record of operational failures that needed attention.

Chapter 7 includes results from a simulation that aims to evaluate the potential contribution of employing the MEC technology. The analysis is divided into a domestic and an industrial scenario, highlighting the scalability and flexibility of the technology whilst simultaneously revealing its main limitations. This chapter also encompasses the general analysis of the MEC perspectives and necessary future developments, as well as some topics that are considered relevant for the broader discussion.

Finally, the conclusions briefly summarise the research study carried out and draw relevant conclusions, proposing recommendations for future works.

1.2 Introduction

Biogas is a gas produced via anaerobic digestion, which is the breakdown of organic matter in absence of oxygen. The obtained gas is mostly composed of methane (CH_4) and carbon dioxide (CO_2), so it can be used as a fuel. Biogas is considered a low-emission fuel; hence, it may play a fundamental role in decarbonisation of the energy matrix. However, anaerobic digestion projects are usually restricted to large-scale due to high capital costs and long payback periods, so Microbial electrolysis cell (MEC) are proposed to enhance the overall performance.

Microbial electrolysis cell (MEC) are a type of bioreactor capable of achieving high-yield production, usually operating under mild conditions and starting from a wide range of organic matter feedstock. This is possible when a low voltage is applied to increase the naturally occurring production rate. Abundant fundamental research has led to significant methane production improvements; developing extensive knowledge of microbiology dynamics, underlying molecular mechanisms, material testing, and complex designs. Nonetheless, this knowledge has been developed isolated from industrial and application concerns, very often ignoring what would be feasible to scale-up and use under industrial conditions.

1.3 Background

There is currently a thorough knowledge of the underlying mechanism involved in methanogenesis and how individual environmental conditions affect them (Park et al., 2018). However, works comparing the relative effect of different design/operational factors on the performance (Fradler et al., 2014; Gil-Carrera et al., 2013; Muñoz-Aguilar et al., 2018), among others are limited and focused on maximising methane production instead of the overall energy efficiency.

The ultimate goal of the study is to operationalise the existing knowledge using an empirical research approach. Due to the number of factors and their interactions, a phenomenological model would not have achieved that goal.

Although some long-term operation studies exist (Guangyin Zhen; Shaojuan Zheng, 2018), it is still not clear how the operation may be adjusted to maintain a reliable and predictable performance when external parameters fluctuate. To close this gap, a set of bio-electrochemical experiments under controlled conditions of methane-producing MECs is proposed.

Chapter 2 Literature Review

2.1 Microbial electrolysis cell (MECs)

Bioelectrochemical systems, particularly waste-to-energy/chemical platforms, have a promising role in a circular bioeconomy (Jung et al., 2020). MECs were originally developed to enhance the biological production of hydrogen. Nevertheless, they have been shown to be useful for many energetically unfavourable reactions. Due to the external energy supply, these systems achieve high production yields of chemicals starting from a wide range of organic matter feedstock despite operating under mild conditions (Zhang and Angelidaki, 2014).

Other applications include the removal of specific pollutants (Zhang and Angelidaki, 2014), so electrochemical technologies are used for wastewater treatment, desalination, remote power sources and other applications. Nevertheless, in the context of energy matrix decarbonisation and energy storage, biofuel production is their most interesting application as it offers a method for long-term energy storage in chemical form, which is easily converted into electricity or heat using commercially available technology.

A MEC is capable of reducing CO_2 to methane when an external voltage is applied using the metabolic capacity of a biocathode (Fu et al., 2013), a current is obtained when redox reactions are driven by the microbial consortium interacting with the solid-state electrodes. The reaction rate of electrochemical systems is linked to the currents and power densities achievable for these systems (Logan et al., 2015); this limitation is overcome by the inherent advantages of accounting with a microbiological component that provides part of the energy required, and a self-adapting capacity. Bacterial and archaeal communities present in the bioreactors are capable of producing a wide variety of fuels and high-value chemicals, self-adjusting themselves to environmental and process changes, which translates into their well-known versatility (Logan et al., 2015). A good case in point is the evolution of a technology developed to produce hydrogen into a platform that produces a variety of valuable chemicals such as methane, formic acid, acetate, and alcohol (Zhen et al., 2016).

When methane is synthesised in an electrochemical reactor it is called electrosynthesis (Liu et al., 2018), or ‘electromethanogenesis’ as previously called (Cheng et al., 2009; Mateos et al., 2020). Electromethanogenesis was proven in 2009 by applying a potential lower than -500 mV (vs. SHE) to a bio-cathode (Cheng et al., 2009). Only one year later, Villano *et al.* demonstrated the technological feasibility of producing gaseous biofuels by treating wastes at ambient temperature in a MEC (Villano et al., 2010).

Particularly relevant is the development of devices capable to produce CH_4 via CO_2 reduction. This possibility offers a way to CO_2 sequestration and fixation, but also a new approach to

renewable energies, as it is less fluctuating than more traditional renewable energy sources as wind and geothermal (Zhang et al., 2019).

The relevancy of methane, when produced as a biofuel and not from fossil origin, is that it is a popular fuel, easily collected and transported when compared to others such as hydrogen. This has led to electromethanogenesis research towards its electrosynthesis, especially focused on the electrodes (materials and architecture), enhancement of electron transfer mechanism (Zhang et al., 2019), and other non-configuration related aspects crucial to achieving the desired off-gas quality such as the microbial consortium composition (Kougias et al., 2017). It has been demonstrated that the methanogenic bio-cathode can reduce CO_2 to methane using hydrogen produced abiotically, or by the polarised electrode acting as an electron donor (Villano et al., 2011); implying that two different mechanisms occur simultaneously (Villano et al., 2010). This capacity of operating on different reaction pathways enables power-to-gas technologies to fit in diverse energetic strategies that are strongly dependent on the available energy infrastructure.

2.2 Basic considerations

This section addresses the discussion regarding common designs, materials selection, and other topics relevant to the design and operation of MEC reactors. The initial MEC design consists of two chambers separated by a semi-permeable membrane, each chamber containing an electrode as shown in Figure 1. Single-chamber reactors have also been demonstrated with both electrodes present in the same chamber which has been designed to avoid direct contact (Clauwaert and Verstraete, 2009). Eliminating the membrane simplifies the design and reduces associated capital and maintenance costs (Moreno et al., 2016), which makes the single-chamber design more appealing for a waste treatment context.

Regardless of the number of chambers, it can be considered that the circuit begins at the anode, where the microorganisms oxidise the organic matter (commonly measured as chemical oxygen demand or COD), generating protons, CO_2, and electrons. An external circuit conducts these electrons to the cathode, where methane is generated from the electrons, hydrogen, and CO_2. The two chambers are separated by a membrane, that prevents the contact between the oxygen present at the anode and the hydrogen generated at the cathode (Kadier et al., 2016a) and avoiding the re-oxidation of the hydrogen (known as hydrogen recycling) that negatively affects the overall performance (Geetha and Raj, 2015).

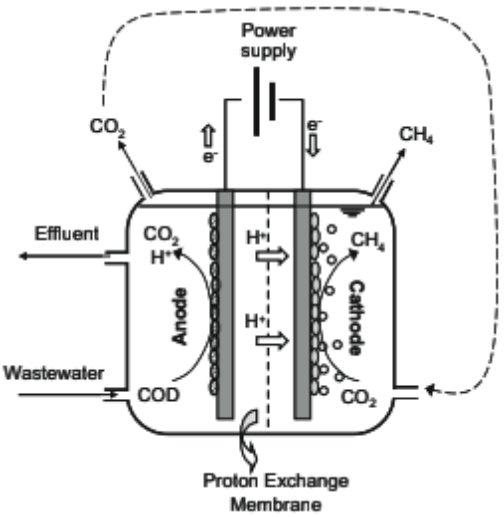

Figure 1: Schematic illustration of a microbial electrolysis cell (Villano et al., 2010)

The membrane can be either anion- or cation-exchange. Anion exchange membranes (AEM) have higher efficiencies than cation exchange membranes (CEM) due to the lower internal resistance consequence of the easier pass-through of ions (Yu et al., 2018). Zeppilli *et al.* evaluated MECs with either an AEM or CEM as a biogas upgrading system, converting 5.4 $gCO_2\ L^{-1}\ d^{-1}$ when the AEM was used, whereas only 3.2 $gCO_2\ L^{-1}d^{-1}$ when using a CEM (Zeppilli et al., 2016).

The implicit costs of using a membrane will inevitably limit the deployment and application of these technologies (Logan et al., 2015). A single-chamber design (see Figure 2) appears more suitable for wastewater treatment simply because it avoids the requirement of a membrane, which represents a direct capital cost, higher maintenance, and overall, a more complex design (Moreno et al., 2016). According to Logan *et al.* for systems such as microbial fuel cells that do not require a membrane, large scale designs capable of achieving similar power densities to those from bench-scale tests need to be developed (Logan et al., 2015), nevertheless, the authors also emphasises that configuration and fuel are the most relevant factors when it comes to power production.

The feasibility of such a design was proven in 2009 (Clauwaert and Verstraete, 2009), and despite the negative energy balance achieved, it attracted attention from many researchers to evaluate the effect of different bacterial sources in a single-chamber device, as well as a variety of parameters such as temperature and substrate (K. S. Choi et al., 2017; Gajaraj et al., 2017; Hara et al., 2013; Kerroum et al., 2014; Kuramochi et al., 2013; Li et al., 2015; Moreno et al., 2016; Yin et al., 2016), including modifications such as the anaerobic baffled reactor (Ran, Gefu, Kumar, Chaoxiang, Xu, & Lin, 2014)

Besides the design simplification and costs reductions, a single-chamber design offers advantages related to pH splitting. When the semi-permeable membrane allows ionic species transport, e.g. protons and hydroxides, a phenomenon known as pH split occurs, where electrochemical reaction promotes the acidification of the anode chamber, and alkalisation of the cathodic chamber

(Zeppilli et al., 2019). Therefore, the absence of a membrane eliminates the associated pH gradient, diminishing both potential losses and the internal resistance thereby reducing the energy input necessary to drive the reaction (A. Kadier et al., 2016) and hence increasing the methane production rate.

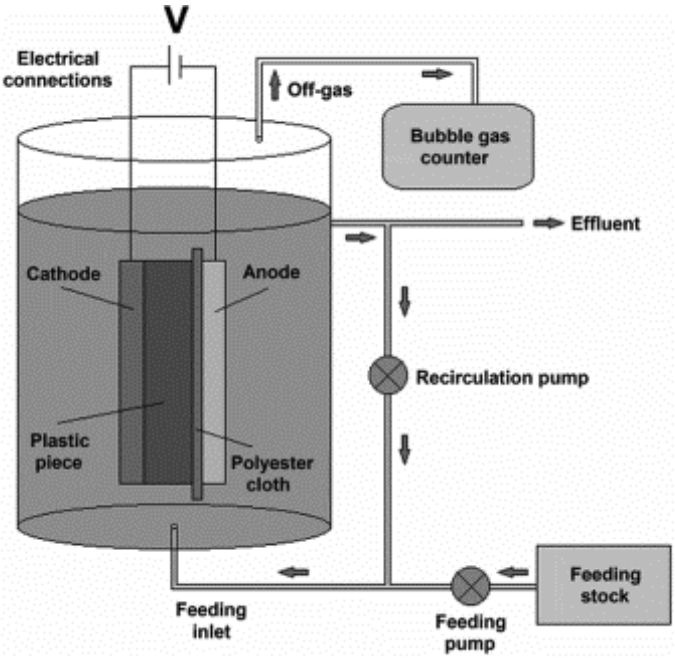

Figure 2: Schematic of a single-chamber MEC (Moreno et al., 2016)

However, since multiple factors such as cell type, design, materials and operational parameters influence the MEC performance, an optimisation for the given application is recommended. Particular attention must be paid to the selection of appropriate electrode material, as this can enhance the electron transfer between the electrode and the bacterial population, achieving higher efficiency and a lower cathodic-overpotential (Zhen et al., 2016).

2.3 Methane producing MECs mechanism (metabolic routes)

MECs produce CH_4 as the main component of biogas, produced as consequence of a series of redox reactions that lead to the production of CH_4 and CO_2, however, the proportion of these within the biogas is determined by the biodegradability and nature of the feedstock. The generic chemical reaction given in Equation (2.1) below shows how the amount of methane and carbon dioxide can be predicted based on knowing the feedstock composition (Achinas et al., 2016).

$$\boldsymbol{C_xH_yO_z + \left(x - \frac{y}{4} - \frac{z}{2}\right) H_2O \rightarrow \left(\frac{x}{2} - \frac{y}{8} - \frac{z}{4}\right) CH_4 + \left(\frac{x}{2} - \frac{y}{8} - \frac{z}{4}\right) CO_2} \qquad \textbf{(2.1)}$$

This stoichiometric reaction shows that different feedstocks will produce different biogas compositions. In general terms, an equal amount of CH_4 and CO_2 production can be expected from carbohydrates such as sugars, cellulose and starch. However, the stoichiometry is different and the ratio rises from 50: 50 to 55: 45 favouring methane production when the waste contains high contents of proteins or fats, although this is highly dependent on the specific protein. An even more favourable case are wastes with high contents of triglycerides (fats and vegetable oil) that can reach CH_4: CO_2 ratio of up to 70:30 (Krich et al., 2005).

The influence of proteins presence in the feedstock not only changes the CH_4: CO_2 ratio, but it also implies the need to account for nitrogen and sulphur compounds in the stoichiometry as shown in Equation (2.2). This leads to the modification of the previous general model to consider the ammonia and hydrogen sulphide typically found in biogas (Achinas et al., 2016).

$$\boldsymbol{C_aH_bO_cN_dS_e + \left(a - \frac{b}{4} - \frac{c}{2} + \frac{3d}{4} + \frac{e}{2}\right) H_2O}$$
$$\boldsymbol{\rightarrow \left(\frac{a}{2} + \frac{b}{8} - \frac{c}{4} - \frac{3d}{8} - \frac{e}{4}\right) CH_4 + \left(\frac{a}{2} + \frac{b}{8} - \frac{c}{4} - \frac{3d}{8} - \frac{e}{4}\right) CO_2 + dNH_3 + eH_2S} \qquad \textbf{(2.2)}$$

The stoichiometric reactions and figure previously introduced are simplifications of the overall metabolic pathways, as these reactions have many deviations due to incomplete reactions, typically by-product accumulation that inhibits specific reactions and other metabolic requirements such as the biomass growth (Krich et al., 2005).

The feedstock variation is intimately linked to the metabolic capacity of the anaerobic consortium, as they will -or not- be capable of breaking down the given waste. The International Water association carried out an exercise to include all these into a single mathematical model, the ADM1(Bensmann et al., 2014). The ADM1 model identifies five basic stages in anaerobic digestion that involve enzymatic action. As seen in Figure 3-B, the process starts with disintegration, where biomass and complex molecules are broke down into lipids, carbohydrates, and proteins (Manjusha and Beevi, 2016). This first stage can often be ignored when looking at stoichiometric reactions, but in reality, and particularly in the waste treatment context, the feedstock is a complex stream constituted with a variety of molecules and nutrients.

The second stage in the ADM1 model is the hydrolysis of the previously formed carbohydrates, lipids, and proteins into long-chain fatty acids, amino acids, and sugars. Later, all these are broken down into volatile fatty acids (VFA) such as propionate, valerate, butyrate, and acetate during a stage called acidogenesis. This fourth stage, acetogenesis, is the transformation of the VFAs into acetate. This acetate is later metabolised to produce the major components of biogas, methane, and carbon dioxide (Manjusha and Beevi, 2016).

The ADM1 model, as described above, does consider in detail alternative metabolic pathways of methanogenesis (Figure 3), such as hydrogenophilic methanogens that use hydrogen and carbon dioxide instead of acetate. Initially, anaerobic digestion (AD) was thought to produce methane mostly from acetate reduction with only a fraction from reactions involving hydrogen or other substrates (Ran et al., 2014). In a typical anaerobic digestion operation, about 70% of the methane is formed through metabolic route including acetate (acetogenesis), whereas about only 30% is produced from hydrogen and carbon dioxide conversion. Figure 3-A summarises the main metabolic pathways related to biologically catalysed methane production, regardless of their relative importance to the overall methane production.

In a bioelectrochemical system context, all the aforementioned reactions take place at an enhanced reaction rate due to the low voltage imposed, typically under 2 V (K.-S. Choi et al., 2017; Ding et al., 2016). This interaction implies the microbial ability to exchange electrons with solid-state electrodes. The CO_2 reduction into CH_4 by microorganisms using electrodes as a direct electron donor was firstly reported in 2009 (Cheng et al., 2009). Nevertheless, it was reported later that this direct extracellular electron transfer (EET) is not the only mechanism of electron exchange occurring in a MEC (Villano et al., 2010). It is well accepted now that there exist two mechanisms, direct and indirect extracellular electron transfer (EET), with both mechanisms having been confirmed to exist simultaneously in methanogenic processes (Van Eerten-Jansen et al., 2012).

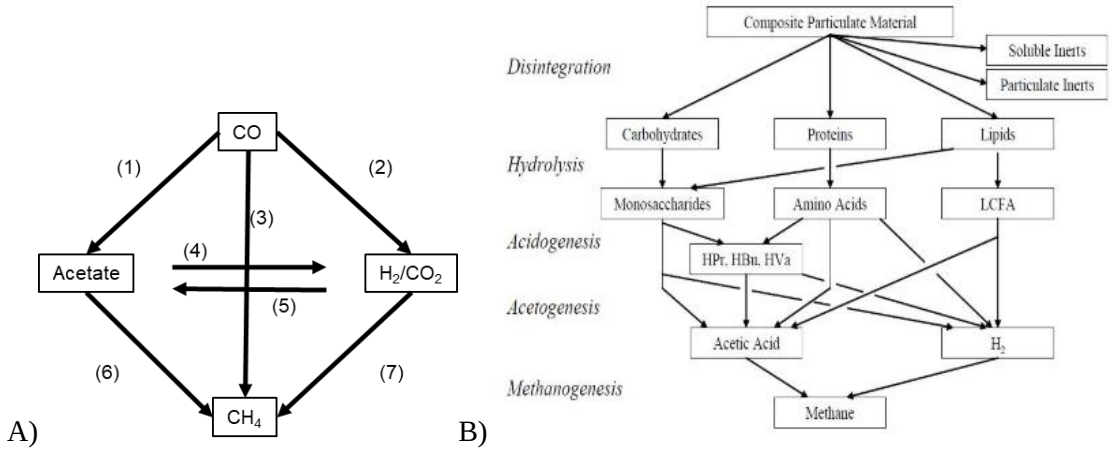

Figure 3: A) Main metabolic pathways involved in methanogenesis, 1) Carboxydotrophic acetogenesis, 2)Carboxydotrophic hydrogenogenesis, 3)Carboxydotrophic methanogenesis, 4)Syntrophic acetate oxidation, 5)Homoacetogenesis, 6)Acetoclastic methanogenesis 7) Hydrogenotrophic methanogenesis (Navarro et al., 2016) B)Biochemical steps considered in ADM1 (Manjusha and Beevi, 2016).

When the CO_2 reduction follows a direct EET pathway, a potential of about -0.244 V vs. SHE is required, whereas an indirect process requires -0.41 V vs. SHE (Arcadis et al., 2003). More negative potentials of about -0.5 V (vs. SHE) are reported to be required to carry the reaction further, mostly due to large overpotentials and imperfect electrode materials (Zhen et al., 2015),

losses due to the pH gradient over the membrane, as well as transport and ionic losses (Zeppilli et al., 2016).

An indirect-EET, unlike the direct-EET, would use a redox mediator instead a direct electron exchange between the bacterial cell and electrode (Zhen et al., 2015), as schematically shown in Figure 4. The existence of the indirect-EET mechanism is indicated by a hydrogen concentration drop as a consequence of the hydrogen-consuming methanogens metabolism, suggesting it acts as an electron shuttle (Zhen et al., 2015).

Furthermore, a microorganism may work as the redox mediator; not just hydrogen as initially thought (Hara et al., 2013). When electrons are transferred from one organism to another it is known as direct interspecies electron transfer (DIET). This requires the ability to produce electrical connections externally to their cells (Zeppilli et al., 2016); this pathway avoids the need for synthesising electron shuttles such as hydrogen, thus it seems to be more efficient than the path where the CO_2 reduction is preceded by hydrogen formation as consequence of electron to proton transfer (Yin et al., 2016).

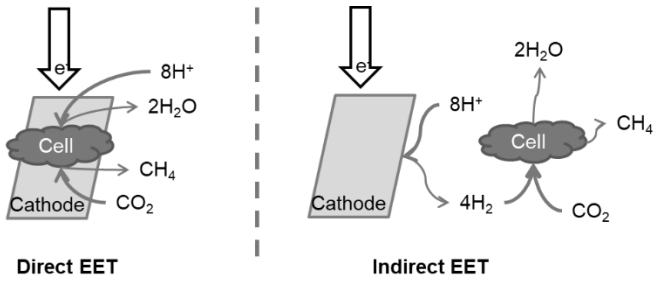

Figure 4: Schematic representation of direct and indirect extracellular electron transfer (EET) mechanisms

A direct mechanism requires a bacteria and a solid electrode interaction, and produces methane by reducing directly the carbon dioxide, following Equation (2.3) (Villano et al., 2010).

$$CO_2 + 8H^+ + 8e^- \rightarrow CH_4 + 2H_2O : E_{CAT} = -0.24\ V\ (vs.\ SHE) \qquad (2.3)$$

The existence of this mechanism is supported by the increment of the current densities and negligible hydrogen generation obtained when comparing a biocathode against an abiotic carbon electrode under -0.8 V (vs. SHE), suggesting the methane is not a consequence of the hydrogen gas reduction of CO_2 (Cheng et al., 2009).

The indirect EET is a two-step mechanism that requires intermediate hydrogen production. Whether a biological or purely chemical process is involved in the hydrogen production is not relevant (Cheng et al., 2009).

$$2H^+ + 2e^- \rightarrow H_2 : E_{CAT}\text{=-0.41 V (vs. SHE)} \quad (2.4)$$

The second step follows the reaction given below, whereby methane is obtained

$$CO_2 + 4H_2 \rightarrow CH_4 + 2H_2O \quad (2.5)$$

Theoretically, the highest efficiency results from the direct mechanism due to its higher standard potential (Van Eerten-Jansen et al., 2012), which is much lower than the 1.8-2 V required for abiotic water electrolysis because part of the energy comes from bacterial activity (Gajaraj et al., 2017). However, the specific application plays a relevant role in this regard, defining both the protons and electrons donor and how the device is integrated, among other factors.

When water is electrolysed at the anode under biologically relevant conditions (pH 7 and 25°C), it has been estimated that 32.7 MJ m^{-3}_{CH4} are needed (Van Eerten-Jansen et al., 2012).

$$4H_2O \rightarrow 2O_2 + 8H^+ + 8e^- : E_{AN}\text{=0.81 V (vs. SHE)} \quad (2.6)$$

The overall reaction would be as follows. The negative potential indicates the reaction will not proceed spontaneously.

$$CO_2 + 2H_2O \rightarrow CH_4 + 2O_2 : E_{CELL}\text{=-1.05 to -1.22V (vs. SHE)} \quad (2.7)$$

The overall efficiency can be monitored via the coulombic efficiency, corresponding to the relationship between the transferred coulombs and the coulombs removed from the substrate. Some authors have reported coulombic efficiencies over 100% (Zhen et al., 2016), hypothesising that it may relate to a methanogenic corrosion and hence the cathode itself would acts as the electron donor for the methane generation (Siegert et al., 2014b) following the reaction given below (Equation 2.8), and later using those protons for reducing the CO_2 (Zhen et al., 2016).

$$2C + 3H_2O \rightarrow CH_4 + HCO_3^- + H^+ \quad (2.8)$$

During the electrode colonisation by electromethanogens, both the coulombic efficiency and corrosion rates (estimated from the electrode mass loss) have shown a downward trend over time. However, according to Siegert *et al.*, a diminishing coulombic efficiency associated with an increase in methane production rate suggests dominance of the bio-methanogenic process over the corrosion phenomenon (Siegert et al., 2014b).

A secondary mechanism that leads to an increased CH_4 content of the raw biogas is related to a series of reactions that take place after the initial digestion of the organic matter. As seen in Table 1, the solubility of the different biogas components differs significantly and this can translate into a preferential re-dissolution of CO_2, (Krich et al., 2005). Thus, the raw biogas in the headspace acts as a secondary source of carbon – as CO_2 – that will re-dissolve. The CO_2 will then either

affect the apparent stoichiometry as more methane will be produced from the same organic load of the feedstock, or a significant amount of CO_2 may leave the system through the digestate.

Table 1: Solubility of typical raw biogas components in water at typical AD temperature operation (T. Al Seadi et al. 2008).

Gas	Temperature (°C)	Solubility mmol L_{water}^{-1}
H_2	35	0.749
	50	0.725
CO_2	35	26.6
	50	19.6
H_2S	35	82.2
	50	62.8
CH_4	35	1.14
	50	0.962

2.4 Reactor design

Microbial electrolysis cells (MEC) can be presented as a bio-electrochemical technology for renewable and sustainable production of chemicals, including biogas. The process can often be considered as a "black-box", where only the inlet and outlet are known, but not the internal process. However, when it is explained that organic matter oxidation is biocatalysed in the anode (Clauwaert and Verstraete, 2009), releasing the protons to the solution and conducting the electrons to the cathode, it can then be understood that to achieve an efficient formation of biogas from organic matter, specific factors are required such as the need of electrochemically active bacteria (Flores-Rodriguez and Min, 2020), electrical connection and the need for an external voltage supply (Kadier et al., 2016).

While the study of many geometries and designs has highlighted some design guidelines, these need to be adapted to the particularities and objectives of the study. A good example is the distance between electrodes, in the microbial fuel cell context was proven that the power increased as the electrodes were closer; probably as the electrical resistance of the electrolyte was reduced (Logan et al., 2015). On the other hand, there is also the detrimental effect of having the electrodes too close, due to the oxygen presence in both, inhibiting anaerobic bacteria.

The electrodes distance gains especial relevancy when working with domestic wastewater, as there is the need to minimise the inter-electrode distance to counteract its low conductivity, simultaneously highlighting the relevance of maximising the electrodes' specific area. Therefore, it is important in understanding the underlying phenomena (Hou et al., 2015) to predict the effect of each design feature within a specific system.

2.5 Electrode Material and Biocathodes

The main difference between AD and MECs resides in the electrodes' design; after selecting the electrode material, the size and separation between electrodes must be decided. A MEC, involves

appropriate electroactive microorganisms and compatible electrode materials to create the bioelectrodes (Zeppilli et al., 2019), capable of converting organic matter into methane when an external voltage is applied. Hence, an appropriate electro-active microorganism must be attached and form a biofilm over the electrode (Fu et al., 2013) known as bio-electrode, electro-active biofilm, or simply biocathode/bioanode. The term emphasizes the role of methanogens present at the cathode and their capacity of establishing EET (Villano et al., 2010).

The bioelectrodes in a MEC aims to maximise the electron transfer between the microbial cells and the power supply, which can be monitored as the volumetric current density (A m^{-3}) of the device. The volumetric current density is the product of the current density (A m^{-2}), and the specific surface area of electrodes ($m^2_{electrode}$ m^{-3}) (Xie et al., 2015). This relates to both the biocompatibility and architectural morphology of the electrodes and their role on the bacterial consortium.

The electrode colonisation begins with the attachment of bacterial cells over the solid surface. This phenomenon is determined by the balance of forces such as the advective flow, preventing the attachment encouraged by electrostatic and Van der Waals interactions. Nevertheless, chemotaxis (the movement of cells along chemical gradients) plays a relevant role here, where the feedstock composition and the availability of divalent ions such as Mg^{2+} and Ca^{2+} can influence cellular adhesion, and biofilm formation (Guo et al., 2015).

In a functional biofilm, bacteria contribute via different mechanisms to the electron transfer between bacterial cells and solid electrodes. Some microbes act as an anchor, while others (exoelectrogens) can carry redox-active membrane proteins over a short-range, although nanowires, being a pilus-like structure capable of electrical conductance (Deutzmann et al., 2015), bind the cells within an external matrix that extends the interaction beyond individual cells (Dykstra and Pavlostathis, 2017). Nevertheless, direct contact is not always mandatory, as a further reach is possible when shuttles or mediators are synthesised and diffused into the surroundings; for example, hydrogen (Xie et al., 2015). Fermentative bacteria enhance the CH_4 production yield, producing H_2 and CO_2 as a substrate for methanogens by recycling cell lysis products.

Regardless of the particular function and composition of the biofilm, increasing the surface area and the roughness of electrodes seems to enhance the bioelectrodes' performance. In bioelectrochemical systems, the electrode surface area can be considered to directly relate to the available reaction sites, and the roughness benefits the bacterial attachment and electrode colonisation, whereas the mass transfer dynamics are partly determined by the 3-D structure as well (Sharma et al., 2014).

It seems then that improving cathode materials and developing highly specialised electro-active microbial communities are needed to obtain the best possible performance achievable for the

given feedstock and operational conditions (Villano et al., 2016). The interaction between the metabolic diversity, cathode material, structure, and potential (Sharma et al., 2014) determines which biochemical pathways can be undertaken, and accordingly, the overall efficiency of the system. This enables biocathodes to produce valuable chemicals from by-products or wastes from a variety of processes. The variations inherent in biofilm maturation and how these interact with the structure of the cathodes, influence the biocathodes' evolution over time, and changes the open circuit potential (OCP) (Sharma et al., 2014).

Carbon-based electrodes have been adopted after an extensive MFC-design due to their stability and low cost (Zhang and Angelidaki, 2014). It has been suggested that the similarity between felts and the natural habitat of the electrogenic bacteria allows them to use functional groups such as carboxylic acids, alcohols, and quinones to attach (Huong Le et al., 2017), a phenomenon essential for the methanogenic biofilm development and hence for long-term operations. However, carbon-based electrodes imply performance limitations, such as current densities reported below 10 Am^{-2}, and their poor kinetics of hydrogen evolution which requires overpotentials and leads to energy losses – estimated at 35% when operating at +200 mV and 62% at -200 mV (Villano et al., 2016).

The EET between the microbial cells and solid-state electrodes takes place at the electrode surface, which is the interface where they directly interact. This cell-to-electrode interaction has at least two highly influential components, namely the electrodes' chemical and topographical features. These components can be designed via materials selection, pre-treatment, and by combining different materials (Huong Le et al., 2017). Based on the manipulation of these components under controlled conditions, electrodes combining high conductivity collectors and biocompatible carbon-based coatings appear to be more adequate than flat bulk metal sheets designs, with a defined topography and chemistry (Guo et al., 2015).

The superior capacity of porous carbonaceous material to interact with microbes and metallic electrodes has led to diverse strategies of electrode designs. Porous materials have been used for coating an electrode with a layer of graphite felt. This being a simple method to improve the electron transfer efficiency, contributing an open three-dimensional structure and fibre interconnectivity whilst maintaining good electronic conductivity (Huong Le et al., 2017).

The properties of the final electrode will be then significantly affected by the felt used, its precursors, and manufacturing procedure. The most common felts are either graphite or carbon felts. Graphite felts are obtained after graphitisation of carbon felts, the operational factors of graphitisation will directly affect the properties of the final material (Huong Le et al., 2017).

An enhanced wettability, via either plasma, thermal or chemical treatment, makes it easier for electrolyte ions to access the voids within the 3-D structure. Additionally, metallic nanoparticles, graphene, and carbon nanofibers have been used to enhance their conductivity (Huong Le et al., 2017). Following this logic, platinum is currently considered a viable alternative due to its low

overpotential and feasibility of coating onto a wide selection of materials such as brushes, cloths, rods, plates, etc.(Sangeetha et al., 2016) and significantly improves the hydrogen evolution necessary for the Hydrogenotrophic methanogenesis (Villano et al., 2010)

Although Pt or Pt-coated electrodes provide high activity and are technically feasible, their high cost, negative environmental impact, and sensitivity to poisoning by chemicals commonly found in waste streams, such as sulphides (Zhang and Angelidaki, 2014), limit its use to foundational studies at the laboratory scale. Consequently, even in the hydrogen production context, where bioelectrodes or abiotic electrodes can be used, the self-regeneration capacity, low cost, and remarkable versatility and specificity to a wide range of reactions make the bioelectrodes has been noted (Villano et al., 2011). Biocathodes, for instance, are known to be particularly resistant to wastewater treatment conditions and have been proven capable of reducing carbon dioxide into bio-methane and other multi-carbon and valuable compounds (Villano et al., 2011).

Additionally, practical issues need to be foreseen and they will modify the geometry and overall architecture requirements of the device for long-term operations. A good case in point is the possible fouling; this can alter the electrode configuration, increase the resistance, or clog the flowing spaces if too small, all these have a detrimental effect on the performance (Guo et al., 2015).

Avoiding direct contact between the electrodes is fundamental too, so rigid supports are commonly used (Guo et al., 2013). For instance, Yang *et al.* operated an H-type reactor with a 4 cm bridge, so their electrodes could only be 6 cm apart (Yang et al., 2018), whereas Guo et al. used a 9 cm diameter cylinder, and thus the electrodes were as close as 2 cm apart. Villano *et al.* used graphite granules as electrodes and support for the bacteria growth, filling the whole compartment so that the electrodes were just 0.5 cm apart. Alternatively, as shown in Figure 2, Clauwaert *et al.* (Clauwaert and Verstraete, 2009) and Moreno *et al.* (Moreno et al., 2016) used a non-woven cloth to keep the electrodes together but without direct contact.

Regarding the design of the electrodes, the literature review suggests that specific surface area shows a positive correlation with the current density obtained, whereas electrode separation has the opposite trend (Rader and Logan, 2010). A summary of relevant literature using different electrodes that have been used under different conditions is shown in Table 2.

Summarising the literature recommendations, an appropriate electrode would be relatively thin (5-10 mm) and have a large surface area with good porosity to facilitate bacterial colonisation and nutrient transport through the matrix to maximise volumetric efficiency (Gil-Carrera et al., 2011). Nevertheless, the inherent characteristics of the materials can drastically affect performance. Conductive materials, for instance, can act as a conduit, improving the direct cell EET and DIET (Zhen et al., 2016) and therefore the overall methane production.

Materials such as carbon and graphite felts have a well-known electrochemical characteristics (Smith et al., 2015), highlighting their good electrical conductivity, mechanical stability, and low cost (Zhen et al., 2016). Additionally, felts have an open 3-D structure that provides large surface areas and porosity at a scale from tens to hundreds of μm, hence are accessible for exoelectrogens (Xie et al., 2015) thereby offering abundant sites for redox reactions and bacterial colonisation (Huong Le et al., 2017). More detailed electrochemical characteristics of graphite felts can be found in the literature (Smith et al., 2015).

Table 2: Summary of relevant literature operational conditions, electrode materials and methane generation.

Reference	Chambers	Vol (ml)	Operation	HRT (H)	OL L_{COD} $L^{-1}d^{-1}$	Temp	applied mV	Control method	Anode	Cathode	ml_{CH4} $L^{-1}H^{-1}$	Current Density A m^{-3}	Current Density A m^{-2}
(Hara, 2013)	1	10	Batch	140			1000	Cell	Carbon paper		0.0014	ND	
(Jang, 2015)	-	5000	semi-continuous	60	108 g/L	55	-				59.3	ND	
(Cerrillo, 2017)	2	500	continuous	6.8			-800	cathode	Graphite granules		0.0096	0.3	-
(Villano G. M., 2011)	2	867	Batch	480			500	anode	Graphite plates		0.75	-	0.021
(Verstraete, 2009)	1	256	continuous	5.3	x	22	-844	cathode	Graphite granules		169.5	0.22	-
(Siegert , 2015)	2	5	Batch	50	2.5 g/L	30	700	cathode	Graphite plates		8.1	8.1	-
(Mieke, 2012)	2	560	continuous	93			-700	cathode	Platinum	Graphite felt	0.25	-	2.5
(Zhen, 2018)	2	400	Batch	24	0.5 g/L	35	-1200	cathode	Platinum	Carbon stick coated GF	87.2	-	2.3E-06
(Kerroum, 2014)	NA	500 (L)	continuous	552		35	-	-	-		16.25	ND	
(Kerroum, 2014)	NA	500 (L)	continuous	552		55	-	-	-		40		

(Gajaraj, 2017)	1	800	Batch	720	3 g/L	35	600	Cell	Reticulated vitreous carbon		40	0.001	-
(Yin, 2016)	1	250	Batch	72	10 g/L	25	1000	Cell	Carbon felt	stainless steel*	78.05	0.3	-
(Moreno, 2016)	1	3000	Batch vs continuous	24			1000	Cell	Carbon felt	stainless steel	0.33	-	0.48
(Choi, 2017)	1	330	Batch	144	2 g/L	35	-835	cathode	Carbon fibre brush		329.2	18.9	-
(Zhen, 2015)	2	800	Batch	6			-800	cathode	Carbon stick		0.58	ND	
(Ding, 2016)	2	800	Batch	72	3 g/L	35	800	Cell	Granular graphite	SS, Ni, Cu	1.1	1.8	-
(Sangeetha, 2016)	1	600	continuous	24	2 g/L	35	800	Cell	Graphite felt		5	14.3	-
(Guo, 2013)	1	300	Batch	720			1800	Cell	Ti/Ru		1	ND	
(Baek, 2017)	2	200	Batch	200		35	-700	cathode	Graphite felt		25.7	25	-
(Yang Li, 2017)	1	1000	continuous	6	1-7 g/L	35	1000	Cell	Graphite		248.5		
(Villano, 2016)	2	860	continuous	8.35	1 g/L	25	-200	anode	Graphite granules		12.5	-	116
(Cai, 2016)	2	700	semi-continuous	48	2 g/L	35	800	Cell	Carbon brush	stainless steel	10.3	ND	
(Rader, 2010)	2	2500	continuous	24	1 g/L	30	900	Cell	Graphite fiber	stainless steel	4.9167	74	-
(Hou, 2015)	1	500	Fed-batch	120	1 g/L	25	900	Cell	Carbon cloth	Niquel foam	7.1	ND	
(Li, 2016)	1	1000	continuous	6			1000	Cell	Graphite		248.5	0.58	-

2.6 Operation of MECs

2.6.1. Operational conditions

As wastes and by-products start to be considered as resources, the interest in platforms such as bioelectrochemical systems that offer the possibility to obtain higher-value products from those streams has increased, with easy integration into existing facilities. Although several proofs of concepts have been reported, the microbe-cathode interactions (more relevant for methane production) are less well understood compared to bioanodes (Sharma et al., 2014).

In this context, power-to-gas applications are particularly appealing as renewable electricity is becoming increasingly available. Producing chemicals that are valuable relative to the electricity cost makes the microbial electrolysis cells more economically attractive (Sharma et al., 2014). The direct energy consumption of electrical power in a power-to-gas device depends on the current circulating and is strongly influenced by the applied voltage, which is a key parameter of the MEC operation.

While the use of a wide range of potentials has been described in the literature, potential between -650mV and -800mV have been reported to enhance both hydrogenophilic methanogenesis and direct extracellular transfer when working with wastewater as feedstock (Cai et al., 2016; D. Liu et al., 2016; Villano et al., 2010).

The applied voltage is not the only relevant operational parameter; a positive dependency on the energy efficiency and electrode size has been reported (Sangeetha et al., 2016) and this is consistent with studies that recommend larger anodes when an anodic reaction is desired, although it does lead to losses on the hydrogenotrophic methanogenic activity (Gil-Carrera et al., 2011). Gil-Carrera and colleagues proved that a higher anode volume increases the current and hydrogen production, whereas increasing the cathode volume enhances the net gas production and boosts the hydrogenotrphic methanogenic activity (Gil-Carrera et al., 2011)

When it comes to methane-producing MECs, the occurring underlying biochemical reactions to go from raw organic matter to biogas use the same basic metabolic pathways as in a traditional AD, therefore, environmental conditions such as temperature of either 35°C or 55°C, HRT of 15 to 40 days, neutral pH between 7.8 and 8.3, and volatile fatty acids concentration correspond to those recommended in the traditional literature (Al Seadi et al. 2008).

Other parameters such as the influent composition's effect on biogas volumetric efficiency (Kerroum et al., 2014), the residence time and organic load (Garcia-Pena, 2015), and the electrode size arrangement (Gil-Carrera et al., 2011) have been studied for hydrogen generation but less is known about their role in methane generation. Efforts have been undertaken to understand the effect of electrode surface area (Hou et al., 2015), electrodes' separation(Park et al., 2017), and organic load (Shen et al., 2017) on the performance of MEC systems. Shen *et al.* focused on the optimisation of the treatment of hydrothermal liquified wastewater rather than potential energy

recovery (Shen et al., 2017), finding that within the range 2-10 g $L^{-1}d^{-1}$, the maximum removal of compounds commonly considered as recalcitrant was achieved at 8 g $L^{-1}d^{-1}$, suggesting that the relationship between treatment efficiency and organic load is not linear. Hou *et al.* studied the effect of the electrode size on the methane production rate of a double-chamber MEC, identifying that a higher voltage (within the range 0.7-1.3 V) increased both the current density and methane production but decreased the energy efficiency (Hou et al., 2015). The effect of the relative size of the electrodes with respect to each other was not studied as part of this investigation. Therefore, it remains unresolved how the relative electrode surface area of the anode and cathode and the organic load affects the performance of MECs designed for methane production.

Despite all this foundational knowledge, MECs are still in an early stage of development, and solving issues related to their operation under industrial conditions is crucial. Some studies have made interesting contributions such as the single-chamber membraneless reactor proving its feasibility, although these did not produce enough energy to offset the running cost (Clauwaert and Verstraete, 2009). The feasibility of methane electrosynthesis at low-temperature operation was also reported with significant reduction of the performance compared to ambient temperature (Kaneco et al., 2002). Some studies have also contributed with simple, low-tech or low-cost MEC-anaerobic digestion systems, achieving up to 3-fold efficiency improvement compared to a traditional AD.

Understanding how operational parameters affect the performance and the microbial component of the system is crucial. For example, the knowledge regarding appropriate/adverse environmental conditions for methanogenic microbes has been used in hydrogen focused studies to eliminate them; using high imposed voltages, short retention times (about 1.6 h), and oxygen pulses were necessary to reduce the methane production, but nevertheless could not achieve a complete elimination (Sangeetha et al., 2016). Incidentally, these studies confirmed that methanogens are indeed attached to the electrodes as part of the biofilm rather than being in suspension (Rader and Logan, 2010).

When methane production is intended, the methanogenic colonisation of the cathode is highly desirable. Many approaches have been evaluated; Mieke *et al*. emphasise the importance of large-surface-area electrode materials (Van Eerten-Jansen et al., 2012), whereas Yang *et al.* and Sasaki *et al.* modified the projected area of the desired electrode (Sasaki et al., 2013). Villano *et al.* opted to use specific conditions for the start-up and the steady operation of the MEC, applying -850 mV vs. SHE to ensure the biofilm development and then changing to +500 mV vs. SHE for the system operation (Villano et al., 2011).

2.6.2. Operational parameters

MECs' operation can be tailored to target production of hydrogen, methane, or waste treatment (reducing its organic matter content). When biogas production is the aim, carbon from the organic matter is used to produce it; hence the design must allow a hydraulic retention time sufficient in extent for the biochemical reactions to occur, while accommodating the entirety of the waste stream to be treated. This means taking into account both technical and economic considerations. In this application, the organic load is an operational parameter that expresses the amount of organic matter fed into the bioreactor per unit of vessel volume and time. This is defined in Equation (2.9), where ORL is the organic load (in kg d^{-1} m^{-3}), m the mass flow of substrate (in kg d^{-1}), c the concentration of organic matter (in %), and V_R the vessel volume (in m^3)

$$ORL = \frac{m \cdot c}{V_R} \qquad (2.9)$$

As noted above, the time required to carry out the biochemical reactions has a crucial role on the overall performance and yield of the process. Under a continuous operation, the time available for the reactions to occur is the hydraulic retention time corresponding to the average time that the substrate stays inside the digester vessel. As seen in Equation 2.1, it is related to the digester volume (V_R in m^3) and the volumetric flow of substrate fed (V in m^3 d^{-1}) (Al Seadi et al., 2008) According to the Equations (2.9) and (2.10), the organic load can be increased by increasing the waste stream concentration without affecting the HRT, Increasing the HRT will typically reduce the organic load, all other factors being equal.

$$HRT = \frac{V_R}{V} \qquad (2.10)$$

The waste treatment is consequence of the bacterial carbon usage for both cellular growth and energy metabolism (Taubner et al., 2015), thus it is inherently linked to the bacterial behaviour and reaction rates. The retention time must be sufficiently long to ensure that the amount of bacterial population removed with the effluent (digestate) in a continuously stirred tanks reactor (CSTR) is not higher than the number of reproduced microorganisms so as to prevent the net loss of the bacterial community. The duplication rate of anaerobic bacteria is usually 5-7 days or more (Zhang et al., 2019). Assuming a fixed feedstock strength, a short HRT provides a good substrate flow rate, but a lower gas yield would be expected in AD. It is therefore important to adapt the HRT to the specific decomposition rate of the substrates. Knowing the targeted HRT, the daily feedstock input and the decomposition rate of the substrate, it is possible to calculate the necessary digester volume.

2.7 Key Performance Indicators (KPI)

When it comes to assessing the performance, there are many indicators used in the available literature, with wide ranges of values for each. This variability corresponds with the inherent search for a "better system" that has led to the use of varied cell configurations, the use of different membranes (or not at all), the fundamental genetic arsenal of the microbial consortium used, and the electrodes' design and materials (Zhen et al., 2015).

The use of metrics or key performance indicator (KPI) is often recommended to compare options, especially when contrasting different approaches aiming to solve the same issue based on different technological principles. In this sense, the use of KPI is a useful tool for ranking alternatives.

KPIs are also important for tracking the operation of one given system, working as an alert system to prevent malfunctions, as it seems there is also the assumption that the operational conditions must be steady and immovable and this underestimates the inherent response-capacity and self-optimisation of such systems. Designing KPIs to fulfil the functions described above is an intricate task. A task that often tends to neglect production rates, focusing on costs or vice versa (Schembecker, 2015). As both production costs and production rate have a significant impact, both should be considered in the decision-making process, as well as any other significant parameter, suggesting that multiple KPIs should be used to effectively compare all the possible conditions.

Bio-electrochemical systems operate under a wide variety of conditions depending on the design and purpose. Therefore, the pH, temperature, electrode material, and feedstock variety, translate into a range of expected performance, but the availability of adequate data and key performance indicators is crucial for the maturation of the technology as it allows an appropriate comparison (Sharma et al., 2014). This comparison is crucial in building the body of knowledge that allows further developments of the technology from foundational tests to deployment at an industrial level.

Currents and current density are the natural response variable to monitor the performance of bio-electrochemical systems, as these indicate the electron flux consequent to the redox reactions taking place. However, technology development and inclusion of new, porous materials have made the projected surface area of the electrodes a parameter that no longer represents the total available surface, as it only applies to smooth and compact materials (Sharma et al., 2014). Fabrics, foams, felts, and brushes have reaction surface available far in excess of their projected surface or macroscopic surface area, hence, current densities are no longer appropriate, and probably an important reason why porous electrodes appear to outperform nonporous electrodes (Xie et al., 2015). For instance, a smooth and flat graphite electrode of 1 cm^2 has a much lower available surface area than a carbon felt electrode of the same dimensions due to the open 3-D structure of the latter.

Due to the inherent limitation of the electrochemical activity to the contact area between the biofilm and the electrode, the biofilm-covered area has been considered for some authors as the base for calculations of current densities. The biofilm-covered area can be estimated with microscopy techniques and offers an assessment of the capacity to transfer electrons when the electrodes are not completely covered by the biofilm. However, this methodology needs to be carefully implemented as not all the members of the biofilm are electro-active, even when mediators and other indirect electron transfer mechanisms are present.

It has been proposed in the literature that the bioelectrochemically-active surface area would be the "one truly valid method" to compare intrinsic activity between bioelectrodes. To calculate this, the total Brunauer-Emmett-Teller active surface and the biofilm-covered area should be calculated first, which needs chronoamperometric response analysis of the porous electrodes, and the diffusion coefficient from an electroactive component (Sharma et al., 2014). This method is accurate but complex to implement, and even harder to establish as a comparison parameter since not all the parameters are commonly known, nor are they easily determined.

When thinking about deploying the technology, simpler and direct performance indicators are more appropriate, especially if complicated techniques are not needed to determine the actual microbial-electrocatalytic activity area. The intricate interaction between the operational conditions and the inherent evolving nature of the biofilm of the bioelectrodes makes them a very dynamic feature of the system. Therefore, global performance indicators seem adequate for highly fluctuating conditions and long-term operations.

Studies regarding the MEC integration into AD systems (MEC-AD) usually report better yield for either methane production or organics removal over conventional AD. However, a systematic comparison can be hardly done, as every study uses different configurations, feedstock, and operational conditions amongst other differences (Zhang et al., 2019).

For the quantitative study of methanogenesis in a MEC mimicking industrial conditions, it is important to account for performance indicators that are simultaneously relevant and that incorporate the multiple aspects involved in a MEC, avoiding the need for over-complicated analysis. The KPI used to describe the performance of a particular system depends on what the author of the work is looking to communicate. Despite the wide variety of KPI used in the literature (as shown in Appendix D), they can be grouped into types. The most common type of KPI is a direct relation between the amount of biogas produced with respect to the physical dimensions of the bioreactor for a given time unit. Within this group, most results are given as $volume_{biogas}\ volume_{reactor}^{-1}\ time^{-1}$, although some authors prefer to report the volume of methane, or some other direct measure of methane such as moles or equivalents as done by (Villano et al., 2011; Zeppilli et al., 2016).

The operational mode used in the study also forces some constraints over the KPI of choice. A popular KPI in studies of bioreactors in batch mode is the accumulated biogas production, whereas continuously feed bioreactors can report their biogas production relative to the organic load input, although (Kerroum et al., 2014; Sangeetha et al., 2016) are some of the few researchers to report any kind of nutrient or energy input effects on yield.

In bioprocesses, the nutrient yield is commonly defined as the proportion between the cellular mass-produced and the amount of nutrient consumed. This establishes a relationship between the rates of biomass change, and substrate consumption as, seen in Equation (2.11) where X represents the biomass, S the studied nutrient, and $Y_{x/s}$ is the yield (how much biomass is obtained per unit of substrate mass).

$$Y_{x/s} = \frac{\Delta X}{-\Delta S} = \frac{produced\ biomass}{consumed\ substrate} \qquad (2.11)$$

However, in the context of this study, where growing the biomass is not the intention, this logic can be directly applied to the product formation yield described in Equation (2.12), where P represents the product. An advantage of this approach is the possibility of calculation directly from experimental data (Acevedo et al., 2002).

$$Yp_{/s} = \frac{\Delta P}{-\Delta S} = \frac{produced\ product}{consumed\ substrate} = MCR\ \langle {g_{CH4}}/{kg_{COD}} \rangle \qquad (2.12)$$

When this yield gets close to the theoretical value, it would indicate that the process is hardly able to be improved, hence investment of limited resources can be better directed to other uses which may improve the technology. In an industrial process, besides the yield, kinetic aspects should also be considered, as the production rate or the volumetric productivity, commonly referred to as a specific metabolic product or cellular/bacterial biomass (Acevedo et al., 2002).

A more realistic estimation would arguably need to consider non-productive times, such as cleaning and maintenance cycles, as this may be significantly different when comparing single and double chamber systems. However, generally it is more important to compare the performance during operation of different sets of operational parameters, using a measure of specific productivity that relates the product formation, time, and bioreactor size (Acevedo et al., 2002), as shown in Equation (2.13)

$$Productivity_{volumetric} = \frac{produced\ product}{time * volume} = MPR\ \langle {ml_{CH4}}/{L_{MEC} * h} \rangle \qquad (2.13)$$

This direct determination of how much methane is being produced by the reactor in terms of its physical design and operation is called methane production rates (MPR, $mL_{CH4}\ L_{reactor}^{-1}\ h^{-1}$). That same methane production expressed as yield relative to the organic matter input is called methane

conversion rate[1] (MCR, g_{CH4} $kgCOD^{-1}$). Finally, the ratio between the energy stored and the total energy input is used as an indicator of the overall energy efficiency, as detailed in section 3.6.

A simple and standardised key performance indicator such as the MPR and MCR allows for easier comparison between different systems operating under different conditions. Appendix D shows that an average MPR of 56 mL_{CH4} L_{MEC}^{-1} h^{-1}, over a wide range of methane production rates from 1 to 340 mL_{CH4} $L_{reactor}^{-1}$ h^{-1} was found. Similarly, bioelectrochemical power-to-gas applications have been reported in the literature to range between 11.25 and 1125 mL_{CH4} $L_{reactor}^{-1}$ h^{-1} (Geppert et al., 2016).

It is noteworthy that performance indicators are necessary but not sufficient in themselves to assess the overall performance, and they should be used in conjunction to offer a broader description of the system's operation. The available literature (Nam et al., 2010) suggests the possibility of optimising the operation of a system to maximise one particular KPI. For instance, it would be possible to achieve higher MPR by increasing the feedstock strength, sacrificing the MCR; or maximise the MCR by increasing the HRT, to the detriment of MPR.

2.8 Energy Balance

2.8.1. Energy Storage

Generally speaking, the energy flow from renewable sources as solar, wind and tidal is not constant but depends on the season, time of day, and weather conditions. Energy demand is not constant either; it depends on the same circumstances but mostly in the opposite sense, with higher demand during winter and night time. So, there is a need for a mediator between the source of energy and its consumer to balance energy demand and supply (Ter-Gazarian, 1994).

Energy occurs in a variety of types, and its ability to be storable depends on its physical form as shown in Table 3. MECs represent an example of the flow between different forms, when used to reclaim energy from wastes in the form of methane using renewable energy to supply the electrical input uncoupling power generation from demand. Following this logic, it has been suggested that AD could produce biogas, or microbial fuel cells could produce electricity from the chemical energy contained as chemical bonds in the organic matter content of wastewater in countries with flushing toilets (Dai et al., 2019), but their yields are not sufficiently high.

Any device in a power system designed with the purpose of converting energy into a storable form can be called "secondary energy storage" (ES). An ES accepts the energy generated in the power system, converts and stores it for a limited time before returning as much usable energy as possible. In nature, the sun's energy has been stored as organic fuels (wood, coal, oil), with water evaporation, and the wind among others, acting as secondary energy storage.

[1] The methane conversion rate calculated here is technically a yield, as it does not include a time reference

It has been defined in the literature that a storage unit must contain three components, where:

-Power transformation system (PTS), works as the link between the power system and the central storage

-Central Storage (CS), is a device that receives energy and stores it for a time. The energy can be extracted on demand within the PTS installed capacity margins until it is discharged. These devices can be based on thermal principles (using sensible or latent heat), or mechanical (using gravitational, kinetic, or elastic energy forms), or chemical (using chemically bound energy), or electrical (using electromagnetic or electrostatic energy)

-charge-discharge control system (CDCS), refers to the unit that controls the charge/discharge power level according to the power system's regime, managing the power flow to respond to the conditions (Ter-Gazarian, 1994).

Energy storage devices operate under three regimes (charge, storage, and discharge). The capacity of CS can be directly measured as the energy storable in the vessel, with different conversion methods from one type of energy to another (mechanical, thermal, chemical, or electrical). Another intrinsic characteristic of the storage device is the charging/discharging power capacity (Ps), corresponding to the maximum between the charge or restoring capacity (Pc) and discharge or generating capacity (Pd) (Ter-Gazarian, 1994).

Table 3 Energy types and how it can be stored according to its physical state (Ter-Gazarian, 1994)

Type	Form	Potential	Quantity	Storable	Example
Gravitational	Altitude	Gravitation potential gh	Mass m	Storable	Dam
Kinetic	Velocity	v^2	Mass m	Storable	Flywheel, Bullet
Spatial	Pressure	Pressure P	Volume V	Storable	Compressed gas
Thermal	Heating	Temperature	Entropy S	Storable	Hot water
Chemical	Electron charge	Chemical potential G	Number of moles n	Storable	Chemical battery
Electric	Electron charge	Voltage U	Electric charge	Storable	Capacitor
Dielectric		Electric field E	Dielectric polarisation P	No	Polarisation
Magnetic	Electron spin	Magnetic field H	Magnetisation M	No	Magnetisation
Electromagnetic	Moving charge	Self-inductance voltage L dl/dt	Electric current	Storable	Magnetic coil
Weak nuclear	Mass change		Mass m	No	Luminous paint

Strong Nuclear	Mass change	Mass m	No	nuclear reactor, stars
Radiation	Photon		No	

The design and power flow within the whole system, as presented in Figure 5, will directly affect the related costs as consequence of the efficiencies. A mathematical model of the costs of energy storing, comprising the three components of the system is introduced in Appendix F.

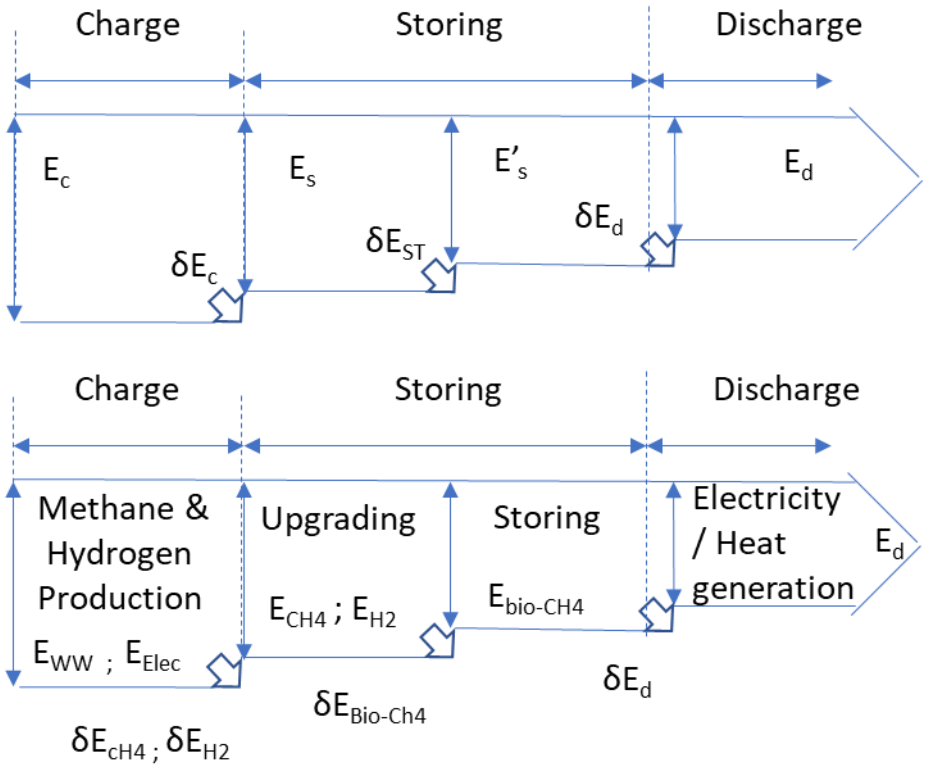

Figure 5 : a) Diagram of a generic storing device operation, indicating losses and energy flow. B) Diagram indicating energy flow and losses in a storing device based on hydrogen methanation in a MEC

Thus, a MEC fed with wastewater and electrical energy to produce methane via bacterial activity would act as a hybrid system (two inputs and only one output), where the Pc would be intrinsically linked to the bacterial activity and its methane production rate (MPR). This Pc is likely to be lower than the methane burning capacity of any device that is used to deliver the energy stored as methane (i.e. the Pd), therefore, the Ps would be limited by the Pc.

The charging/discharging capacity becomes relevant when several consumers are connected, as many energy storage devices (E_S) would be at different phases with different reserves available at any given time. Isolated consumers, on the other hand, are more efficient due to their forced autonomy (Ter-Gazarian, 1994).

Each one of these regimes has losses (δE) inherent to the operation as shown in Figure 5 and the equations 2.14 and 2.15 below. This overall efficiency can be used as an indicator of these losses, and calculated as the ratio between the final energy delivered and the total initial energy input

$$\boldsymbol{\delta_E = \delta_{Ec} + \delta_{Es} + \delta_{Ed} = E_C E_d} \qquad \textbf{(2.14)}$$

This efficiency (ξ) is traditionally time-dependant; hence, the overall efficiency can be defined as follow:

$$\boldsymbol{\xi_S = \frac{E_d}{E_C} = \xi_C * \xi_S(t) * \xi_d} \qquad \textbf{(2.15)}$$

Then, the energy losses (δE) can be written as

$$\delta_{Es} = E_C - E_d = \frac{E_S}{\xi_C - E_d + \frac{E_S}{\xi_C} * \left(1 - \xi_C * \frac{E_d}{E_S}\right)} = \frac{E_S}{\xi_C} * (1 - \xi_C * \xi_S(t) * \xi_d)$$

$$\boldsymbol{\delta_{Es} = \frac{E_S}{\xi_C} * (1 - \xi_S)} \qquad \textbf{(2.16)}$$

Bacterial cells use carbon for both, energy metabolism and as a building material for construction of new cells. This results in a discrepancy when it comes to the energetic and growing yield of the culture, especially as these changes according to the conditions, as explained in Section 2.10. In a typical MEC system there is only one carbon input corresponding to the organic matter in the wastewater or CO_2 injection in a methanation operation, whereas multiple outlets exist. although The most important carbon outlet is forming part of the biogas CO_2 and CH_4, although it will also leave the bioreactor in the digestate, as a constituent of the organic matter not metabolised during the process or dissolved gases (Steed and Hashimoto, 1995). This simple carbon balance shown in Equation (2.17) can be used to estimate the accuracy of energy storage calculations, but it should also take into account the carbon sequestered in the biofilm as structural component of the new bacterial cells when the conditions are appropriate for cellular growing.

It has been estimated that about 3% of the input carbon will be used for methanogenic cellular growth in conditions similar to those in a typical mesophilic operation (Taubner et al., 2015), a similar range was reported by (Steed and Hashimoto, 1995)

$$\boldsymbol{C_{input} = C_{digestate} + C_{CO2} + C_{CH4} + C_{cell}} \qquad \textbf{(2.17)}$$

2.8.2. Biogas production energy balance

Domestic wastewater is not just a waste stream that needs to be disposed of, but a potential source of chemical and heat energy (Hao et al., 2019). In Switzerland it is even used to produce hydroelectricity (Samora et al., 2017). There are many technological solutions under development to seize this opportunity. In this context, even the recovery of heat from wastewater has been proposed (Hao et al., 2019), with claims that up to 90% of that energy can be recoverable, although it will depend on the temperature difference between the wastewater stream and the

environment. Nevertheless, assuming a 4 °C of gradient, it was estimated at 4.64 kWh m^{-3} (Hao et al., 2019)

When approaching wastewater treatment, the chemical energy is typically perceived as the most relevant energy source recoverable while turning wastewater plants towards carbon neutrality (Hao et al., 2019), but the previous examples open an interesting discussion to evaluate the different technologies currently under development. How much energy is possible to retrieve from it, what are the efficiencies of each technology and how to compare them are important questions that may change the perception about different processes and, hence, their deployment.

The chemical oxygen demand (COD) is the measure of how many oxygen equivalents are necessary to achieve the total oxidation of the organic matter present in the sample (Hu and Grasso, 2005), and has been extensively used as the reference measure of the organic matter content in wastewaters, and hence as an indicator of the chemical energy present in it.

Despite the lack of a standard relationship between the COD and the energy content, there is a long-established agreement that the internal chemical energy of wastewater is about 6.3 kJ/L, although more extensive and accurate research proved it to be about 20% higher at 7.6 kJ/L (Heidrich et al., 2010). Subsequently, part of the same team reported an empirical mathematical factor of 16.1 kJ of energy in the wastewater per gram of COD (Dai et al., 2019).

Each technology has advantages and disadvantage against other options, but when it comes to energy reclaiming from wastes, the energy balance is a crucial tool to compare the efficiencies of alternative processes, as there is no benefit in using more energy than the energy reclaimed. It is particularly useful to contrast the performance of systems that operates under completely different technological bases, as occurs between the AD and MECs comparison throughout several different conditions, or the heat versus organic energy reclaiming in the wastewater previously mentioned.

Considering E_{out} as the energy output of the system, either as fuel, heat, or any other form produced at the PTS. E_{in} would be the energy required in the system, including in this case both the electrical energy needed for running the MEC and the chemical energy present at the wastewater inflow. Then, the energy balance can be estimated as shown in Equation (2.18).

$$E_B = E_{OUT} - E_{IN} \qquad (2.18)$$

From an energy balance point of view, MEC operation requires the direct spending of energy to carry on the desired reaction, mostly in the form of electrical energy used to apply the corresponding voltage to the electrodes. Nevertheless, there is also a series of indirect energy costs to be considered such as the construction, delivery of raw material, maintenance, waste collection amongst others. These indirect costs are essentially equal for both traditional AD and

MECs, and are highly system dependent. The energy flow through the system can then be defined as shown in Figure 6.

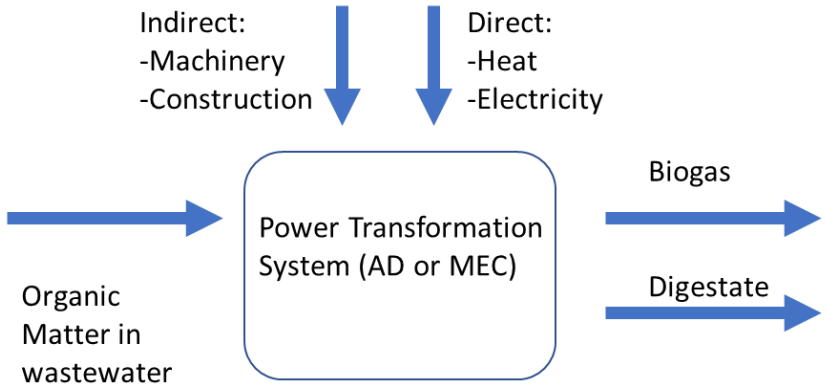

Figure 6 Diagram depicting the main energy inputs and outputs of the AD and MEC plant.

The main energy output corresponds to the energy contained in the biogas, which is then considered stored for effects of efficiency calculation, calculated as proposed in section 3.6. The empirical factor 16.1 kJ g_{COD}^{-1} allows estimation of the input (Dai et al., 2019), multiplied by the organic load (flowrate in L day^{-1} multiplied by the organic matter concentration COD in mg L^{-1}). Finally, the direct electrical energy required by MECs is calculated by directly multiplying the imposed voltage (according to the design of experiments) by the time it was imposed per day (24 hours) and the resultant current.

2.8.3. Overpotentials

In the literature there are reports of needing a potential much higher than the theoretical potential of -0.244 V vs SHE (standard hydrogen electrode) via direct EET, or -0.410 V via indirect EET to achieve methane electrosynthesis (Zhen et al., 2016). This is likely due to imperfect electrode materials and mass transfer-related overpotentials, which translate into more energy consumption and hence poorer energy efficiency overall.

A key element in energy efficiency is the interface between microbe and electrode, which is the physical place where the electrode reactions occur. This reaction usually includes a series of basic electrochemical steps:

1.-Mass transport, including the transport of the reactants from the bulk to the electrode surface, which can be enhanced by agitation and mixing

2.-Preceding reactions; some molecules may need to be absorbed, or chemical reactions such as protonation or disassociation may need to take place in advance.

3.-Electron transfers at the interface

4.-Surface conversions, which can include chemical reactions, desorption, etc.

5.-Mass transport from the interface into the bulk of the electrolyte.

As in any process, the overall reaction rate is limited by the slowest step. Every step takes place at a specific rate and can be a cause of overpotential, which opens the classification of overpotential into three categories: ohmic (η_o), activation (η_a), and transportation (η_c). The overpotential can be defined as the sum of those three (Wang et al., 2015), as shown in Equation (2.19)

$$\eta = \eta_o + \eta_a + \eta_c \qquad (2.19)$$

Ohmic overpotential relates to Ohm's Law, combining the resistances of electrodes, electrolyte, membrane (when present), current collector, and the contact. Thus, when the current flows through the system, the ohmic potential drop varies linearly with the current obtained. Nevertheless, the ohmic overpotential is predominantly controlled by the ionic resistance rather than electronic; the latter being higher for semiconducting materials or when the electrode is passivated with a coating film (Wang et al., 2015).

The activation overpotential is intimately linked to the steps 2 and 3 previously described, caused by the build-up of electrons over the surface, making it more difficult for new electrons to arrive. Therefore, the activation overpotential is the potential difference over the equilibrium necessary to achieve the activation and produce the current. However, electrode potential departure from the equilibrium potential can also be caused by slower preceding or following surface reactions, such as catalytic decomposition or crystallisation (Wang et al., 2015).

Different reaction rates, bioreactor feeding, lack of appropriate mixing, etc. may also cause a concentration gradient between the bulk of the electrolyte and the surface of the electrodes – phenomena related to the preceding reactions and mass transport (steps 2 and 5 above). This translates in practice to a reaction rate faster than mass transport, so the reactant reaching the reaction site, or rate of product leaving it are the limiting steps. Thus, depletion of reactants or accumulation of products will be produced over the electrode.

It has been reported that fluid dynamics have a great effect on the overpotential and thus over the energy consumption of the whole process (Zeppilli et al., 2016). It seems noteworthy that new electrode materials with 3-D open structures, such as felts, tend to create zones where there is very little or no mixing at all. In this sense, mixing/stirring would greatly help to increase the convection component of the overall mass transport that takes place in electrochemical processes. Otherwise, mass transport would depend entirely on the diffusion and migration mechanisms. Diffusion is proportional to the concentration gradient, whereas migration refers to the mass transport driven by the electrical field (Wang et al., 2015).

If a reaction occurs sufficiently rapid, the electrode reaction rate can be controlled by the mass transport, so a rapid change of the reactants' concentration at the electrode surface will decrease

their concentration and increase the current. The critical current, or limiting current is defined as the current when the reactants react instantly upon arrival and the concentration over the electrode is null. This would be the maximum rate allowed by the mass transfer conditions, when it is a diffusion-controlled reaction, the current density can be estimated with Equation (2.20), where *F* is the Faraday constant, *n* the number of electrons involved, *D* the diffusion coefficient of the reactant, *C** the concentration at the bulk, and δ the thickness of the diffusion layer (boundary where the concentration is different to that on the bulk of the electrolyte) (Wang et al., 2015).

$$i_l = \frac{n*F*D*C^*}{\delta} \qquad (2.20)$$

Different approaches have been taken to reduce the effect of overpotential and increase the overall energy efficiency of the process. One approach is to tailor the electrode materials to enhance the electrode-microbe electron transfer (Zhen et al., 2016). This strategy was proved to enhance the microbial electrocatalysis activity and reducing the overpotential needed for methane production when graphite felt was used, thought to be due to the reduction of the activation overpotential.

Another strategy looked to minimise the overpotential influences through imposing different voltages to improve the mass transfer stage (Zeppilli et al., 2016). This approach probably addresses issues with ohmic and transport overpotential in their system. The authors claimed that the change of potentiostatic control from the anode to the cathode reduced the anodic reaction overpotential by 30%, while the cathodic overpotential remained steady.

It seems that a mass transport capacity limited to diffusion and migration, combined with the chemical nature of the electrode material and architecture are the major sources of overpotentials. Therefore, the most effective measures to counteract the limitations will depend on the specific constraints each system faces. It can be understood as a general guideline the necessity for having electrodes with an architecture and open design that facilitate the mass transport phenomena, whilst offering a good activity to avoid formation of gradients and build-up of any components in general. It can be understood from the literature that the integration of agitation to the bioreactor is therefore necessary to avoid the complete dependency on diffusion and migration.

2.8.4. Heating and pumping

It has been previously mentioned that heating and pumping energy demands are very system dependent and similar between AD and MEC plants, so they have not been considered in the efficiency calculations. Nevertheless, a short introduction of which are these energy demands, and how to estimate them is given below to provide a picture of what would it be needed outside the laboratory.

A generic representation of the equipment needed in a working plant is shown in the Figure 7, allowing an estimation of the main energy cost involved in the operation.

The pump sizing process considers many factors, nevertheless, it can be simplified to the use of Equation (2.21) where P_h is the hydraulic power (in kW), q the flow capacity (in $m^3\ h^{-1}$), ρ the fluid density (kg m^{-3}), g the acceleration of gravity (9.81 m s^{-2}) and h the differential head (m). Also considering that P_h (in HP)=P_h(in kW)/0.746 (Ter-Gazarian, 1994)

$$P_h\langle kW\rangle = \frac{q * \rho * g * h}{3.6 * 10^6} \qquad (2.21)$$

When referring to heat requirements, these include both the energy needed to take the wastewater to bioreactor temperature and the heat losses throughout the walls, floor and roof of the biodigester, etc. Here, peculiarities of the facility such as the insulation of the bioreactor and the ambient temperature among others have a significant effect as the heat losses (*hl* in kW) depend directly of the overall heat transfer coefficient (*U* in $Wm^{-2}C^{-1}$), which depends on the heat transfer area (*A* in m^2) and the temperature difference across that area (Δ*T*, °C); the relative importance of this factor strongly depends on the ambient temperature where the operation takes place.

$$hl\langle kW\rangle = U * A * \Delta T \qquad (2.22)$$

This simple Equation (2.22) hides the underlying effect of the biodigester design, as the heat transfer coefficient is specific for each material and the design and shape will determine the heat transfer area.

When it comes to the feedstock heating (*hf*), the heat requirement is directly dependent on the volume to be heated (*Q* in m^3), the temperature difference between the operation and initial feedstock (Δ*T* in °C) and the specific heat capacity of the feedstock (*MJ* $tonne^{-1}$ $°C^{-1}$), as shown in Equation (2.23) for estimating the heating feedstock requirement.

$$hf = Cp * Q * \Delta T \qquad (2.23)$$

Therefore, the total heat requirement is influenced by many factors such as the feedstock, its flowrate, the temperature difference with the environment and the biodigester design, each factor affecting either the heat losses or direct heat requirement (Ter-Gazarian, 1994).

A more complex system allows more interactions, altering the energy balance. For instance, a MEC integrated as a biogas upgrading stage to an AD biodigester and supplemented with *in situ* hydrogen generation will allow the recovery of fuel with a higher energetic value, but also need the installation and maintenance of electrodes and additional machinery. All of this will affect the net energy flow presented in Figure 6.

Summarising, to determine the energy balance it is necessary to clearly establish the system boundaries to account for direct and indirect energy usage, including the energy necessary to produce/transport the biomass and the energy to produce the biomass into bioenergy. If the energy balance is negative this means that more energy is needed to produce the biofuel than that which

it contains, however, this could be affected by many factors. Some of these factors are not easily managed, such as the feedstock used or ambient temperature, but others such as the thermal insulation, working flowrate or even the use of passive waste collection and transfer or heating/cooling heat exchange could significantly reduce the overall energy requirement of the operation.

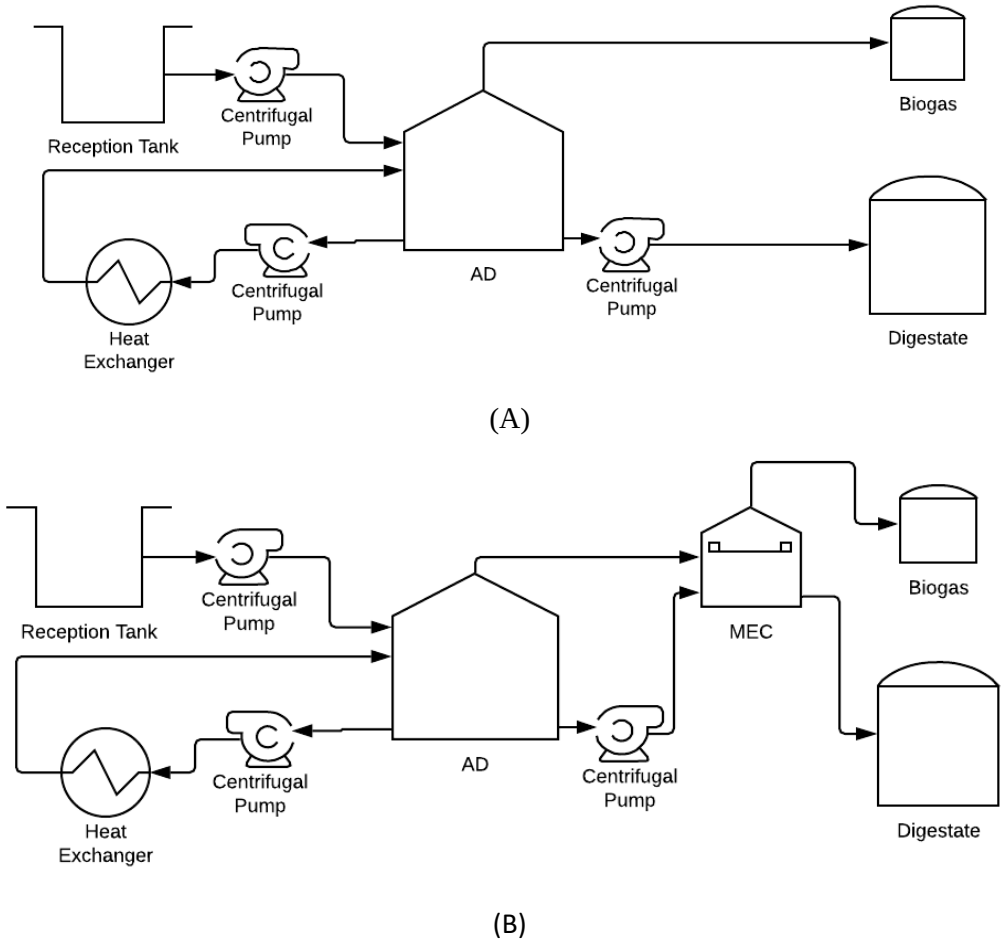

Figure 7 : A) Generic traditional anaerobic degradation biogas plant, B) Biogas plant with Ex-situ upgrading stage integrated.

Particularly relevant for the MECs is the electrical energy input. If this is surplus energy, produced as consequence of renewable generation fluctuation, the actual operational cost will be reduced due to the excess nature of the electrical energy used. However, the use of fossil energy produced solely as an electrical input would clearly introduce an additional economic and environmental cost.

2.9 Voltage Imposition

The performance of MECs depends on a complex system of parameters and their interactions, including electrodes design and operational conditions. However, the energy efficiency and

overall performance are mainly determined by the metabolic pathways and mechanisms of the bioelectrochemical energy conversion (Schröder, 2007). The link between microbiology and electrochemistry are key and define the maximum limits of the overall performance.

In this sense, the method used to control the applied potential has been found to influence bacterial activity. Hence, by controlling the applied voltage, the overall methane-producing MEC performance would be affected due to the biological base of its operation (Zeppilli et al., 2016). The applied voltage may be controlled via A) maintaining the potential difference between both electrodes (cell potential method) or B) setting the desired potential over one electrode relative to a reference electrode.

When the potential is imposed following strategy A, is possible to accurately know the energy input, but there is no further control over the electrode potentials. Additionally, the cell potential method is particularly easy for operation capable of simultaneously providing a stable and identical voltage to a group of cells (Zhang et al., 2019).

On the other hand, strategy B allows controlling perfectly the potential of one electrode but leaving the other free, and hence, there is no control over the energy input (Zeppilli et al., 2016).

Strategy B would allow further control of every stage of the process, enhancing different phenomena at different moments. As suggested by Villano *et al.*, a faster start-up of the organic matter oxidation may be obtained when an anodic potential is applied, hence, taking over the bacterial activity; the cathode must then adjust its potential to sustain the current production from the anode (Zeppilli et al., 2016). According to this data, a higher anode potential would lead to the maximum ATP yield (based on the moles of substrate consumed) that a microorganism can produce.

2.10 Bacterial growth

Bio-electrochemical systems, such as MECs, based their operation on the metabolic capacity of bio-cathodes, which implies the relevance of the microbiological component. Therefore, providing appropriate conditions for them to thrive is important, especially in bioreactors operating continuously, since part of the population is continuously discharged and replaced by fresh medium or wastewater having insufficient bacterial population.

Understanding microbial dynamics is of great importance for many applications, as these will determine the overall performance in, for example, the food industry, waste removal in bioreactors, pollution clean-up in soils and sediments, among others. Most microbiological models acknowledge the benefits of incorporating microbial growth. Some models even include energy expenditure measures involved in maintaining healthy the living cells, a concept commonly referred to as “maintenance”, which is recommended to consider to provide a more appropriate description of microbial kinetics (Bodegom, 2007).

Prokaryotic bacterial cells reproduce by binary fission, making it impossible to differentiate the mother from the daughter cell. So, the maximum age of each cell is the time between two successive replications. A different concept is the age of the culture, for a batch operation this corresponds to the time since inoculation. This implies that in a bacterial culture there are no important differences among the physiological states of the cells (Acevedo et al., 2002). This uniqueness makes the consortium within a vessel different and allows for the self-adaptation and self-optimisation of the culture as a whole beyond individual cells.

The microbial cells of the consortium can be present individually or in small groups associated as a biofilm. A biofilm is a thick layer of prokaryotic organisms forming a community attached to a substrate with an exopolysaccharide to increase their survival by improving availability of nutrients and the resistance mechanisms to environmental conditions and chemical responses (McCarty et al., 2014). These depend on the material and architecture of a substrate such as the electrodes and are key to encourage biofilm development

To predict the microbial behaviour, fermentation performance, yields, production rates, and overall process optimisation it is necessary to know the growth kinetics and metabolites production to allow for a quantitative treatment of the fermentation processes. The kinetic behaviour is determined by a group of environmental and genetic factors, such as the culture modality (batch, continuous, etc), operational conditions (temperature, feedstock, pH, etc.), and the inoculum composition (Acevedo et al., 2002). All these factors affect the typical growing curve, characteristic of the culture kinetics.

A particularly relevant case for many industrial applications is bioreactors operating under a continuous regime that aims to maintain the chemical environment steady over time, known as a chemostat. Different parameters affect differently the overall performance. The inoculum composition has a qualitative influence, as it will determine the metabolic capacity of the system, whereas environmental conditions have a more quantitative influence offering possibilities to modulate the level of activity (Acevedo et al., 2002). The nature of the feedstock, particularly the carbon and nitrogen sources will determine the specific growth speed as suggested by the Monod model (see Equation (2.24), where μ_m is the maximum specific growth rate, S is the limiting substrate concentration, and K_S is the constant of saturation (substrate concentration to achieve $\mu_m/_2$)

$$\mu = \mu_m \frac{S}{K_S + S} \qquad (2.24)$$

The specific growth rate is inherently linked to the time required by a population to double. This is known as the doubling time (*Dt*), where $Dt = ln2/\mu$. Interestingly, in a chemostat, the specific growth rate equals the dilution rate, defined as the number of reactor volumes passing through the

vessel per unit of time. In this context, the uniqueness of a chemostat is that $\mu = D = {flow}/{volume}$ (Najafpour, 2007).

This explains how the consortium composition (μ depends partly on the bacteria present) constricts the relationship between the volume of the bioreactor and the waste inflow (see section 2.6) (Acevedo et al., 2002). Since the actual specific growth rate depends on many factors, it can be determined for each particular system, and optimised to minimize the risk of washing out and maximise the productivity. Nonetheless, as a general rule, it is known that *acetoclastic methanogenic* bacteria have a longer duplication time (5-7 days) than *hydrogenotrophic methanogens*, ranging between 4-8 hrs (Zhang et al., 2019), thus determining two very different HRT according to the desired operation.

When it comes to biogas production, bacterial growth is only part of the dynamics and not the focus of the whole bioreactor operation. Electroactive microorganisms cultured on the cathode, including archaea and bacteria, play an important role in CO_2 electro- methanogenesis (Zhang et al., 2019). Compared with pure strains, mixed strains possess more complicated microbial communities and more versatile metabolic pathways. Furthermore, there may be an interdependent relationship between different microbial species (Bretschger et al., 2015), giving a wider range of applications for mixed strains.

The factors that affect microbial communities, such as the operational conditions and the type of biomass inoculum, have been investigated to enhance biological CH_4 production. Interestingly, it was found that two systems operated under analogous conditions reached similar final consortium compositions despite starting up from inoculums coming from different bioreactors. Additionally, it was also found that the organic load of an AD system can be doubled when integrated with a MEC recirculation loop (Cerrillo et al., 2017a, 2017b).

The bacterial growth and incomplete digestion have a minor effect on the biogas production, as they require about 5% of the carbon present in the substrate, but they may also affect the CH_4:CO_2 ratio. This relationship between the carbon availability, the presence of complex molecules such as lignocellulose to the CH_4:CO_2 ratio leads not only to different biogas productions but to different methane contents, and overall yields. Thus, the CH_4 content has a maximum of about 70% if oils are included, but ranges between 55% to 60% are more likely for typical dairy wastes (Al Seadi et al., 2008).

In the first attempt to understand and work with the inherent variations of yield, the “Maintenance” concept was first introduced during the 1970s, as a mathematical constant to equilibrate the mass balance of bacterial cultures. It was later noticed that this mathematical constant would change for different culture conditions, increasing when those were less favourable for the bacterial population (Bodegom, 2007). Since then, it has become an important microbiology concept as it offered a mathematical explanation of the changes in behaviour seen in the laboratory.

Nevertheless, its quantification is not exempt from debate. It has been suggested that this debate is due to a) the definition of the coefficient includes non-growth components different from maintenance, b) overlapping of different concepts, c) the evolution of variable as constants, d) the neglect of cellular death in the microbial dynamics (Bodegom, 2007).

It has long been known that bacteria use nutrients for both obtaining energy and cell-growth simultaneously, the relative proportions of each function depend as much on the population composition as on the environmental conditions, with a predictable behaviour under steady-state operation of the bioreactor (Taubner et al., 2015). According to the literature review by Lecker and colleagues, between 0.28 and 0.43 % of the H_2 and around 3 % of the carbon dioxide available inside the bioreactor are used to produce new bacterial cells. Nevertheless, there is a specific ratio for each microbial group, which depends, among other factors, on the cellular composition, being the information used to prepare specific culture media. However in the anaerobic digestion context, it would be expected to be within the range of 3–9 % for carbon dioxide (Lecker et al., 2017). This cell composition dependency produces diverse results of different mixed cultures between the methanogenesis ratio and cell growth, as they are formed by bacteria with different nutritional requirements (Lecker et al., 2017).

Methanogens are capable to prioritise energy generation rather than growth when nutrients are limited. This would allow them to survive but also to recover quickly after a period where nutrients were unavailable (Taubner et al., 2015).

2.11 Project Aims

A reliable MEC operation requires knowing how to adapt the operation to respond to external variations and it is particularly relevant to overcome the challenges of matching power generation and demand, which are inherent in energy matrices with high shares of renewable energy generation.

It is known that many factors influence the MEC overall performance, and their individual effect on methane production has been studied (electrodes material, voltage, hydraulic retention time, inoculum, temperature, etc.). Nevertheless, methane production is just a part of the overall energy storage.

In the context of the development of a low emission economy, bridging the gap between mechanism knowledge and operational understanding is crucial to push forward the development of MECs toward industrial deployment as an alternative to renewable energy storage, raising the questions:

1. How sensitive is the MEC performance to the main operational conditions?

2. What effect has the hydraulic retention time and voltage variations over the MECs performance?
3. Could MECs contribute with existing technologies to pivot towards a low emission economy?

This study aims to operationalise the existing knowledge, closing the gaps by linking energy storage efficiency and operational parameters of a MEC. For this, single-chamber MECs were designed, built and used over the different stages of the study, to allow a direct, and reliable comparison of reaction rates, efficiency, and overall performance

This study relies on a laboratory setup that provides empirical data to discuss the influence and interaction of different anode-to-cathode relative surface area, and operational parameters such as hydraulic retention time (HRT), organic load, voltage, and hydrogen injection, over the performance of MECs as a long-term energy-storage solution.

A set of bio-electrochemical cultures systematically organised allows a direct comparison of results, and to identify the most influential factors and interactions that affect the overall performance in the context of energy storage. Additionally, design and operational recommendations derived from the empirical data and the literature review are discussed.

Chapter 3 Materials and methods

3.1 Overview

This chapter introduces the equipment and methods used to perform a set of tests, aiming to provide information regarding the influence of relevant factors, both individually and combined, that have a significant effect on MEC performance. The basic operational unit is an MEC, operated under different bio-electrochemical controlled conditions to produce methane. An overview of the experimental design is given in Table 4.

Table 4: Methodology overview, indicating both the objective and operational conditions compared

	Stage I (Chapter 3)	**Stage II (Chapter 5.1)**	**Stage III (Chapter 5.2)**	**Stage IV (Chapter 6)**
Objective	Prototype design and construction	Sensitivity Analysis	Comparing mechanisms	Performance and operational conditions effect
Operation	Start-up anaerobic digestion	Variation of Organic load and relative electrode surface areas	Effect of Hydrogen and voltage supplements	Variation of Hydraulic residence time and applied voltage

ANOVA tests assess the statistical relevance of the results and the relative effect of each factor in Sections 5.1 and 5.2 of Chapter 5. Chapter 6 relates overall performance and operational conditions, presenting the results as a surface response, or contour plot, as a rule of thumb for operational guidelines and factors' interactions.

By basing the study on laboratory and empirical data, the results are inherently linked to the set of conditions tested, so key performance indicators are established and compared to relevant reported values, so that the results broadly reflect common scenarios. Additionally, operating the systems under a variety of conditions makes it possible to experience first-hand operational issues and how design affects the reliability of the device beyond methanogenesis.

3.2 MECs design and operation

There are two different bioreactors design used in this study, a traditional anaerobic digester and two MECs for the bio-electrochemical essays.

Anaerobic digestion (AD) was carried out in a 20 L HDPE unstirred vessel, fitted with gas and wastewater inlet connections along with biogas and treated water outlets. Wastewater feeding/discharge flow provides the mixing, relying on automatic peristaltic pumps to ensure continuous operation with a 20 days HRT (unless otherwise specified).

MECs consisted of a 1.2 L single-chamber membraneless reactor made of Tritan ™ (1 L working volume and 0.2 L headspace) mixed by the feeding/discharge flow of automatic peristaltic pumps, equipped with the same functional connections as the anaerobic digester for gas and wastewater inlet/outlet (see Figure 8). The MECs also had electrical connections between 3 mm thick carbon felt electrodes without any pre-treatment, and the DC power supply, with titanium collectors, which continuously applied 800 mV to the MECs (unless otherwise specified). The off-gas passes through a condenser to reach the bag (aluminium multilayer bag resistant to 10 kPa) where it is stored and sampled to monitor the volumetric production and composition.

The only difference between the otherwise identical MEC reactors is the size of the anode. The cathodes of both MECs were 8 cm wide x 5 cm high, whereas the anodes were 8 x 10 cm and 8 x 2.5 cm for MECs denoted MEC A and MEC B respectively.

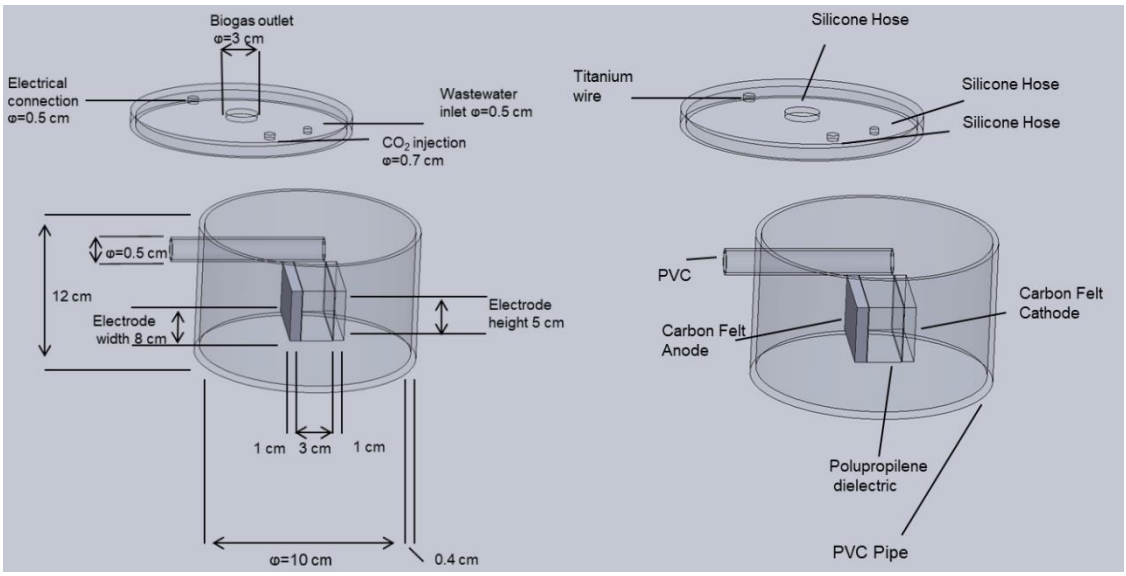

Figure 8: Schematic of the main reactor design, detailing the material and size of the main components

The connection between the electrodes and the power supply depends on how the voltage is imposed. There are two main strategies, A) maintaining the potential difference between both electrodes, in other words, the total cell potential; B) setting the desired potential over one electrode relative to a reference electrode. Strategy B would allow further control of every stage

of the process, enhancing different phenomena at different moments. As suggested by Villano *et al.*, a faster start-up of the organic matter oxidation may be obtained when an anodic potential is applied and hence takes over the bacterial activity, the cathode must then adjust its potential to sustain the current production from the anode (Zeppilli et al., 2016). According to this data, a higher anode potential would lead to the maximum ATP yield (based on the moles of substrate consumed) that a microorganism can produce, which is relevant since the ATP is an essential mediator of the energy metabolism across unicellular and multicellular species (Rajendran et al., 2016).

A total cell potential control (strategy A), on the other hand, does not control the electrode potential, but it makes it possible to determine the energy input. Additionally, the operation is simplified by requiring a simple power supply instead of a potentiostat and, probably more importantly when considering industrial deployment, it can provide a stable voltage to different cells in parallel (Zhang et al., 2019). Therefore, in order to work with a system design more likely to be scaled up and adopted by the industry, the total cell potential strategy has been used.

Thus, the electrodes were directly connected to the power supply, the same carbon felt was used to prepare the electrodes, ensuring the surface areas could be compared. On this basis, the MEC A anodic surface area was approximately 4 times larger than for MEC B, with the total electrode surface area double that of MEC B. To reduce the internal resistance and avoid direct contact between the anode and cathode a layer of Teflon was used in between both carbon felt sheets, forming a sandwich like 3-layer electrode without affecting the active electrode surface as the Teflon is not suitable for bacterial colonisation nor electric conductive.

All bioreactors were operated under the same conditions to allow a direct comparison between AD and MECs. These were operated as a chemostat with feeding and discharge flowrates controlled with automatic peristaltic pumps to achieve an HRT of 20 days (unless otherwise indicated). The temperature was maintained via immersion in a water bath at 35 °C, and the pH was maintained within 6.8-7.2, aligned with the International Energy Agency guidelines (Bachmann, 2015). As a control to assess the effects due to the electrodes only, experiments were also performed under identical conditions in the MECs but without an applied potential (MEC OCP).

Besides checking the applied voltage and measuring the obtained current in the MECs, the operation of all bioreactors was monitored and productivity followed by sampling both the digestate and off-gas. The off-gas composition (CH_4, CO_2, H_2) and volumetric productivity were measured as described in Section 3.3.

3.3 Analytical methods

The biogas volumetric productivity was measured by the volume displacement method as detailed in the literature (Kougias et al., 2017). The biogas composition (in terms of CH_4, CO_2, and H_2) was monitored every 2 days using an infra-red online sensor. The CH_4, CO_2 were monitored via a GA2000 Plus gas Analyzer from Geothecnical Instruments Ltd. (U.K.), whereas the hydrogen used a Sino Hitech HT-XS handheld pump sensor, with a 0.1 ppm resolution.

Liquid samples were taken from a fixed sampling point, filtered through a 0.22 μm syringe filter to monitor the pH and chemical oxygen demand (COD) both at the feeding and digestate stages of each bioreactor. A sewage effluent kit, based on the colorimetric alkaline potassium permanganate oxidation method (Goh and Lim, 2008) was used to monitor the COD as an indicator of the organic matter concentration.

The current produced as a consequence of the reaction was monitored using a UNI-T UT803 multimeter connected in series between the power supply and the cathode immersed in the MEC liquor. To verify the read value, an evaluation of the transient was made by stopping the applied potential at steady-state operation and recording the instantaneous current produced upon reapplying the 800 mV potential.

The different organic loads, assessed in chapter 5, were achieved by decreasing the wastewater strength from 4000 to 200 ppm to the three bioreactors. A new set of operational conditions was established only after obtaining a constant operation for a minimum of 3 HRTs. These results were used to calculate the methane production rate and methane conversion rate (see Section 3.6), comparing them using ANOVA tests.

3.4 Design of experiments

The difference between the bio-electrochemical runs is based on specific operating conditions changes, organised as a Placket-Burman experimental design (Chapter 5) and a complete factorial experimental design (Chapter 6). The operative unit is a 1 L vessel with relevant connections for both inlet and outlet of synthetic wastewater and H_2/biogas, as well as electrical connections for the carbon felt electrodes.

A total cell potential strategy is used for imposing the voltage, so the power supply is directly connected to the electrodes. The positive lead is directly connected to the anode, whereas the negative goes through a multimeter and then to the cathode, providing the required potential control and electrical current reading simultaneously. Such connections allow both an accurate control of total cell potential whilst gathering information to estimate the power input.

Stage I includes both the bacterial acclimation and the design and engineering of an appropriate bio-electrochemical bioreactor MEC A and MEC B. The off-gas volumetric production and

composition (CH_4, CO_2, and H_2) is monitored at the headspace, as well as the energy input (monitored online) and COD removal (initial and final readings), as further described later.

In section 5.1, the effect of relative anode-to-cathode surface ratio and organic load is evaluated, feeding both MEC A and MEC B with synthetic wastewater with strengths varying between 4000 ppm and 200 ppm while maintaining other operational parameters unaltered.

In section 5.2 the relative importance of different mechanisms is evaluated through performing anaerobic digestion where external hydrogen is injected (when appropriate), and the applied voltage is switched on or off (according to the design of experiments). Runs with applied voltage are used as a control to verify the electroactivity of the bacterial community. Operation on open circuit mode (power supply off) provides information regarding the effect of the electrodes' presence as a substrate for bacterial growth. Hydrogen injection will provide information to assess the relative weight of the *hydrogenophilic methanogenesis* within the overall methane production.

Finally, in Chapter 6 the relationship between the performance and the two main energy inputs is studied, modifying according to a complete factorial design the HRT (changing the inflow) and the applied voltage. All the work on these stages is made on the basis of continuous operation of the MEC, and utilising the bacterial community developed during the prototype MECs start up (Chapter 4).

3.5 Inoculum and substrate

In this study, raw cow manure is used as an initial bacterial source, cultured under similar conditions to those to be tested in the MECs to select the most adequate consortium. Mixed strains or consortiums have more complicated dynamics, due to the complex communities, but offer a greater metabolic versatility that translates into a wider range of possible applications (Zhang et al., 2019), which is crucial for electromethanogenesis through CO_2 reduction by microorganisms on the cathode.

The greater metabolic variety aids the development of an appropriate biofilm over the carbon felt to effectively form a biocathode that has all the available metabolic tools needed, which is unlikely to be achieved with a single strain inoculum.

Raw cow manure taken multiple times from different organic farms was used as initial inoculum for the AD system, cultured in the AD digester previously detailed (35°C) and adapted to synthetic wastewater containing (in g L^{-1}): KH_2PO_4, 0.462; K_2HPO_4, 0.143; NH_4Cl, 0.9; NaCl, 0.2; $CaCl.2H_2O$, 0.3; yeast extract, 2; CH_3COONa, 0.2; and 1 mL L^{-1} of trace metals as detailed in appendix I. The inoculum adaptation was carried out in the AD reactor over 3 months and then used to inoculate the MECs. Inoculation of the MECs followed the same procedure as for AD except that a 800 mV potential was applied to enhance bacterial attachment to the electrodes, as has been described in (Zeppilli et al., 2016).

3.6.MEC performance parameters

Three general performance indicators are used in this study, Methane production rate (MPR, $ml_{CH4}\ L^{-1}\ h^{-1}$) works as a reference of how much methane is being produced by the reactor in terms of its physical design and operation, while the methane conversion rate (MCR, $g_{CH4}\ kg^{-1}{}_{COD}$) is the yield relative to the organic matter input. Finally, the energy efficiency allows evaluation of the energy input.

The storage energy efficiency of all three bioreactors is calculated as the ratio between the stored energy – as methane in the biogas – and the total energy input, considering both chemical and electrical as corresponds. The chemical energy input was estimated using the empirical mathematical factor of 16.1 kJ g_{COD}^{-1} (Dai et al., 2019), multiplied by the organic load (in g day^{-1}). The energy contained in the biogas is calculated according to Equation (3.1), where H_{CH4} corresponds to the enthalpy of combustion for methane (890.5 $kJmol^{-1}$) (Hao et al., 2019).

$$\boldsymbol{Energy_{Biogas} = \frac{M_{CH4}\langle g\rangle \cdot - H_{CH4}}{16\,{}^{g}/_{mol}}\,.} \qquad \textbf{(3.1)}$$

The electrical energy consumption was calculated by directly multiplying the imposed voltage (according to design of experiments) by the time it was imposed per day (24 hours) and the obtained current.

Chapter 4 Design of MECs and methanogenic consortium establishment

4.1. Context and hypothesis

The design described in Section 3.2 was developed taking many factors into account such as materials used, size, and specifications of the MEC vessel, diffuser, wires, and biogas bags. This section describes the process of selecting these components as well as assembling and starting-up the MECs operation to test the hypothesis that it is possible to develop an electroactive biofilm on carbon felt electrodes to produce methane.

The design of experiments includes the evaluation of hydrogen injection; this requires a supply of hydrogen on demand. The process of design and evaluation of the operation of a small bench-scale hydrogen generator to supply the required hydrogen is also described.

4.2. Materials and methods

At the process-engineering stage the design of the AD and MECs specifies the volumes and fluxes, however its complete implementation requires many decisions to be made regarding the specific construction. This includes the selection of hose materials and diameter to match the fittings of the chosen pumps subsequent to the design of experimental requirements; this is an example among many other seemingly simple choices that may prove to have downstream consequences.

The final mechanical design of the single chamber bioreactors, without membrane (single chamber), including carbon felt electrodes and a complete cell voltage imposition strategy was defined and calculated before starting the operation. Simultaneously, the AD system was prepared and operative for bioaugmentation, to allow the adaptation of the bacterial consortium to the synthetic wastewater before inoculating the MECs.

All connections of both liquid and pressurised gas use John Guest ™ fittings as they are can manage pressure, gases, liquids and are available in a range of sizes. After assembling and setting up the MECs at the desired location, hydraulic and gas-tightness were evaluated with water and CO_2, ensuring that the systems were operating properly, and no leaks were present. The sealing tests were performed by starting the operation with water and CO_2 injection into the headspace, taking the system to the appropriate HRT and temperature, confirming there was no gas leaking from the headspace nor leaking from the hosing system nor pumps.

The start-up operation was carried out as a feed-batch mode, starting with 100 mL of synthetic wastewater prepared as indicated above in Section 3.5, then 100 mL of inoculum from the AD bioreactor was pumped into each MEC. After 24 h, the feed started with the flow adjusted to

ensure 20 days of HRT (50 mL d^{-1}), although the discharge was delayed until the full 1000 mL working volume was attained, before switching on the imposed potential voltage.

Although hydrogen generation is beyond the scope of this study, the efficiency of hydrogen production at different voltages is of interest when considering an integration of the two technologies. Integration that would allow, for instance, the use of excess solar energy during summer time

The hydrolyser constructed consists of 4 plates for each electrode (refer to Figure 9), each plate made of stainless steel 316 measuring 8 x 12 cm and a copper wire connection to a variable DC power supply. Each set of plates, connected in parallel, formed respectively the anode or cathode contained in a chamber that allows collection of the gases (hydrogen and oxygen) separately, however, these chambers were located inside a single unstirred 8-litre vessel containing the electrolyte (62.5 g L^{-1} of $NaHCO_3$)

Every run started with fresh electrolyte and allowed to run for 5 hours, with sufficient electrolyte to avoid loss of performance due to $NaHCO_3$ exhaustion.

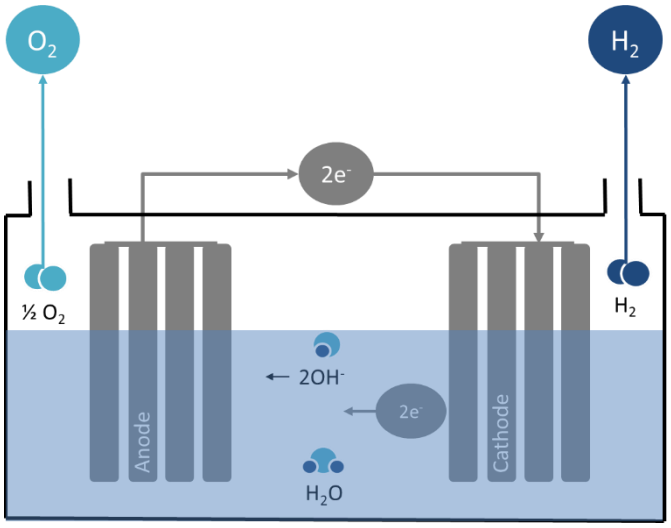

Figure 9: Schematics of the hydrolyser used to produce hydrogen.

4.3. Results and Discussions

In the context of bioprocesses, where the device's performance is based on the use of a biocatalyst (enzymes or living cells) to carry out the desired reactions, the electron transfer between the electrodes and, in this case, the biofilm that colonised them is of paramount importance so choosing a suitable electrode material is essential.

The electrode material is one of the many electrode design features that will impact the development of the future stages of the study. As noted earlier, carbon-based materials are widely used for bioelectrochemical systems due to their electrical conductivity, low cost, light weight, and chemical stability. However, its hydrophobic nature makes it hard to investigate its intrinsic properties, or the essential properties of the material (Huong Le et al., 2017). This is not of particular concern in this study as only one material, carbon felt, was selected for both electrodes. Nevertheless, many methods and techniques have been developed to modify its surface to overcome the poor wettability of such carbon-based materials.

Enhanced wettability of carbon-based electrodes, via either plasma, thermal or chemical treatment, makes it easier for electrolyte ions to access the voids within the 3-D structure. Metallic nanoparticles, graphene, and carbon nanofibers have been used to enhance the conductivity. According to Huong Le *et al.* the best pre-treatment will depend on the purpose of the fabricated electrode (Huong Le et al., 2017).

In the context of this study, which aims to explore inexpensive and commercially viable options, no further modification of the electrodes was investigated. Nevertheless, during the selection process, it was considered that the inherent open 3-D structure of felts with smooth randomly dispersed fibres, allows nutrient and metabolite mass transfer, while offering an ideal substrate for bacterial attachments and colonisation due to the high surface area.

When defining the architecture of the electrodes, adding or subtracting sheets of felts allows the modification of the thickness and overall 3-D architecture, as noted in the literature (Huong Le et al., 2017). This provides indirect control over two important features. Firstly, the available surface to carry out the desired reactions. Although the specific surface area value will vary depending on the method used. There are standard techniques, including physical methods, physical adsorption of gases, structural methods, as well as electrochemical methods for determining this value if necessary. The MECs design in this study uses the same carbon felt for both electrodes, hence, the relative surface area is directly proportional to the ratio between the external dimensions of the sheets, so detailed measurement of the available surface area was not necessary.

The second important architectural feature is due to the fluids flowing through felts following Darcy's law describing the velocity of a fluid flowing via a volume unit of a porous medium per unit of differential pressure (Huong Le et al., 2017). Hence, by modifying the architecture, and depending on the porosity of the felt, the flow of a fluid can be improved by allowing a better

mass transfer through the electrode structure, thus avoiding an inhibitory concentration of metabolites.

At the initial start-up operation of the bioreactors, the MECs included overflow as discharge, but it was observed that it would drag some gas, making harder to ensure the seal. To avoid these issues, commercially available airtight containers were used as vessels for the bioreactors, with all the inlets and outlets located in the lid, which makes necessary another peristaltic pump for controlling the discharge and maintain the volume constant. This avoids water tightness issues and ensured the John Guest ™ fitting was located in a flat area for maintaining the airtightness, as depicted in Figure 10

Once the MECs airtightness was proven, and all the supplementary services were operating adequately (CO_2 and H_2 injection, charge and discharge, temperature control, off-gas quantification), the cells were inoculated. As described in section 3.5, the bacterial consortium present in the MECs comes originally from a composite sample of raw manure acclimated in a AD. This was expected to provide a wide microbial diversity that would translate into a more flexible inoculum.

A diverse consortium translates into a robust operation, as it would self-optimise for the operational conditions offered. A similar strategy has been reported in the literature, successfully achieving up to 97% of methane content. According to their microbiological analysis, the most abundant microbes were uncultured and not available in public databases (Kougias et al., 2017), this highlights that a diverse population in the inoculum enables the development of unusual communities suited to the environmental conditions.

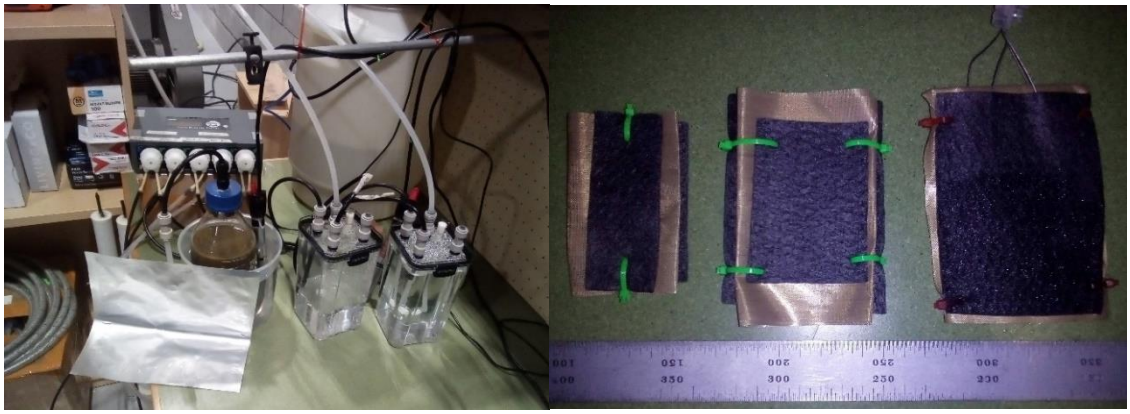

Figure 10: Left, Picture of the MECs during hydraulic and airtightness tests, before installing the electrodes. Right, electrode assembly.

The starting up operation was initiated three times, with the whole system cleaned and sanitized by rinsing for 30 min with a solution of sodium percarbonate (5g L^{-1}) between each attempt, as the medium would become cloudy approximately 30 hrs after inoculation. The excessively fast-

growing speed, pungent odour, and thick yellow biofilm were unexpected, as methanogenic consortia tend to display slow metabolisms. As a molecular biology study of the consortium diversity was out of scope, but having an active methanogenic culture is essential for carrying on with the design of experiments, samples from the biofilm and planktonic cell were examined in the microbiology laboratory (in the biosafety chamber).

The observation of samples under the microscope confirmed the growth speed and provided morphological insights that suggested a dominance of coliforms rather than the microorganisms directly involved in methanogenesis. Although no specific confirmation test was performed, the sample proved to be gram negative, the morphological and size description and gas (not methane) production under anaerobic conditions suggests the coliforms dominance.

The presence of microorganisms different from those found in the inoculum (digestate from the AD bioreactor) suggested that another source of bacterial diversity (inoculum) was being unintentionally introduced, which could have come from the water used for the synthetic wastewater preparation, or most likely from any contaminated reagents. Therefore, and despite this problem had not been indicated in the literature protocol (Moreno et al., 2016), the synthetic wastewater was autoclaved under standard conditions of 121 °C for 15 minutes before the start-up operation, ensuring that the developed consortium came only from the raw manure used as inoculum.

The MECs were operated from the beginning with a wastewater strength of 4000 ppm COD, 20 days HRT, 35 °C and 800 mV applied potential. The selection of the operating conditions was based on typical values reported in the literature (T. Al Seadi et al. 2008; Villano et al., 2010), achieving an steady MPR of about 6-7 mL_{CH4} L^{-1} h^{-1}, requiring approximately 30 days of steady, continuous operation. Although the timeframe required for establishing the culture is hard to predict, some works highlight the labour-intensive and uncertain nature of this task (Zhen et al., 2015) while others mention the need for up to 8 months to achieve the maximum methane content (Angelidaki et al., 2018). In comparison, the 30 days needed by the MECs seems short, but these MECs were inoculated from the AD, where 3 months of previous adaptation of the raw manure had already taken place.

After re-starting the MECs operation with sterilised fresh medium, and having disinfected the bioreactors with ethanol 70% and UV radiation in the microbiology laboratory, the cells started the biogas production. The methane content in the off-gas was initially low, translating in the fact that the methane production rate of both MEC A and MEC B during the starting-up operation was initially slow, and built up as shown in Figure 11,

As shown in Table 5, the steady operation of both MECs reached a steady performance in terms of MPR, a performance level that would be recovered after altering the operational conditions. Therefore, an MPR of 6.0 and 6.4 ml_{CH4} L^{-1} h^{-1} was considered as the baseline for MEC A and

MEC B respectively. To compare these results to previous studies, the MPR of selected studies was estimated (Appendix D), revealing a wide range between 0.0014 ml_{CH4} L^{-1} h^{-1} (Hara et al., 2013), and 340 ml_{CH4} L^{-1} h^{-1} (Zeppilli et al., 2019), which does not provide a clear reference. However, there are reports of a MPR within the same range between 5-7 ml_{CH4} L^{-1} h^{-1} using organic loads close to 1000 mg_{COD} $L_{reactor}^{-1}$ day^{-1} (Hou et al., 2015; Rader and Logan, 2010; Sangeetha et al., 2016), these are higher than the 200 mg_{COD} $L_{reactor}^{-1}$ day^{-1} used here.

Surprisingly, the MECs' performance was comparable to the performance of AD bioreactor. When operated under similar conditions, AD achieved an MPR 7 ±1.5 ml_{CH4} L^{-1} h^{-1}, and the MCR of all three bioreactors was calculated in 0.5±0.1, 0.47±0.11, 0.5±0.15 g_{CH4} kg_{COD}^{-1} for AD, MEC A, and MEC B respectively. The low MCR and similar performance between the three systems suggests that the biogas production was metabolically limited, as the high wastewater strength of 4000 ppm would supply a sufficient source of carbon to satisfy the consortium requirements. Nevertheless, a significantly higher performance in terms of MCR is expected from MECs under carbon scarcity conditions due to the preferential carbon usage on the energy related metabolism against cellular growth (Taubner et al., 2015).

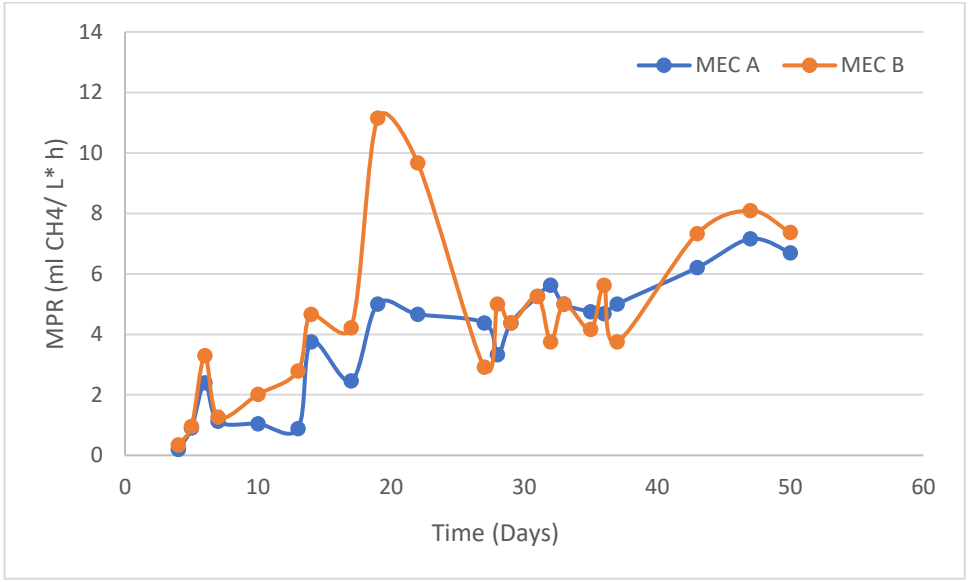

Figure 11 MPR (in ml_{CH4} L^{-1} h^{-1}) during start-up of MEC A and MEC B

Having established a baseline reference, verification of the reliability of operation was needed to make sure that the performance changes obtained during the controlled bio-electrochemical test corresponded to the operational conditions tested, and not to another disturbance of the microbial consortium. To disturb the system performance, the voltage application was turned off (maintaining the electrodes in place) for 4 days (affecting the MPR). After restoring the voltage,

and maintaining all other operating parameters constant, the baseline was recovered in approximately 6 days, as seen in Table 5.

Table 5: Methane production (in ml_{CH4} L^{-1} h^{-1}) rate of MECs during start-up operation.

	Day	43	47	50	55	61	65	74	76	78
	MEC A	6.2	7.2	6.7	7.5	6.3	3.7	6.2	6.4	6.3
MPR	MEC B	7.3	8.1	7.4	7.5	6.3	2.4	6.8	7.1	7.2
Operation		Baseline					No Voltage	Baseline		

Parallel to the performance reference -baseline- operation, a hydrogen generator was designed and engineered. The design of experiments includes the injection of hydrogen, which needs to be self-supplied and produced on demand. The hydrogen requirement comes from the intention to recruit two different metabolic pathways simultaneously. There are two main metabolic routes that lead to methane production, *acetoclastic methanogenesis* that uses the organic matter present in the wastewater as raw material, and the *hydrogenophilic methanogenesis* that starts from hydrogen and carbon dioxide produced by the fermentative bacteria in the initial stages of the anaerobic digestion process (Burkhardt and Busch, 2013).

The bacterial-based phenomenon of the technology supposes an inherent rate limitation that can be mitigated by enhancing simultaneous operation of as many metabolic paths as possible, which translates into searching approaches to promote *hydrogenophilic methanogenesis*. The off-gas produced here has a content of about 50% carbon dioxide but barely 30 ppm of hydrogen; this suggests that the hydrogen availability is likely to limit the achievable methane production, as predicted in the literature (Lecker et al., 2017).

Thus, injection of externally produced hydrogen seems a reasonable solution and implies the need to produce hydrogen *in situ* or to obtain it from an external source. Therefore, a hydrolyser based on Figure 9 was designed and engineered to self-source hydrogen for the hydrogen injection tests considered in the design of experiments detailed in Chapter 5.

The relationship between current and the hydrogen production rate (HPR) of the simple apparatus engineered is necessary for its operation, and on demand hydrogen production, thus, facilitating the possibility of *in-situ* integration between this technology and the MEC at bench scale. As seen in Figure 12, the current obtained increases proportionally to the increment of the applied voltage – and thus the energy used however, the hydrogen production rate (HPR, in L h^{-1}) decreases significantly within the evaluated range of 3 to 10 volts. The ratio between these two indicators is considered as efficiency, and shows clearly that, with between 3 to 5 volts applied, the efficiency slope is significantly steeper than between 5 to 10 volts. It can only be theorised here

that a mass transport limitation plays a significant role in this, and is not due to $NaHCO_3$ consumption as the hydrogen production could have continued after stopping the experiments, which confirms that availability of $NaHCO_3^-$

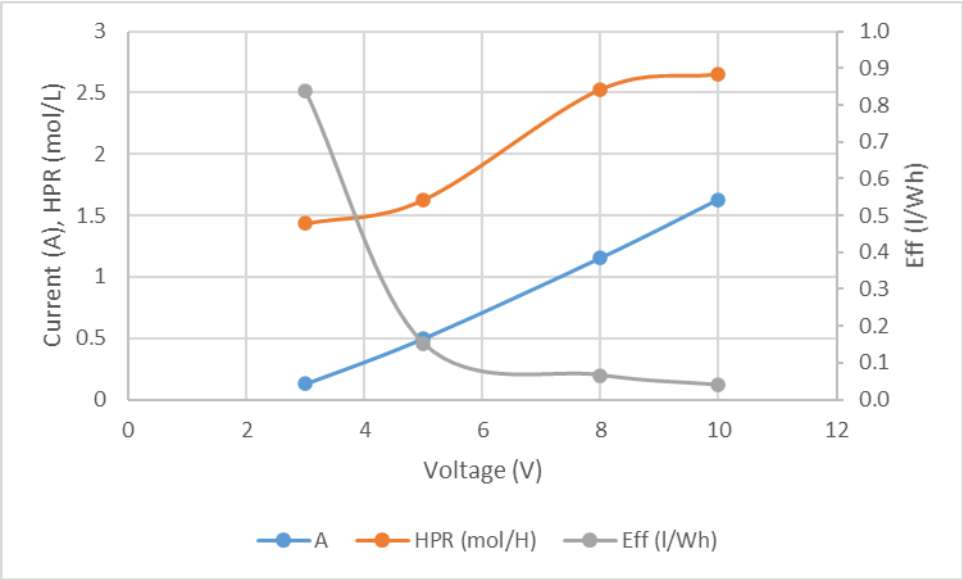

Figure 12: Hydrogen production in a hydrolyser to provide hydrogen for injection in MECs.

The efficiency is calculated as the inverse of the energy required to produce 1 L of hydrogen, the power consumption is obtained multiplying the voltage applied and the current obtained for each case, whereas the time necessary for producing 1 L of hydrogen at atmospheric pressure is estimated from the HPR.

4.4. Conclusions

A stable and reliable gas production was achieved for both the methane and hydrogen systems; hence, the systems were considered appropriate for proceeding with the design of experiments. The methane production achieved was considered as the baseline for the bioreactors, and used as reference for the assessment of the effect of operational conditions modifications, as will be described later in Chapter 5 and 6.

Chapter 5 Main factors effect on MEC performance

5.1 Context and hypothesis

Wastes are beginning to be considered as resources, such as in the case of typical domestic wastewater with an estimated chemical energy content of 6.3 kJ L^{-1} (Guo et al., 2015; Heidrich et al., 2010). This energy can be reclaimed to produce synthetic fuels that can act as long-term energy-storage vectors (Dou et al., 2018).

It has been proposed that synthetic fuels can be prepared from wastewater streams in MECs. MECs are a type of bioreactor first reported in 2005 to produce hydrogen from acetate and other dissolved organic matter in wastewater (Liu et al., 2005; Rozendal et al., 2006). Over time a thorough knowledge in the context of hydrogen generation has been built up regarding how the gas volumetric efficiency is affected by the influent composition (Kerroum et al., 2014), the arrangement of the electrodes (Gil-Carrera et al., 2011), the hydraulic retention time and organic load (Garcia-Pena, 2015), However, less is known about the role of these in methane generation.

When methane production is targeted, the influent carbon is simultaneously used for cellular growth and as a carbon feedstock for the electromethanogenic production of methane, with the relative proportion depending on the consortium present and environmental conditions (Taubner et al., 2015). Under nutrient deficit conditions methanogenic bacteria prioritise survival metabolism rather than cellular growth (Taubner et al., 2015), leading to a reduction in the methane production rate (MPR) which measures the methane production of the bioreactor, and an increment in the methane conversion rate (MCR) which indicates the yield with respect to the organic matter input.

Although the microbiology dynamics and molecular pathways involved in methane production have been thoroughly studied (Cerrillo et al., 2017; Hara et al., 2013; Jang et al., 2015; Siegert et al., 2014b; Urrutia et al., 1997; Xu et al., 2015; Zhen et al., 2016), how the organic load affects the MEC performance has not been paid the same attention. Shen *et al*. evaluated the organic load effect focused, on the optimisation of the treatment of hydrothermal liquified wastewater rather than in methane production as potential energy recovery (Shen et al., 2017).

The electrode material and design play an important role in the overall performance and the underlying mechanism of MECs. The three major design characteristics recommended in the literature are a large surface area of electrode per volume of bioreactor (Rader and Logan, 2010), a reduced distance between the electrodes due to the poor conductivity of the wastewater (Escapa et al., 2012), and good porosity to facilitate bacterial colonisation and nutrient transport through the matrix to maximise volumetric efficiency (Gil-Carrera et al., 2011).

It has been also been found that increased electrode surface area will improve energy efficiency (Sangeetha et al., 2016). In an investigation of MECs for hydrogen production, it was identified that electrodes that occupy a larger volume favour the formation of methane as a by-product (Gil-Carrera et al., 2011) although the effect of the relative size of the electrodes to each other was not considered.

There have been reports that suggest that the relative surface area of the electrodes should be configured to favour the rate-limiting reaction (Li et al., 2016; Sasaki et al., 2013). This raises the question of whether it would be best to favour the anodic or cathodic half-reaction when methane is targeted, and whether this strategy is affected by the availability of nutrients which changes the relative priority of cell growth and energy generation by the microbial consortium. Hitherto it remains unresolved how the relative electrode surface area (anode to cathode), and the organic load affect the performance of MECs designed for methane production for energy storage.

Furthermore, and despite the development of the field knowledge previously mentioned, the key limitations of the biogas production are the low yield when treating diluted streams or complex organics (Schildhauer, T.; Biollas, 2016; Villano et al., 2016) and the lack of control to avoid methanogen inhibition due to volatile fatty acid accumulation (Zhen et al., 2016); these factors translate into a low methane content in the final biogas.

A typical biogas plant, purely based on biological reactions produces an off-gas with a common content of CH_4 between 50-70%, 30-50% of CO_2, and some minor amounts of hydrogen sulphide (H_2S) (Voelklein et al., 2019). Even though this biogas is flammable, in order to be considered exchangeable with natural gas (from fossil origin), the current legal requirements usually imply a two stages improvement process. The first is cleaning, where H_2S is removed before the upgrading stage, which aims to enhance the calorific value; the effective requirement is a methane content over 96% (Persson et al., 2006).

The raw biogas methane content can be increased by upgrading either via CO_2 transformation into methane or, more commonly, achieved via CO_2 scrubbing (Angelidaki et al., 2018). More than 280 upgrading plants were connected to anaerobic digesters as in 2012, achieving the clean and upgraded biogas – called bio-methane- via processes based on membrane filtration or cryogenic separation, which are technically viable but questionable due to the inherently high energy costs (Kougias et al., 2017).

The transformation of CO_2 into methane can be approached by separating the biogas generation into a two-stage operation. Separating the initial hydrolysis stage of the influent from the final methanogenic stage allows optimisation of each operation separately. A two-stage process would be expected to perform at a higher overall rate, translating into reduced HRT, operational costs, and energy yield (Premier et al., 2011). On the other hand, this option implies a significant up-

front cost increase, requiring a setup and operation different from those used in this study, therefore it is not considered further.

Another approach is the MEC-AD integration. This integration implies the application of MEC principles to AD, which accelerates substrate degradation (including recalcitrant and complex compounds), avoids methanogenic inhibition by improving volatile fatty acid degradation (Yu et al., 2018), shortens the hydraulic retention time (Li et al., 2016), and increases biogas production because of the exoelectrogen and methanogen enrichment of the microbial community (Yu et al., 2018).

MECs appear then as an interesting platform to produce biogas, but also for biogas upgrading through enhancing the hydrogenotrophic methanogenesis, using externally produced hydrogen. This means it could be nicely integrated to store surplus energy beyond the MEC's direct capacity, as water hydrolysis is considered an environmentally friendly technology to use the excess renewable energy produced during peak generation events (Gondal, 2019), generating hydrogen that can be utilised in a MEC to produce methane.

By using an external source of hydrogen, it would be possible to maximise the contribution of the called indirect extracellular electron transfer (EET) mechanism. The indirect EET is a two-step mechanism that requires intermediate hydrogen production following equation 5.1. Whether a biological or purely chemical process is involved in the hydrogen production is not relevant (Cheng et al., 2009).

$$2H^+ + 2e^- \rightarrow H_2 : E_{CAT} = -0.41\ V\ (vs.\ SHE) \qquad (5.1)$$

The second step follows the reaction given below in equatioin 5.1, where methane is obtained

$$CO_2 + 4H_2 \rightarrow CH_4 + 2H_2O \qquad (5.2)$$

In the literature two main strategies for biogas upgrading are highlighted, and a third that results from the combination of them (Kougias et al., 2017), as in Figure 13.

a) *In-situ* biogas upgrading implies the injection of hydrogen directly into the biogas-producing bioreactor. Therefore, it is inherently coupled to the CO_2 produced within the reactor
b) *Ex-situ* biogas upgrading relies on the hydrogenotrophic methanogenic capacity of the consortium, injecting a balanced amount of hydrogen and CO_2 from external sources, as biogas from a different bioreactor.
c) Hybrid biogas upgrading results from combining both strategies.

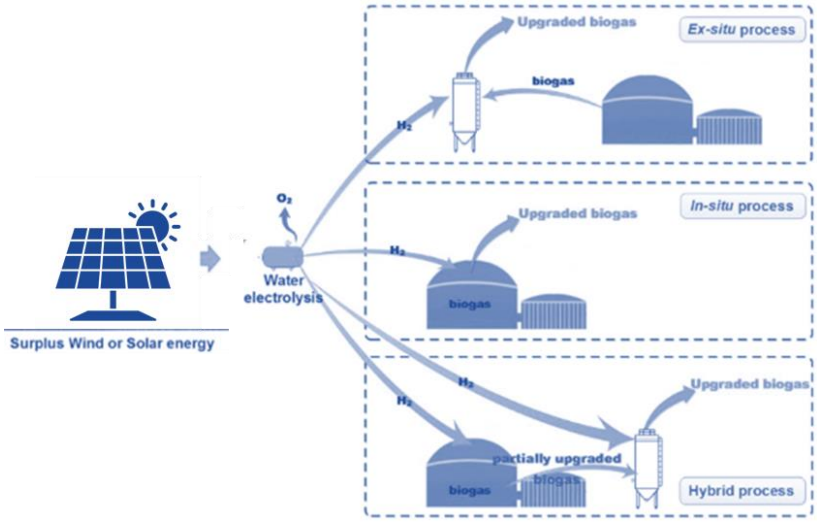

Figure 13: Biogas upgrading strategies, based on hydrogen methanation, modified from (Angelidaki et al., 2018)

Overall, MEC-AD integration has proven to consistently have a higher methane production rate than AD alone. Although, regardless of the underlying molecular mechanism, the effect of applying a voltage has been considered minor compared to the presence of the electrodes by some authors (Gil-Carrera et al., 2011). This statement seems to question the very fundamental difference between a traditional AD system and a MEC, notwithstanding, the effect of the applied voltage and the mere presence of the electrodes tend to be confused as they occur simultaneously.

The logic of the Gil-Carrera *et al.* statement regarding the rather insignificant role of the applied voltage relies on the development of a mature biofilm over the electrodes that works as a substrate. This phenomenon is known, and highlighted as a source of the robustness of bioelectrochemical systems due to what is called the hybrid consortium (Dou et al., 2018), as the main reaction vessel accounts with both planktonic and attached bacterial cells.

Nevertheless, as biofilms develop naturally over a wide variety of substrates and surfaces, the colonisation of electrodes is a matter of concern for many applications. In this sense, as has been discussed in Section 2.5, both the design of the electrodes in terms of material and architecture (Guo et al., 2015; Moreno et al., 2018) and a particular voltage during start-up operation (Villano et al., 2011) have been addressed in the literature to ensure colonisation occurs.

In a traditional AD system, the formation of biofilm can also be encouraged by including some surface to help developing a biofilm, but no voltage can be applied to modulate the occurrence of different underlying molecular pathways. In this sense, and following the logic of the *in-situ* biogas upgrading, biogas *in-situ* recycling could work as a secondary CO_2 source, enhancing the hydrogenotrophic methanogenesis.

All these options suppose that there are significant differences between the operational conditions and even in the process flowchart of an eventual industrial operation. To fulfil the goal of this study to operationalise the knowledge of methane electrosynthesis, it is necessary to assess the effects of the main factors on the MEC's performance.

Therefore, this chapter aims to evaluate the individual and combined effects of selected factors not commonly considered in the literature. The joint evaluation of hydrogen injection and applied voltage allows surveying the contribution of the electrode's presence, emulating an *in-situ* biogas upgrading operation.

The influence of organic load on the performance of two MECs with different relative electrode surface areas (A:C) is also evaluated, to identify whether this design feature plays a role in the final performance. Additionally, two different strategies of biogas recycling, including the variations of continuous and intermittent *in situ* biogas recycling as secondary CO_2 source are performed in a traditional AD system and compared to the MECs results. The performance evaluation is based on the same information and analysis as the rest of the study, focusing primarily on the MPR, and MCR.

5.2. Materials and methods

To determine whether applying a voltage has the same effect when the electrodes are not of the same size, two MECs with different anode-to-cathode ratio (A:C) are used in a full factorial design of experiments with 3 factors (hydrogen injection, electrodes size and voltage applied), considering 2 extreme levels of each factor to determine whether is there an effect, rather than to look for a predictive model.

The voltage applied for each run and the specific conditions modified are detailed below in Table 6 that, summarises the operational conditions of each run for this stage. When hydrogen is injected, the stoichiometric ratio shown in (Equation (2.4))??? is used to calculate the amount of hydrogen necessary, following an *in-situ* strategy, hence using the amount of CO_2 in the off-gas as base of calculation.

Table 6 Design of experiments, indicating whether hydrogen is injected, relative electrode surface area, and voltage applied (800mV or Open Circuit Potential)

Hydrogen	COD mgL^{-1}	A:C area ratio	Voltage mV
No	200	0.5	800
No	200	2	800
Yes	200	0.5	800
Yes	200	2	800
No	200	0.5	OCP
No	200	2	OCP
Yes	200	0.5	OCP
Yes	200	2	OCP

In the MECs, 800 mV was applied after the addition of the inoculum to enhance the bacterial attachment to the electrodes as has been proposed elsewhere (Zeppilli et al., 2016). Unless explicitly mentioned, all tests were carried on under similar operational conditions of 20 days of HRT, 35°C, and 800 mV for the MECs. Figure 14 depicts the set-up used for the tests that need gas injection into a bioreactor. A peristaltic pump and a 3 mm internal diameter hose were used to inject and diffuse the gases into the digestate.

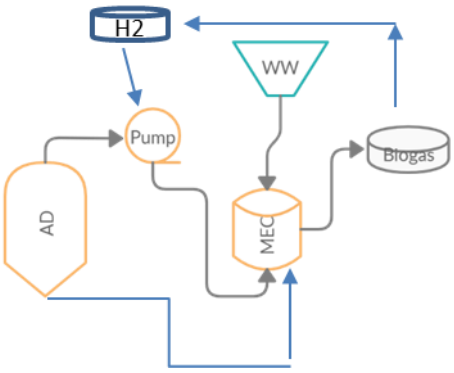

Figure 14: Schematic diagram of the functional connection for In-situ biogas upgrading for AD-MEC integration. All connections previously detailed are omitted here for simplification of the diagram.

The same MECs with different relative electrode sizes were operated with two extreme organic loads, to evaluate the effect on the overall performance (see Table 7). The different organic loads assessed were achieved by decreasing the wastewater strength from 4000 to 200 ppm sequentially to the three bioreactors (AD, MEC A and MEC B). Changes to the organic loads were achieved while maintaining a constant flowrate (to maintain a constant HRT) by modifying the amount of yeast extract to produce synthetic wastewater with low (200 ppm COD) and high strengths (4000 ppm of COD), providing organic loads of 10 mg_{COD} $L_{reactor}^{-1}$ day^{-1} and 200 mg_{COD} $L_{reactor}^{-1}$ day^{-1} respectively.

A new set of operational conditions was established only after obtaining a steady operation for a minimum of 3 HRTs. These results were later used to calculate the methane production rate and methane conversion rate, and compared via ANOVA tests. Both MEC A and MEC B have a different anode-to-cathode area, and the operational conditions are kept as indicated earlier unless otherwise mentioned.

Table 7: Design of experiments indicating the voltage and wastewater strength for each run.

Reactor	A:C	Voltage (mV)	COD (ppm)
AD	-	0	4000
MEC A	2	800	4000
MEC B	0.5	800	4000
AD	-	0	200
MEC A	2	800	200
MEC B	0.5	800	200

Additionally, two different strategies of *in-situ* biogas recycling were evaluated in the AD bioreactor, and compared to results obtained with MECs under similar conditions. The design of experiments summarised in Table 8 was performed in the same AD system described in Section 5.3. The analytical methods and key performance indicators used also correspond to those used across the study.

Table 8: Summary of the design of experiment for in-situ biogas upgrading strategies, describing factors and level evaluated.

Factor	**Levels**	
Re-circulation	Intermittent	Continuous
Wastewater strength (ppm)	200	4000

The synthetic wastewater strength was changed between 4000 ppm and 200 ppm adjusting the yeast extract content, according to the methodology described above. For the different recirculation strategies, the biogas was collected for one day before starting the continuous re-injection of it into the AD. When intermittent injection is assessed, the biogas injection only lasts 1 day to repeat the cycle again, whereas the continuous re-circulation implies the collection of gas for one day and then recirculation at a constant rate of 4L h^{-1}, maintaining the gas receiver at a constant volume to determine the daily volumetric production.

5.3. Results and Discussions

The average biogas composition, MPR, and MCR for each set of operating conditions are given below in Table 9. These values were obtained after three sets of 3-HRT periods had passed and the steady-state operation had been attained. Firstly, it is worth comparing the performance of AD with MECs that had no applied potential (MEC-OCP). There is no significant difference (p-value>0.05) in MPR or MCR for either of these two setups although the biogas volume is reduced for the MECs relative to AD. This indicates that the mere presence of the electrodes does not significantly affect the performance of these reactors with regard to methane production and that the differences between AD and MEC performance can be primarily ascribed to the applied potential.

Across the MECs and AD, it is evident that higher wastewater strength increases significantly (p-value,0.05) the volumetric biogas production (mL_{biogas} L^{-1} d^{-1}). This increase in biogas is accompanied by a reduction in the methane content with increased hydrogen and carbon dioxide concentrations.

The MPR is a measure of the average rate of methane production normalised to the working volume of the reactor. Table 9 demonstrates that the MPR increases with increasing organic load across the three systems. MPR increased for AD, MEC A, and MEC B by 263%, 207%, and 240% respectively between these conditions, if MEC-OCP is used as a baseline for MECs. That the MPR increases with organic load is not surprising given the greater availability of carbon, although it is clear the MPR did not increase proportionally to the factor of 20 increased in the organic load (see Appendix for statistical analysis)

Under the low organic load conditions, the MPR increased in the order AD < MEC A < MEC B. This was altered under the high organic load conditions with the MPR increasing in the order MEC A < MEC B < AD. MEC B outperforms MEC A based on MPR under both conditions, however, AD appears to maintain a better MPR performance relative to the MECs under high organic load.

The MCR is a measure of the amount of methane produced relative to the organic load. In contrast to the MPR results, the MCR results decrease as the organic load is increased with the MCR values across all three conditions being an order of magnitude greater under low organic load. The MCR for MEC B is greater than for AD and MEC A at low organic loads, with no significant difference between the MECs and AD at high organic loads. These results highlight that the conversion of organic matter appears to be rate-limiting at higher organic loads regardless of whether AD or MEC conditions are employed. The effect of organic load on MPR and MCR was found to be significant at the 5% level of confidence across all 3 conditions (see Appendix B) whereas the differences between the MECs in terms of MCR and MPR were only statistically significant at low organic loads (Appendix A).

The literature recognises a positive effect of supporting material for biofilm development over the methane production and degradation efficiency (Sasaki et al., 2013), however, here both performance indicators (MPR and MCR) of the MEC-OCP controls are almost identical to those from AD, therefore, the difference in performance can be attributed to the application of voltage, and not to the presence of electrodes.

From the MPR reported is possible to note that the CH_4: CO_2 ratio does not directly respond to the stoichiometry previously explained, but the carbon mass balance is satisfied when estimating the total amount of carbon input and output, considering both the off gas and digestate carbon content, and between 1-3% of carbon usage for cellular growth. This apparent inconsistency is probably the consequence of a series of reactions that occurs after biogas production. Where the formed biogas is liberated to the reactor headspace, then the CO_2 would be preferably re-dissolved into the digestate (Krich et al., 2005), as CO_2 is about 400 times more soluble in water than CH_4. Consequently, the biogas becomes a secondary source of CO_2 for alternative methanogenic pathways. This is particularly relevant for MECs when voltage is applied, as the methanation of

hydrogen and carbon dioxide is favoured (Villano et al., 2010). Therefore, the off-gas composition is not an indication of the methanogenesis stoichiometry as the digestate acts as a CO_2 sink, altering the CO_2: CH_4 ratio.

Table 9: Average gas composition (CH_4, CO_2, H_2), and performance indicators for both low (200 ppm) and high (4000 ppm) strength.

Bioreactor	Wastewater Strength	Voltage	CH_4		CO_2		Biogas		MPR		MCR		H_2	
	mg COD L-1	Volt	%		%		ml L^{-1} Day^{-1}		ml_{CH4} L^{-1} h^{-1}		g_{CH4} g^{-1} $_{COD}$		ppm	
AD	200	No Electrodes	57%	±8	42%	±8	107	±54	3	0.68	3.1	±1	154	±47
	4000	No Electrodes	47%	±4	50%	±5	371	±71	7	±1.51	0.5	±0.1	228	±94
MEC A	200	OCP	38%	±3	60%	±9	125	±44	2	0.24	3.1	±0.3	18	±33
	200	800	52%	±8	43%	±8	228	±5.4	5	±0.3	7.7	±0.5	66	±2
	4000	800	42%	±6	55%	±7	337	±53	6	±1.46	0.5	±0.1	162	±50
MEC B	200	OCP	37%	±14	60%	±14	123	±69	2	0.96	3.0	±1.5	18	±2
	200	800	59%	±6	48%	±6	245	±5.1	6	±0.2	8.8	±0.4	42	±1
	4000	800	42%	±9	54%	±8	358	±82	6	±1.93	0.5	±0.1	182	±25

To calculate the energy-storing efficiency, as the bioreactors are then considered as a black box and the total energy content of the wastewater is compared to the energy content of the final off-gas (from the methane content), regardless of the different mechanisms that may occur in each bioreactor.

5.3.1 Organic load effect

It is evident from the results in Table 9 that increasing the organic load leads to an increase in methane production, however, the proportion of the organic load converted into methane drops substantially. This effect was more notable for the MECs compared to AD.

To explain these trends in reactivity, it is important to consider the underlying mechanism of these processes. The methanogenic stage has been suggested as the bottleneck for both AD and MECs (Zeppilli et al., 2016). This limits the overall performance as the bacteria are not capable of metabolising CO_2 and H_2 at the same rate as they are produced. As acidogenic bacteria have faster metabolisms than methanogens (T. Al Seadi et al. 2008), the fatty acids and CO_2 produced by these bacteria are not metabolised by the methanogenic consortium and released into the final biogas. While some reports highlight hydrogen limitations (Zhen et al., 2015), here it appears that under high organic load conditions methane production is metabolically rate-limiting. This indicates that the *acetoclastic methanogenesis* and/or *hydrogenophilic methanogenesis* pathways are not sufficiently efficient under these conditions.

Further evidence for the enhanced activity of acidogenic bacteria can be observed from the consumption of alkali required to maintain the pH of the solution. These results are shown in Table 10. There was also a positive correlation between alkali consumption and organic load as well as a significant difference between AD and MECs. This trend parallels that of hydrogen

production in these systems and is further evidence of the dominant role of acidogenic bacteria over methanogens in the presence of an excess of nutrients.

When feeding with wastewater strength as at 4000 ppm, AD performance was similar to MECs, with a high volumetric productivity and low %CH_4. The MPR of all systems (see Figure 20) fell when lowering the strength to 200 ppm, although the conversion of COD to methane became more efficient, as indicated by the MCR improvement.

In terms of MCR (g_{CH4}/kg_{COD}), MECs are similar to AD when COD is high, which suggests bacterial activity limitations. The higher COD may favour acidogenesis, accumulating volatile fatty acids, and more CO_2. Evidence for this can be observed by the high alkali consumption under the high organic load condition. The greater alkali consumption with a high wastewater strength can be noticed in the traditional anaerobic digester (AD) going from 1.5 to just 5.27 $mL_{1M\ NaOH}\ L^{-1}\ d^{-1}$(71% more), whereas MECs rose from 2.14 to 6.4 $mL_{1M\ NaOH}\ L^{-1}\ d^{-1}$(66% more), also explaining the increased gas production and lower CH_4 content.

The ratio of carbon usage for methanogenesis and cellular growth is dependent on the availability of nutrients, an effect referred to as 'uncoupling'(Lecker et al., 2017). This allows methanogens to change the proportion of carbon flux used to produce energy compared to cellular growth based on the organic load. This uncoupling effect can be observed here with relatively larger proportional production of methane under restricted organic load conditions which is consistent with energy production being metabolically favoured (Taubner et al., 2015).

In terms of MPR, AD seems to benefit more than MEC from the phenomenon described above. However, MCR improvement of MECs is double that from AD, and therefore, the effect over the MPR is partly hidden by the fact that MECs (applying 800mV) are already operating closer to the rate limitation imposed by the methanogenic consortium.

MECs are expected to show greater resilience to organic load changes as they form a hybrid consortium, including both planktonic bacteria and the biofilm attached to the electrodes. This has been shown to provide a greater capacity to withstand shock organic loads (Dou et al., 2018) although in this study the feed was steady and continuous rather than having high/low strength shocks. When the wastewater strength was lowered from 4000 ppm to 200 ppm the MPR drop was larger for the AD reactor compared with the effect on the MECs. This suggests that the MECs are more resilient to changes in organic load. MEC B which contains the larger relative cathodic surface area provides the greatest resilience to these changes.

Table 10: Average alkali consumption (mL L^{-1} d^{-1}) for each bioreactor, at low (200 ppm) and high strengths (4000 ppm).

Alkali consumption (mL L^{-1} day^{-1})

Strength	AD		MEC A		MEC B	
200 ppm	1.51	±0.03	2.15	±0.13	2.15	±0.24
4000 ppm	5.23	±0.11	6.37	±0.39	6.59	±0.66

5.3.2 Effect of the relative size of electrodes

It has been proposed that applying a low voltage would enhance the methanogenic activity (Cheng et al., 2009; Moreno et al., 2016; Villano et al., 2011), however, it is not clear whether this voltage has the same effect when the electrodes are not of the same size. Figure 15 compares the MCR and MPR values across a series of bio-electrochemical tests where 800 mV or no voltage (OCP) were applied to MECs with different relative electrode sizes. Given the anode size difference between both MECs, Figure 15-B shows the normalised MPR and MCR to the total electrode surface area for both MEC conditions to evaluate any effect of surface area on performance.

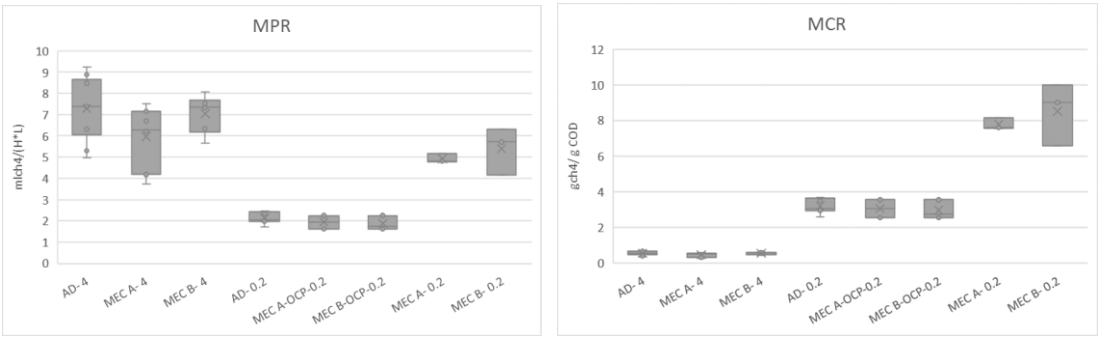

(A)

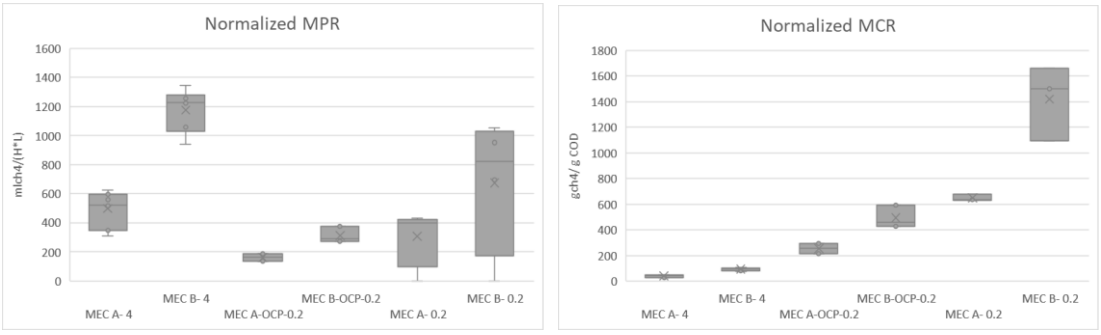

(B)

Figure 15: A) Methane production rate (MPR) and methane conversion rate (MCR) in mL_{CH4} $L_{reactor}^{-1}h^{-1}$ and g_{CH4} kg_{COD}^{-1} respectively. B) The normalized (by total electrode area) methane production rate and methane conversion rate are expressed as mL_{CH4} $L_{reactor}^{-1}$ $h^{-1}m^{-2}$, and g_{CH4} kg_{COD}^{-1} m^{-2}

The performance of MEC B surpasses MEC A under both high and low organic load conditions despite possessing a smaller electrode surface area. When normalised to the surface area this effect becomes even more pronounced, highlighting that increased relative cathodic surface area appears to favour methane production. This is consistent with the observations of Gil-Carrera *et al.*, who identified that the residual methane content in the off gas of their hydrogen-producing MECs nearly doubled when they modified their MEC electrode arrangement from 4 anodes and 1 cathode to 4 anodes and 2 cathodes (Gil-Carrera et al., 2011). They also identified that increasing the relative anode to cathode surface area increases the current density, which is consistent with our findings (Table 11).

Sasaki *et al.* suggested using a larger cathode when the optimisation of methane production rather than organic matter oxidation is desired (Sasaki et al., 2013). An explanation of these results is simply that larger anodes offer more suitable conditions for the attachment of fermentative bacteria and exoelectrogens, whereas larger cathodes provide more appropriate conditions for methanogens. The relatively larger concentration of methanogens in MEC B will ensure greater conversion of the carbon flux into methane following its oxidation at the anode. It also ensures that the cathode is operating under lower nutrient conditions which favour energy formation as has been previously discussed. According to Shen *et al.*, when methanogens control the overall rate, a lower current density is expected (Shen et al., 2017), which is a possible scenario for MEC B.

Table 11: Normalized current densities.

	Current Density (A m^{-2})			
Strength	**MEC A**		**MEC B**	
200 ppm	0.97	±0.3	0.09	±0.06
4000 ppm	1.04	±0.13	0.12	±0.03

5.3.3 Energy storage efficiency

A key parameter when considering MEC for energy storage is the proportion of energy input converted into the energy storage vector (methane in this case). From an energy storage perspective, AD and MECs have similar operations with the exception that MECs require an electrical input that must be accounted for. In our calculations only direct energy consumption has been considered with energy inputs such as pumps or heating excluded as these will be unlikely to vary significantly between AD and MEC, and highly dependent on the particular facility. Hence the AD energy input corresponds solely to chemical energy input, whereas MECs have both chemical and electrical inputs.

Table 12 shows the MPR and MCR, as well as the energy input calculations described in Section 3.6. The heat of combustion of the final biogas is considered to be "stored-energy", and the chemical and electrical energy inputs are used to calculate the energy storage efficiency.

These calculations highlight that the electrical energy consumption of the MECs can be considerable, particularly for MEC A which had a greater current density. Hence, despite having a similar MPR under low organic load conditions, MEC A exhibited a total proportion of energy saved significantly lower than MEC B, due to the electrical energy input. MEC B, however, showed an increase in the proportion of total energy saved compared to MEC A and AD under low organic loads. At high organic loads, a relatively small difference between the three bioreactors was observed indicating that the use of MECs under these conditions did not lead to significant improvements over AD. This highlights that MECs are better at coping with low organic load wastewaters but offer limited advantages at high organic loads.

Table 12: Stored-energy as % of the energy input, considering both electrical and chemical inputs.

Reactor	A:C	Voltage (mV)	COD (ppm)	Energy (Wh)			% Saved	
				produced	chemical	Electrical	Total	Chemical
AD	-	0	4000	1.407	64.00	-	2.2%	2.2%
MEC A	2	800	4000	0.061	3.20	0.239	1.8%	1.9%
MEC B	0.5	800	4000	0.065	3.20	0.014	2.0%	2.0%
AD	-	0	200	0.388	3.20	-	12.1%	12.1%
MEC A	2	800	200	0.046	0.16	0.223	12.0%	28.7%
MEC B	0.5	800	200	0.057	0.16	0.010	33.3%	35.4%
MEC A	2	0	200	0.020	0.16	-	12.3%	12.3%
MEC B	0.5	0	200	0.019	0.16	-	11.9%	11.9%

The storing energy efficiency rose from around 2% to 12%, 12.1%, and 33.3% for AD, MEC A, and MEC B respectively when the high organic load is replaced by the low organic load. All controls (AD and MECs-OCP) fell within the range of 10-14%, consistent with those found in the literature (Hao et al., 2019) for a similar wastewater strength (200 ppm). The increased MPR showed by MEC A did not suffice to overcome the extra energy expenditure, hence the overall energy-storage efficiency remains at 12%. MEC B, however, showed a storage efficiency almost three times higher, probably due to the positive interaction of immobilised biomass (as biofilm attached to the electrodes) and the voltage imposition which enhances the net metabolic reaction rate.

This also illustrates that using relatively larger cathodes than anodes for MECs increases their overall efficiency for methane production. The negative correlation between the storage efficiency performance and the organic load found in this study is consistent with similar studies

of single-chamber microbial fuel cells (Nam et al., 2010) where a negative correlation between coulombic efficiency and the organic load was found.

The MPR is important but it does not suffice to assess the performance of future industrial-scale operation. The biogas produced must meet certain standards if it is to be injected directly into a city grid and the MCR indicates the chemical efficiency element of the stored energy efficiency. A comparison of the performance under both high and low organic loads for each of the three reactors are summarised in Figure 16, including all the parameter previously described. Interestingly, despite all three bioreactors showing a similar MCR trend and values, it appears that the methane content in the off-gas drives the performance difference in terms of MPR. This suggests that favouring the cathodic surface could lead to greater cathodic reaction capacity, enabling more hydrogenophilic activity. However, the setup and operation of this study are not adequate to elucidate this, and further study would be beneficial.

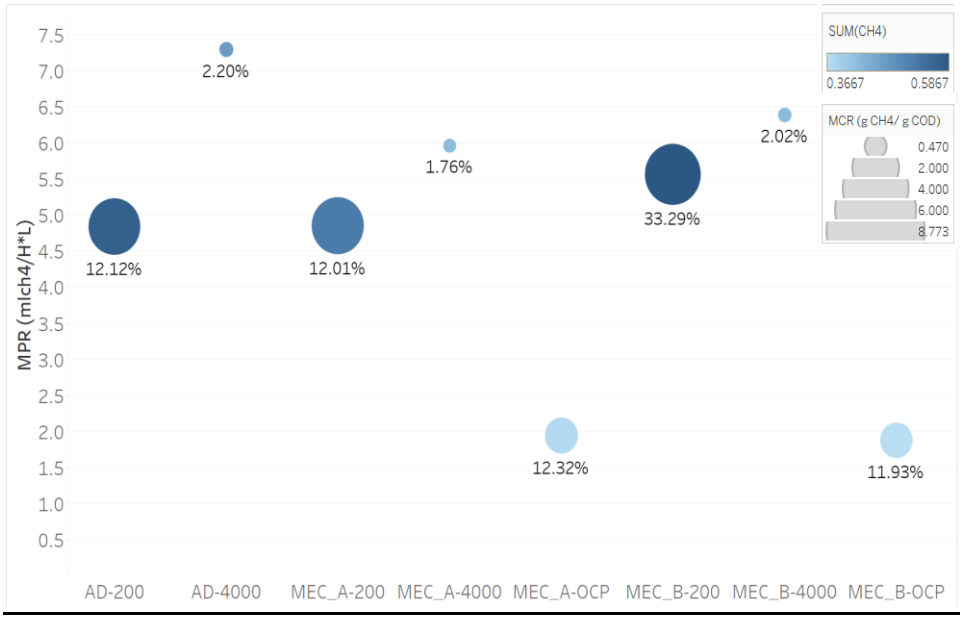

Figure 16: Performance overview for each bioreactor (AD, MEC A, MEC B), at high and low wastewater strengths (4000 and 200 ppm). MPR is represented in the Y-axis, MCR as the diameter of the circle and the biogas methane content as the intensity of the colour.

5.3.4 Hydrogen Injection and Voltage

The inoculum composition has a crucial effect on the dominant methane-producing pathway, and hence over the performance. This topic has been studied from many perspectives (Cerrillo et al., 2017; Li et al., 2016; Siegert et al., 2014a; Xu et al., 2015; Yin et al., 2016), some studies used isolated CO_2-consuming methanogens, or *hydrogenophilic methanogens* (Cheng et al., 2009; Zhen et al., 2015); this partly explains the great variability of performance outcomes between different studies. When both the inherent metabolic capacity of a given consortium and the operational conditions are changed, a structured and systematic analysis of the effect of those

operational conditions becomes complex. However, by exposing the same consortium to different levels of selected parameters, the effect of a set of those operational conditions can be assessed.

As previously described in Section 3.5, the microbial consortium used in this study came from raw cow manure, without any previous MEC system adaptation, just allowing time and application of 800 mV for the electrode colonisation. The resulting inoculum was then exposed to a designed set of different operational conditions. As seen in Table 13, there is a clear effect of applying voltage, as the performance indicators (volumetric production, MPR, and MCR) exhibit an outstanding increment, unlike with hydrogen injection (see Appendix B).

Table 13 Average biogas composition and performance indicators, indicating the standard deviation (StD) for voltage is application (800 mV or not), and hydrogen injection (stoichiometric proportion or not).

MEC A

		800 mV				No Voltage			
		No H_2		Stoichiometric H_2		No H_2		Stoichiometric H_2	
Parameter	Units								
CH_4	%	52%	±9.9%	54%	±5.0%	38%	±8.2%	33%	±2.7%
CO_2	%	45%	±9.9%	44%	±5.0%	60%	±8.2%	65%	±2.7%
Biogas	mL L^{-1} Day^{-1}	228	±43.8	208	±11.6	125	±5.4	117	±2.7
MPR	mL_{CH4} L^{-1} h^{-1}	4.85	±0.23	4.65	±0.5	1.94	±0.3	1.59	±0.09
MCR	g_{CH4} Kg^{-1}_{COD}	7.65	±0.37	7.34	±0.9	3.06	±0.53	2.50	±0.1
H_2	ppm	123	±103.4			18	±2.1		

MEC B

		800 mV				No Voltage			
		No H_2		Stoichiometric H_2		No H_2		Stoichiometric H_2	
Parameter	Units								
CH_4	%	59%	±22.6%	52%	±3.62%	37%	±6.8%	36%	±2.1%
CO_2	%	38%	±22.7%	45%	±3.6%	60%	±6.8%	61%	±2.1%
Biogas	mL L^{-1} Day^{-1}	244	±68	235	±47.2	123	±5.1	115	±5.4
MPR	mL_{CH4} L^{-1} h^{-1}	5.56	±0.9	5.13	±1.1	1.88	±0.2	1.73	±0.2
MCR	g_{CH4} Kg^{-1}_{COD}	8.77	±1.5	8.09	±1.7	2.96	±0.4	2.73	±0.3
H_2	ppm	73	±53.7			18	±1.7		

*Hydrogen content in off-gas saturated the sensor when hydrogen was injected

Figure 17 graphically shows the influence of each factor and their interactions. The statistical analysis (see appendix H) confirmed that applying 800 mV actually improves the performance of both systems significantly, regardless of the hydrogen injection, whereas the influences of relative electrode size and hydrogen injection influences are not significant.

The factors' interaction tends sometimes to hide the actual contribution of a particular factor. Probably this is the case for the null effect of the different electrode sizes which is a consequence of the really poor performance when voltage is not applied. However, if the performance of both MECs is compared only when voltage is being applied the conclusion is different, as a significant improvement is achieved by using a relatively bigger cathode, as seen in Figure 17(B).

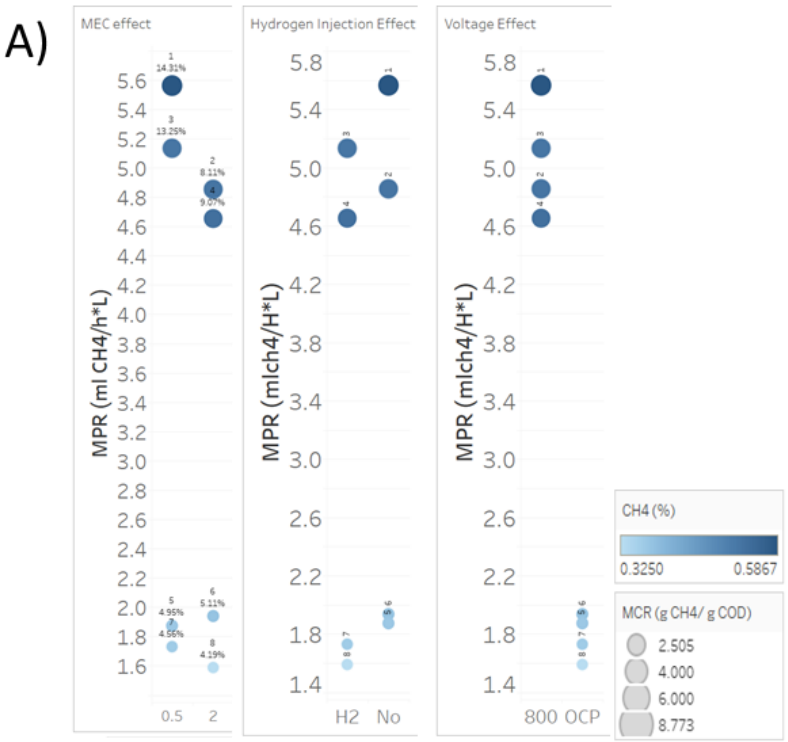

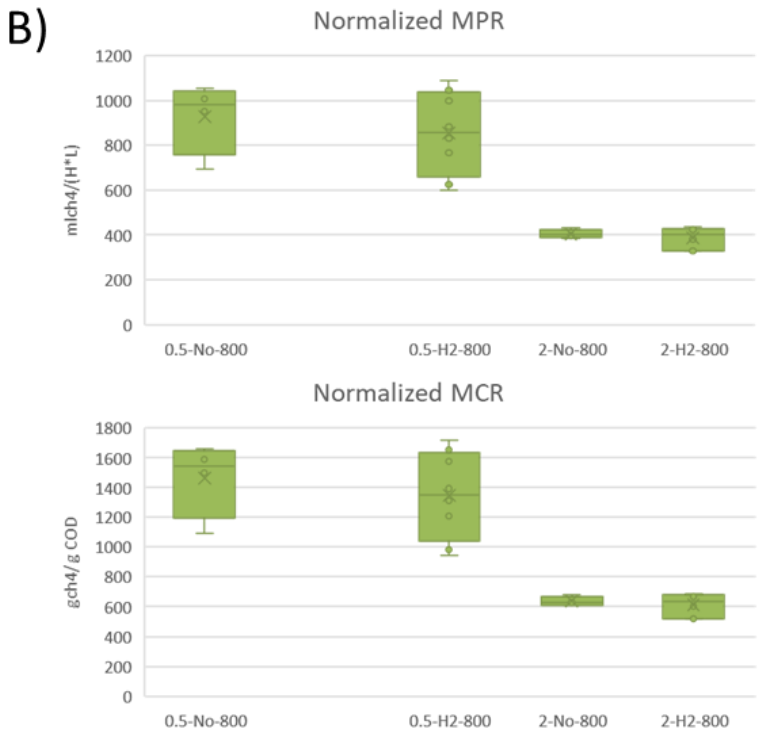

Figure 17 A) Performance indicators outcome for each design factor considered, B) MPR and MCR distribution for each MEC when 800 mV are applied, normalized to the total electrode area.

Additionally, the injection of hydrogen into the MECs vessel increases operational complexities. In this study, some operational issues had to be solved in order to carry on the design of experiments as desired. The most notable, the accidental injection of air into the strictly anaerobic MECs system, was caused by the failure of a hose, making it necessary to halt the experiments and re-start them (details are given in Appendix G).

5.3.4.1 Voltage application effect

As seen in Table 13 and Figure 17, the effect of applying versus not applying a voltage is remarkable, more than doubling the methane production rate regardless of the relative size of the electrodes to each other. Hydrogen production also increased from around 18 ppm for both MECs to over 120 and 70 ppm for MEC A and B respectively when voltage is applied.

The bio-electrocatalysis is effectively promoted when voltage is applied, enhancing the electron transfer between electrodes and electrochemically active bacteria, with an effect over the electron-supply chain for the methanogenesis, but not directly affecting these pathways as also concluded by (Zhen et al., 2015)

By applying voltage, the MPR significantly improved from 1.94 to 4.85, and 1.88 to 5.56 mL_{CH4} $L^{-1}h^{-1}$ respectively for MEC A and MEC B and the MCR also significantly improved by 150% and 197% respectively for MEC A and MEC B, suggesting that the applied voltage has a direct effect over both methanogenic mechanisms (direct and indirect EET).

The voltage influence over the *hydrogenophilic methanogens* could not be completely established in this study, as the hydrogen content of the off-gas increased instead of diminishing. This could be a consequence of either a large effect over the acetoclastic and oxidative electroactive bacteria or simply due to a relatively low presence of *hydrogenophilic methanogens* within the consortium. The MCR could be considered to some extent as indicative of direct EET (*acetoclastic methanogenesis*), as it is related to the methane production from organic matter instead of CO_2.

When it comes to assessing the contribution of a surface as a substrate to develop a biofilm of methanogenic bacteria, as has been suggested (Gil-Carrera et al., 2011), the “non-voltage” experiments were carried out with MECs that already had a mature biofilm and healthy operation, with both MPR and MCR being within the expected ranges when 800 mV, 20 days of HRT and 200 ppm organic strength are used.

These tests simply maintained the operation without any change besides cutting off the voltage imposition, however, that raises the issue of using the current as an indication of bacterial activity,

since the current reading needs a voltage to be applied. Therefore, the voltage was briefly connected at the moment of current reading and disconnected immediately after.

Initially, the currents were about three times higher than those readings obtained from the steady operation at 800 mV, leading to the hypothesis that, due to the open 3-D structure of the carbon felt used for the electrodes, the bacterial activity generates a gradient of metabolites that are harvested when voltage is applied, hence the short-term high current. This scenario is implicit in the literature which recommends the use of 3-D electrodes with large surfaces to promote bacterial attachment, but notes the importance of porosity to facilitate the transport of nutrients through the matrix (Gil-Carrera et al., 2011).

To test this hypothesis, a continuous operation was maintained, reaching a steady-state without voltage applied, maintaining every other operational condition as per section 5.2.2. For measuring the current 800 mV was applied while monitoring the current with a Unit T-80 multimeter as usual, but the current was recorded until it reached a new plateau.

It can be seen in Figure 18 that the current readings drop from the initial anomalously high values 38 and 1.2 mA for MEC A and MEC B respectively, about 3 times those obtained when 800 mV were applied. More importantly, the drop followed a two-slope kinetic path, where the first minute accounts for about 90% of the drop.

The two slopes seen in Figure 18, suggest the occurrence of two different phenomena. Following the Gil Carrera *et al.* statement logic, it is possible to theorise that the two slopes correspond to different stages, where the thickness of the electrode offers a mass transport limitation, hence concentrating mid-products of the process that are quickly harvested if sufficient voltage is applied to overcome the concentration overpotential.

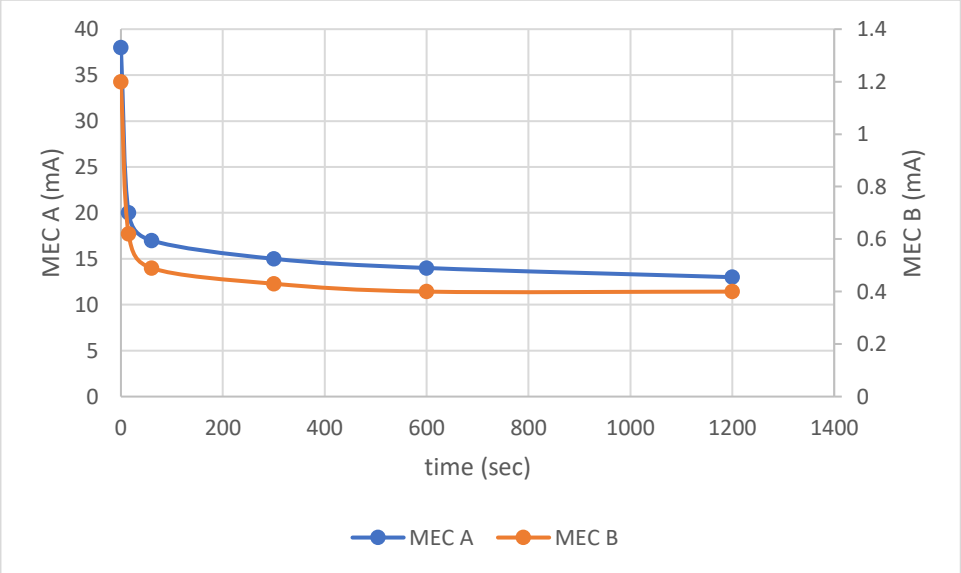

Figure 18: Instantaneous current response when 800 mV are applied to MECs operating as chemostat without voltage imposition.

Therefore, the higher current would correspond to a momentary increment of the Faradaic current. The higher current is consequence of heterogeneous reactions occurring at the electrode-solution interface (Zoski, 2007), linked to the greater gradient between the bulk of the digestate and the momentary higher metabolite concentration within the 3-D structure of the electrode.

At a small laboratory scale, mass transfer-related resistances tend to be negligible, but are indeed sensitive to design materials (mainly electrodes and membrane), electrodes distance, etc (Park et al., 2017). Whether these two-slope kinetics are related with a mass transfer limitation is out of this study's scope, but further investigation is necessary as mass transfer resistance is likely to be related to activation and concentration overpotentials. Consequently, mass transfers restrictions would add to the ohmic resistances (charge transfer resistance and electrolyte resistance), resulting in elevated costs related to the electrodes' material in order to avoid an overall high internal resistance (Park et al., 2017), and affecting the overall energy efficiency of the operation because of increased overpotentials.

Nevertheless, simultaneously these results open the discussion of whether an intermittent operation could result in a higher overall Faradaic efficiency. It has been proven that intermittent voltage imposition does not result in detrimental methanogenic performance (Mateos et al., 2020). Potentially, an intermittent electrical enhancement of the bacterial activity would maintain the overall methanogenic activity and reduce the electrical energy consumption, with consequent energy storage efficiency improvements.

5.3.4.2 Hydrogen injection

Using a broad inoculum makes tests with a variety of conditions more technically feasible, as a consortium is more likely to provide the enzymatic arsenal needed, but also it is more attractive from an engineering standpoint to compare the effect of a variety of conditions over the performance of non-specific systems. This offers relevant information on how the operational conditions influence the performance, and provides a guide to the operational changes required should the feeding, hydrogen injection, or input voltage vary. Although the consortium adaptation is not just a time-consuming task, but also very laborious and expensive, as the time frame is uncertain (Zhen et al., 2015).

As seen in Figure 17A, hydrogen injection does not seem to have a clear effect on the methane production performance. Nevertheless, and despite it can only be theorised here, there is the possibility of self-adaptation of the existing bacterial consortium in the MECs if the operational conditions were to be maintained for a period long enough to allow this. Zhen *et al.* reported an increasing bio-electrosynthesis during the continued operation (Zhen et al., 2015), suggesting the self-optimisation of the bacterial consortium resulting in a relatively higher *hydrogenophilic methanogenic* capacity. However, unlike how it was done in this study, the recommendation is to

slowly ramp up the hydrogen injection so as to avoid the accumulation of intermediates such as volatile fatty acids (Kougias et al., 2017).

Despite the performance upgrading effect of long-term operation, these improvements would be limited by design factors, such as the electrode material and its capacity to transfer electrons to the bacteria (Zhen et al., 2015). However, the interaction between these factors and the effect of a long-term hydrogen injection has not been studied here nor thoroughly addressed in the available literature, and further work is both desirable and recommended to facilitate the successful deployment of this technology.

As seen in Table 13, the hydrogen content of the off-gas increased when voltage was applied. On one hand, a strong dependency has been reported between both methane and hydrogen formation on the cathodic potential (Zhen et al., 2015), meaning that the hydrogen content increased in the off-gas despite increasing the indirect EET (*hydrogenophilic methanogenesis*). This would suggest a minor *hydrogenophilic methanogenic* presence relative to direct EET driving microbes (*acetoclastic methanogenic* bacteria).

However, on the other hand, a study by Kougias in 2017 evaluated different bioreactor designs, concluding that a bubble column seems to be the most efficient design for biogas upgrading, reaching 73% of methane content in the off-gas and consuming 84% of the injected hydrogen. They attributed this success to a poor bioconversion in other designs – as CSTR – and their limited capacity for gas-liquid mass transfer as a consequence of the low solubility of hydrogen (Kougias et al., 2017); this is shown in Table 1. The MECs used in this study are mixed only by the feeding and discharge of synthetic wastewater, resulting in poor mixing and consequent mass transfer limitation and low hydrogen solubilisation. The effects of this feature can be demonstrated by the two-slopes trend that indicates a two-stage process typical of mass transfer limitations when the no-voltage confirmation tests were run and probably associated with the depth of the carbon felt sheets used as electrodes (see no voltage test in Chapter 5).

Working with bacteria implies certain constraints, for instance, using vigorous mixing to improve mass transports and avoid dead zones in a CSTR would mechanically disrupt the biofilm formation and individual cells with a consequent detrimental effect on the performance. A gentle mixing instead – as a bubble column design does – allows counteracting these limitations, avoiding nutrients limitation and reducing mass transport related internal resistance (not ohmic resistance) (Park et al., 2017). Increasing the biogas recirculation flow rate has been reported to achieve 97% of methane content with just 12 L h^{-1} of recirculation (Kougias et al., 2017). No issues were observed even at recirculation rates as high as 40 times the produced gas (Lecker et al., 2017).

Based on those reports, it would be surprising the hydrogen injection used in this study would have had a detrimental effect due to the mechanical injection of the gas. However, an adverse

effect over the microbial dynamics has been reported when an excess of hydrogen is injected into a bio-electrochemical system such as the MECs used here, due to the accumulation of acetate, a product of the combined effect of acetoclastic activity reduction and increased homoacetogenic activity (Agneessens et al., 2017). This could then have counteracted the expected benefit of the extra hydrogen availability, leading to a negligible net effect.

Contrarily, an increment of the overall hydrogenotrophic capacity was reported after long-term exposure to hydrogen injection (Angelidaki et al., 2018) due to preferential growing and overall greater utilisation of the hydrogen available, which overcomes the aforementioned inhibition. This acclimatisation, or adaptation period, is necessary to achieve the highest biomethanation efficiencies regardless of the operational temperature. It can require up to 8 months before a 95% methane content in the off-gas is reached. Nevertheless, a 60% higher hydrogen consumption has been reported when thermophilic (55-65°C) and mesophilic operations were compared (Angelidaki et al., 2018).

In retrospect, in this study, the inoculum did not have the time to self-optimise for these conditions nor did the design favour the hydrogen solubilisation into the digestate, leading to the null effect of hydrogen injection over the MPR. Therefore, these results suggest that hydrogen injection will not have an effect unless accompanied by an appropriate design for its purpose. This highlights the relationships between the design, operation, and microbiology involved.

5.3.5 Overall efficiency

According to Katuri *et al.*, MECs cannot be used as standalone technologies as they usually do not fulfil the required wastewater treatment level to either reuse or finally dispose of the water (Katuri et al., 2019). Nevertheless, in this study, MECs are thought of as a device to link both chemical and electrical energy networks bi-directionally rather than as a wastewater treatment technology, which leads the efficiency analysis in a different direction.

In this sense, MECs can be used either as an *in-situ* or *ex-situ* upgrading stage, where the main difference – beyond the operation itself – is that an *ex-situ* approach is not inherently limited by the internally produced biogas, hence, a higher amount of mixed carbon dioxide and hydrogen can be injected in the pursuit of a greater methane production rate (MPR).

This energy-storage approach makes the wastewater treatment of secondary importance to methane production. It also increases the importance of the energy efficiency, calculated from the energy present in the final off-gas as methane as a percentage of the total energy directly fed into the MEC consisting of chemical energy from wastewater and directly applied electrical power.

In this study, the hydrogen injection was matched to the stoichiometry needed to react with the carbon dioxide produced in the MEC. Although no positive effect of the hydrogen injection was

found here, the amount of hydrogen to inject to optimise methane upgrading remains unknown and will likely depend on the adaptation of the system to *hydrogenophilic methanogens*, with an uncertain timeframe.

The temperature of operation also plays a role, affecting both the gas dissolution and metabolic activity of the microbial consortium. Here, in common with many other studies, a mesophilic operation temperature was used. Nevertheless, Lecker and colleagues have reported that 15°C and 98°C are the optimal temperatures for the hydrogenotrophic methanogens from the genus methanomicroiales and methanopyrales respectively, whereas 35°C (the temperature used here) is closer to the Acetoclastic methanogenesis optimal temperature (Lecker et al., 2017), which would clarify the marked effect over the methane conversion rate (in $g_{CH4}\ kg_{COD}^{-1}$) regardless of the hydrogen injection.

These factors can make an important difference in industrial-sized methanation plants, hence, the gas injection systems should be optimised for the particular system and tested for scalability and ideally should have a low maintenance cost (Lecker et al., 2017) whilst ensuring high mass transfer performance.

It can be seen in Table 14 that applying 800 mV produces an unquestionable gain to the energy stored as methane. MEC B achieved a 3-fold improvement in its efficiency, mostly due to the *Acetoclastic methanogenesis* enhancement suggested by the growth of the chemical energy saved and MCR improvement. MEC A on the other hand, despite doubling its MPR (see Table 13), does not exhibit the same improvement on the overall energy storage efficiency, as the direct energy input increases with the voltage imposition. Hence, MEC B which has a bigger cathode than anode, is more efficient at storing energy than MEC A, which has a bigger anode than cathode, when voltage is applied but they remain equal without it. This implies that, despite literature conjecture to the contrary (Gil-Carrera et al., 2011), the sole presence of a substrate for bacterial attachment and development is not enough to optimise energy storage, and a voltage needs to be imposed in order to increase the methane production. These results are consistent with those from the organic load and electrode size test (Section 5.1), where the relative anode and cathode size has a greater influence over the MPR than the total volume of the electrodes.

A different scenario is hydrogen injection, where no difference was obtained regardless of whether a voltage was applied. This is evidence of the dominance of *acetoclastic methanogenesis* over *hydrogenophilic methanogenesis* under the conditions imposed.

The Faradaic efficiency is used as a ratio between the stored energy and the electrical input, although in this case the analysis needs to consider the previously mentioned "apparent stoichiometry" of the biogas affected by the re-dissolution into the digestate and the fact that most of the energy input comes from the synthetic wastewater rather than the direct electric input.

Nevertheless, MEC B is even more favourable compared to MEC A when the Faradaic energy efficiencies are compared. This is consistent with the reported results from literature stating that a bigger anode will increase the current (Gil-Carrera et al., 2011), favouring oxidative and electroactive microbes, which translates to lower Faradaic efficiency as the higher current does not produce a proportionate increase in methane production.

Table 14 Summary of energy inputs and output. MEC A has an anode-to-cathode ratio (A:C) of 2, MEC B of 0.5.

Hydrogen injection	A:C	Voltage (mV)	COD (ppm)	Energy (Wh)			% saved		Faradaic efficiency
				produced	chemical	Electrical	Total	Chemical	
No	0.5	800	200	0.057	0.16	0.010	33%	35%	24
No	2	800	200	0.049	0.16	0.223	13%	31%	0.9
Yes	0.5	800	200	0.052	0.16	0.008	31%	33%	26
Yes	2	800	200	0.047	0.16	0.136	16%	30%	1.5
No	0.5	0	200	0.019	0.16		12%	12%	-
No	2	0	200	0.020	0.16		12%	12%	-
Yes	0.5	0	200	0.018	0.16		11%	11%	-
Yes	2	0	200	0.016	0.16		10%	10%	-

-Hydrogen injection was made according to the stoichiometric requirement for the CO_2 produced
-Faradaic efficiency cannot be calculated when voltage is not applied

However, whether the off-gas can be directly injected into the city grid or not depends on specific standards. For instance, a methane content above 95% is usually required, meaning that the conversion of the gas injected into the MEC needs to be almost complete, which is not the case in this study (see Table 13). The conversion is ultimately controlled by the microbial activity within the bioreactor, although many precautions can be taken to favour this, such as high mixing velocities, good injection systems design -small bubbles-, high pressure working vessel, etc. It is noteworthy that there is an energy balance that needs to be positive, or all these design and operational improvements will consume more than the energy contained in the final off-gas.

The higher MCR obtained (see Table 13) possibly reveals the change in the metabolism suggested when nutrients are scarce (Taubner et al., 2015). As the working wastewater strength is just 200 ppm, it seems fair to assume that the methanogenic bacteria worked under the “survival mode” that directs more carbon usage to energy generation instead of cell growth, which is exactly the metabolic path enhanced by the applied voltage in the MEC used here, resulting in a significantly greater MCR.

An overview of the performance for each run is shown in Figure 19, which highlights that imposing a voltage increases the MPR of both MECs leading to an increase in the methane content

of the off-gas. A secondary role is the relative size of electrodes with the effect obscured as a consequence of the interaction between these two factors.

When the influence of the relative electrodes' sizes is assessed regardless of any other factor, there is no effect. However, when the results are evaluated in conjunction with the voltage application, MEC B is significantly better.

Figure 19 shows an overview of MEC performance under different regimes for the hydrogen tests. As noted above, the difference between MEC A and MEC B in terms of MPR and MCR was only noticeable when examining the applied voltage results. This difference is also highlighted when comparing energy storage efficiencies, as both MECs show a similar chemical energy storage efficiency (around 12%) with no voltage applied. However, MEC B outperforms MEC A (33% against 16%) when the overall energy efficiency is evaluated with applied voltage. The Faradaic efficiency is proof of a different phenomenon occurring in both cells, as MEC B reached over 20% of Faradaic efficiency, whereas MEC A attained an efficiency of barely over 1.5%

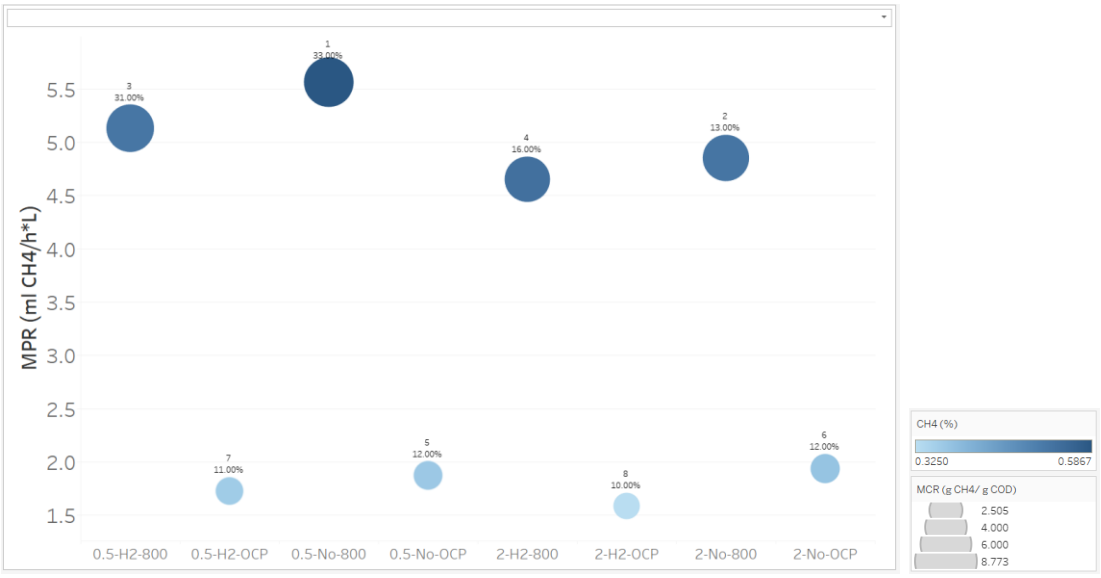

Figure 19 Summary of major performance indicators, MPR in Y-axis, methane content as colour intensity and MCR as circle size for each condition.

5.3.6 Effect of the Biogas recycling set-up

Based on what was discussed in Section 5.1, it was expected that the change in organic load had a much greater impact on both MPR and MCR results than the *in-situ* upgrading strategies (continuous or intermittent). In terms of MPR, both recycling strategies have a rather detrimental effect on the AD performance, diminishing the MPR. from 8 to about 6 mL_{CH4} $L^{-1}d^{-1}$ at high organic load, and from 5 to barely over 4 mL_{CH4} $L^{-1}d^{-1}$ when the low wastewater strength is used, which are statistically different wit p-value >0.05.

It was also noticed that, when starting the recirculation of the biogas, the hydrogen content of the off-gas consistently fell from 250 ppm until it reached the new steady condition of 110 ppm, which, despite not directly complying with the stoichiometric reaction, could partly explain the methane content increment from 45% to nearly 80%. This would suggest that *in-situ* recycling enhances hydrogen utilisation.

It could be possible then that the in-situ upgrading has successfully engaged the hydrogenophilic methanogens, translated in the hydrogen content drop of the off-gas. However, as the hydrogenophilic methanogens population is fewer than the acetoclastic methanogens – due to the unfavourable operational conditions-, the overall MPR would have been diminished despite increasing the methane content. Nevertheless, such population dynamics should be confirmed by microbiological analysis to monitor the consortium diversity.

Figure 20 depicts the MPR and MCR for MECs and AD, including the variants of continuous and intermittent in-situ upgrading, allowing to compare the ex-situ strategies against both in-situ upgrading strategies at both low and high wastewater strengths.

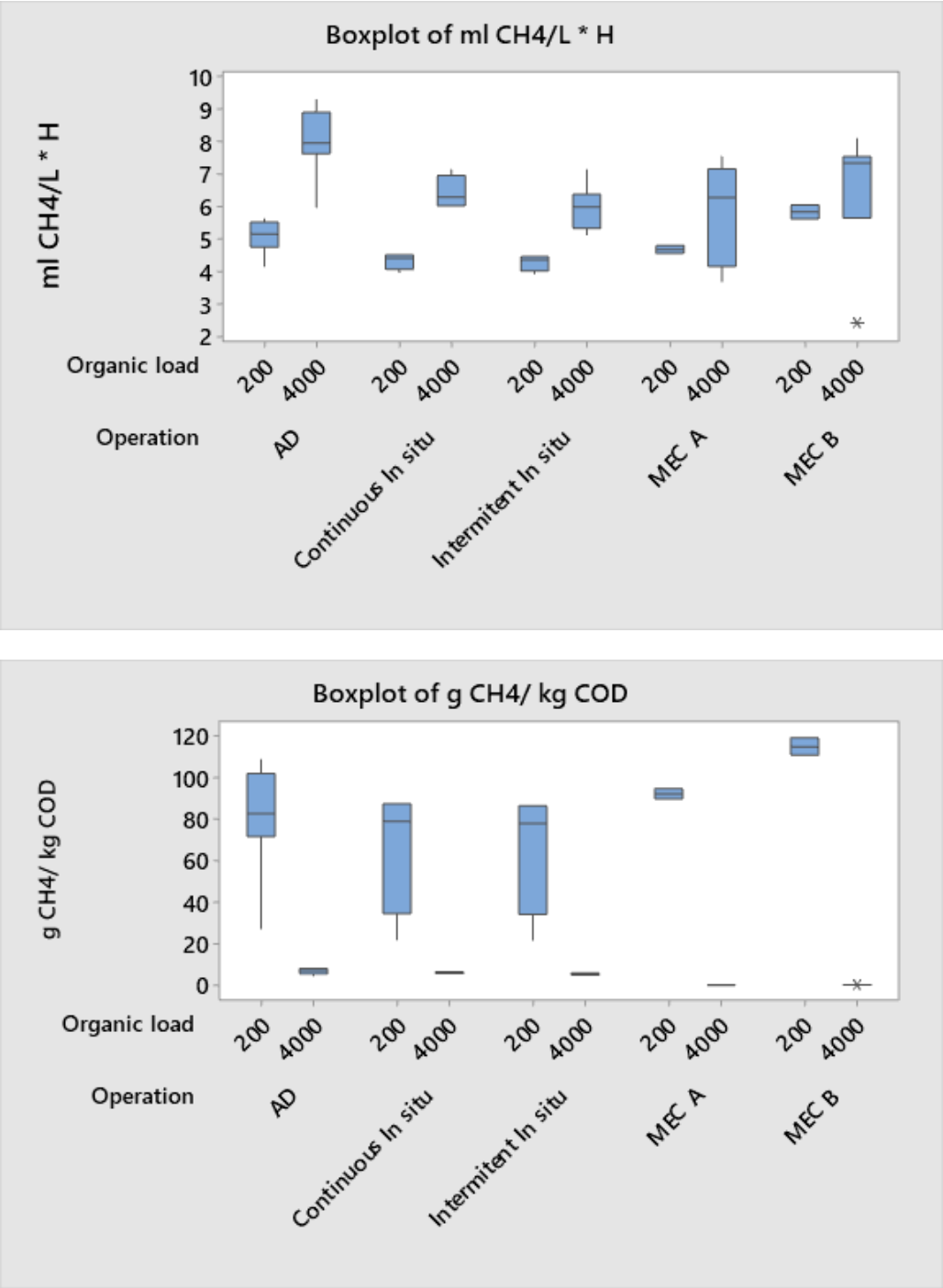

Figure 20: Performance of different upgrading strategies A) up, as MPR (in $mL_{CH4}\ L^{-1}d^{-1}$), B) down, as MCR (in $g_{CH4}\ kg_{COD}^{-1}$).

5.3.7 Final Comments

The addition of hydrogen did not significantly influence the outcome of the MEC operation in terms of methane production or energy storage efficiency. In retrospect, these results were expected, as having an active methanogenic consortium and hydrogen injection is not guaranteed to enhance the *hydrogenotrophic methanogenesis* unless it is accompanied by appropriate operation and the corresponding time for self-optimisation.

To begin with, the system is likely to offer insufficient mass transfer to effectively dissolve the hydrogen into the digestate. The mixing relies on the influent/effluent flows, creating low mixing zones. In addition, the 3-D open structure of the electrodes is convenient for bacterial colonisation but also creates nutrient gradients that increase overpotentials. Finally, the injection system used was appropriate for dissolving the carbon dioxide from the biogas, but hydrogen is far less soluble (Henry's constant at 25°C of 29.41 and 1282.05 L atm mol^{-1} respectively for CO_2 and H_2) (Perry and Green, 1997). These would explain the results from Kougias *et al.* where their bubble column was more efficient than a CSTR, achieving 84% of injected hydrogen usage (Kougias et al., 2017).

These design details would have minimised the hydrogen availability, but some level of MPR increment was expected. So, the null effect of the hydrogen injection suggests an insufficient *hydrogenotrophic methanogenic* population, or the unlikely significant counteraction of homacetogenesis that accumulate acetate. Although this can only be theorised here as a thorough microbial diversity study would be needed.

It has been mentioned before that bacterial consortium has the capacity of self-optimisation for the given environmental conditions, which brings flexibility and robustness to the system to treat a wide variety of wastes. However, as literature noted, this process has an uncertain time frame besides being a time-consuming and laborious task (Zhen et al., 2015). The uncertain time frame may be relevant as the tests performed here achieved a steady-state and constant performance, but most likely the operation including hydrogen injection was shorter than the time needed for the consortium to adapt and not sufficient to allow the *hydrogenotrophic methanogenic* population to grow. A *hydrogenotrophic methanogenic* population that according to (Lecker et al., 2017) can operate in a range of 0 to 122°C, with optimal temperatures of 15°C and 98°C (for Methanomicrobiales and Methanopyrales orders respectively), means that the 35°C used for this study was less than favourable for this particular metabolic route. This highlights the inherent complexity of working with a bacterial consortium, where different metabolic routes requiring different conditions take place simultaneously under one set of conditions.

5.4 Conclusions

MEC B outperforms MEC A in terms of energy-storing efficiency, despite producing a lower current. These results highlight that both cells operate differently, as the chemical energy storage efficiency is similar but the Faradaic efficiency of MEC B is about 20 times that of MEC A.

By comparing MECs with different electrode sizes it was found that both MECs show a similar behaviour, responding positively to voltage application regardless of the hydrogen injection, increasing from 1.94 to 4.85 mL_{CH4} L^{-1} h^{-1}, and from 1.88 to 5.56 mL_{CH4} L^{-1} h^{-1} for MEC A and MEC B respectively.

It was found that MECs are more efficient at converting low organic loads into methane than AD but are similar in performance at high organic loads, implying a bacterial metabolism being rate-limited. These results suggest that for maximum energy storage efficiency, methane-producing MECs should be used where low organic load wastewaters are present and designed with relatively larger cathode surface areas. When it comes to the *in-situ* biogas recycling into the AD system, both *in-situ* strategies increase the methane content, inducing a higher apparent hydrogen utilisation., but have a detrimental effect on the overall MPR. Additionally, biogas recycling implies a more complex operation, and higher operational costs. In this sense, the MECs appear as a more attractive option as the performance emulates the best AD methane production, achieving around 80% of methane content with a fraction of the organic strength.

Chapter 6 Interaction of the primary factors for energy storage efficiency

6.1. Context and hypothesis

The operation and design of a bioelectrochemical system (BES) needs to be optimised accounting for factors such as the electrode material, size, and separation, as well as HRT, and the inoculum. Despite many studies exploring the ideal voltage for different electrode materials (Villano et al., 2016), the different experimental conditions used define the relationship between the applied voltage and other factors such as HRT and the physical design of the bioreactor, connection that remains unclear.

This section aims to identify the effect and potential interactions between the relative electrode size (A:C), hydraulic retention time (HRT), and the voltage imposed on representative MEC systems and to operationalise that knowledge to motivate the deployment of the technology, as the relative A:C surface area will favour different rate-limiting reactions.

6.2. Materials and methods

The same two MEC bioreactors used in previous stages were operated continuously, controlling the feeding and discharge flowrates with automatic peristaltic pumps to achieve the desired hydraulic retention time (HRT) as per the design of the experiments detailed in Table 15. The temperature was maintained by immersion in a water bath at 35 °C, and the pH was maintained within 6.8-7.2, in accordance with the International Energy Agency guidelines (Bachmann, 2015).

To evaluate the influence of the 3 factors (anode-to-cathode area, applied voltage, and HRT), a full factorial design of experiments considering the levels shown in Table 15 was built with the aim of establishing whether a given performance is achievable with different combinations of these factors, thus counteracting with one factor the unmanageable real-world fluctuations of another, mimicking a full-scale operation.

Table 15 Detail of the factors and levels used to construct the matrix of conditions (24 conditions)

Factor	Levels				
Anode-to-Cathode	0.5		2		
Voltage (mV)	600		800	1000	
Hydraulic Retention Time (d)	2		5	10	20
Organic Load (g L^{-1} d^{-1})	0.01	0.02	0.04	0.1	

The MECs with different anode-to-cathode surface area (A:C) are run in parallel at identical conditions, starting with the lowest voltage and organic load (ORL). Then, the voltage is sequentially increased as shown in Table 15 before initiating the cycle again at a shorter HRT (increasing ORL). The operational conditions are modified only after obtaining a steady operation for a minimum of 3 HRTs when the organic load is changed, and at least 5 days for voltage changes.

The biogas composition (CH_4, CO_2, and H_2), volumetric production, digestate pH, chemical oxygen demand (COD), and current are monitored as previously explained; to calculate the Methane production rate (MPR, $mL_{CH4}\ L^{-1}\ h^{-1}$), Methane conversion rate (MCR, $g_{CH4}\ kgCOD^{-1}$), and the storing energy efficiency.

6.3. Results and Discussions

6.3.1 Methane production

The influences of HRT, voltage, and relative electrode size on the MPR and MCR of the MECs have been investigated using an identical inoculum and operating under otherwise identical conditions. The average biogas composition, the MPR, and MCR for each set of operating conditions are given below in Table 16. These values were obtained after three sets of 3-HRT periods had passed and the steady-state operation had been attained. Table 17 provides the concentration of H_2, alkali consumption, and the current density obtained under these conditions.

Table 16: Summary of operational conditions and biogas performance results.

HRT	Volt (mV)	CH_4 (%)	CO_2 (%)	Biogas (mL L^{-1} d^{-1})	MPR ($mL_{CH4} L^{-1} h^{-1}$)	MCR (g_{CH4} kg_{COD}^{-1})	
20	600	35±0.07	59±0.05	143±23	2.1±0.5	3.3±0.8	MEC A
10	600	85±0.06	14±0.09	315±8	11.1±0.6	8.7±0.5	
5	600	65±0.03	32±0.04	314±11	8.6±0.5	3.4±0.2	
2	600	63±0.02	35±0.01	323±11	8.5±0.3	1.3±0.0	
20	800	79±0.07	16±0.07	136±13	4.5±0.4	7.0±0.7	
10	800	83±0.03	16±4	342±10	11.8±0.6	9.3±0.4	
5	800	60±0.11	41±0.16	309±56	7.6±1.3	2.9±0.5	
2	800	61±0.09	42±0.06	329±28	8.3±1	1.3±0.2	
20	1000	87±0.08	14±0.1	160±23	5.8±1.1	9.2±1.7	
10	1000	79±0.04	18±0.05	391±20	12.9±0.7	10.2±0.5	
5	1000	79±0.02	19±0.01	257±22	8.5±0.8	3.3±0.3	
2	1000	77±0.02	22±0.01	283±29	9.1±0.9	1.4±0.1	
HRT	**Volt (mV)**	**CH_4 (%)**	**CO_2 (%)**	**Biogas (mL L^{-1} d^{-1})**	**MPR ($mL_{CH4} L^{-1} h^{-1}$)**	**MCR (g_{CH4} kg_{COD}^{-1})**	
20	600	33±0.07	67±0.19	141±26	1.9±0.5	3.0±0.8	MEC B
10	600	92±0.03	8±0.04	299±16	11.5±0.3	9.0±0.2	
5	600	76±0.03	22±0.03	323±13	10.3±0.6	4.0±0.2	
2	600	73±0.01	25±0.01	345±14	10.5±0.4	1.7±0.1	
20	800	81±0.19	28±0.28	161±37	5.9±1.7	8.6±3.2	
10	800	86±0.04	13±0.01	329±13	11.8±0.8	9.3±0.6	
5	800	74±0.09	21±0.05	341±27	10.6±1.9	4.2±0.8	
2	800	71±0.06	26±0.07	346±23	10.2±1.2	1.6±0.2	
20	1000	85±0.08	19±0.08	154±25	5.5±1	8.6±1.6	
10	1000	86±0.03	13±0.05	357±13	12.8±0.7	10.1±0.5	
5	1000	79±0.02	19±0.01	257±22	8.5±0.8	3.3±0.3	
2	1000	77±0.02	22±0.01	283±29	9.1±0.9	1.4±0.1	

The overall storage efficiency depends on the MPR and energy input. Therefore, analysing the main factors affecting the MPR provides insight into how operational parameters are likely to influence the overall performance. A positive correlation between the applied voltage and the obtained MPR is observed as shown in Figure 21 alongside the positive effect of decreasing the relative anodic surface area on the MPR. An HRT of 10 days provides the best MPR performance

with a marginal decrease for shorter HRTs. A longer HRT of 20 days provided substantially reduced performance.

Table 17: Summary of alkali consumption in ($mL_{NaOH}L^{-1}d^{-1}$), hydrogen (in ppm) content and current density (in mA m^{-2}) at different HRT and voltages applied.

		MEC A			MEC B		
HRT	**Voltage (mV)**	**H_2 (ppm)**	**Alkali consumption ($mL_{NaOH}L^{-1}d^{-1}$)**	**Current density (mA m^{-2})**	**H_2 (ppm)**	**Alkali consumption ($mL_{NaOH}L^{-1}d^{-1}$)**	**Current density (A m^{-2})**
20	600	18.1±3	1.4±0.5	225±2.9	17.1±4	0.2±0.4	45±1.3
10	600	21.9±4	1.7±0.6	261±3.5	21.3±2	2.5±0.7	63±0.8
5	600	32±4	3.7±0.6	266±2.4	29.7±3	3.3±0.6	125±1.1
2	600	35.1±3	4.3±0.6	262±1.2	31.6±1.9	4±0	137±0.9
20	800	60.3±6	2±1.4	295±4.5	60±4	2±1.4	27±0.7
10	800	62.9±20	3±0	259±2.8	73.9±4	2.5±0.7	187±3.6
5	800	75.4±4	3.8±0.3	277±2.6	74.1±3	3.5±0.4	208±3.5
2	800	78±3	4.3±0.6	284±1.7	70.8±16	4.3±0.6	251±3.3
20	1000	79.3±3	2.5±0.7	293±2.3	80.7±3	2±1.4	6±0.57
10	1000	88.1±3	2.3±1.2	317±1.3	89.5±3	2.7±1.5	239±3.6
5	1000	102.9±4	4±0	324±2	102.9±4	4±0	222±1.9
2	1000	109.1±5	4.5±0.6	327±1.5	110.6±7	4.2±0.3	234±0.6

Due to the increased energy input, energy storage efficiency does not increase significantly when a greater potential is imposed as shown in Figure 22. The factors underlying these key trends and their finer details will be discussed in the sections below.

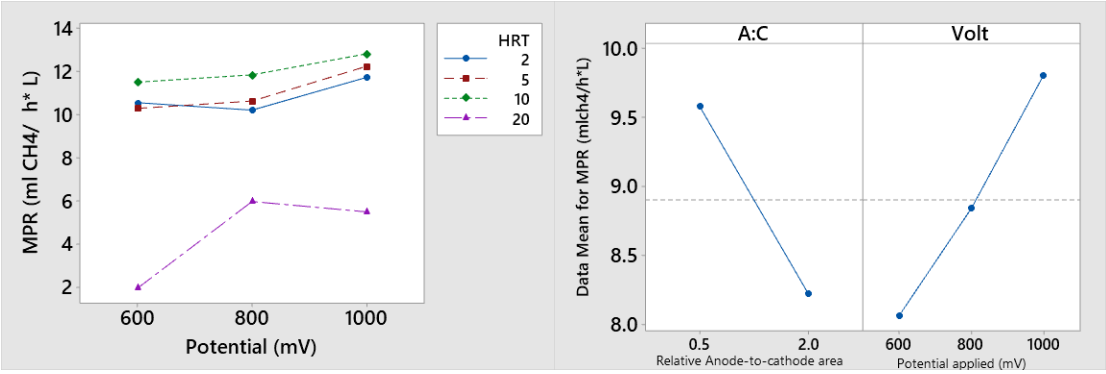

Figure 21: Methane Production Rate (MPR in mL_{CH4} L^{-1} h^{-1}) change with HRT (days), applied voltage (mV) and anode-to-cathode surface area ratio.

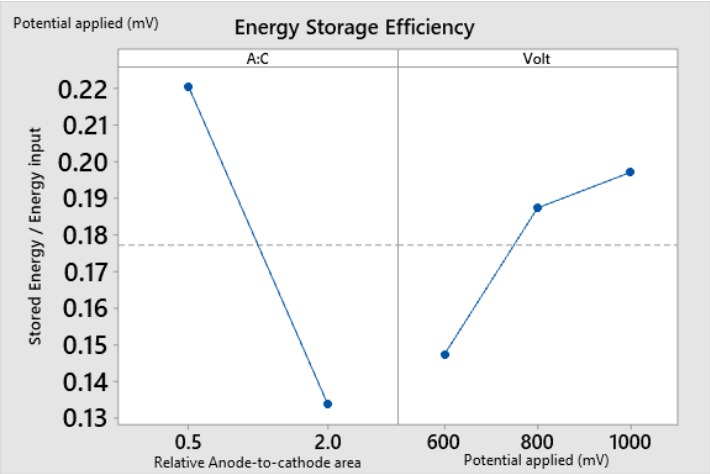

Figure 22: Effect of anode-to-cathode surface area ratio and applied voltage on energy storage efficiency.

6.3.2 Anode to cathode surface ratio

Despite the similar MPR and MCR between MEC A and MEC B under extended HRTs, MEC B appears to be more resilient than MEC A as the HRT decreases. As can be seen in Figure 23, reducing the HRT from 20 to 10 days results in a significant increase in the MPR and MCR for both the systems. Further reductions of the HRT had an overall negative effect on MEC A's performance, reducing both the MPR and MCR. However, the MPR for MEC B was not significantly affected although the clear MCR reduction reflects that at shorter HRTs the higher organic load is less efficiently used. This trend suggests that the uncoupling effect where energy production is favoured over cell growth is optimised near to 10 days HRT (Lecker et al., 2017).

Additionally, further reductions of the HRT led to an increment of organic load beyond the metabolic capacity of the methanogenic consortium. This created conditions more amenable for acidogenic bacteria, hence increasing the alkali consumption in both systems (Table 17). The acidogenic dominance translates into a larger volume of biogas produced but with a reduction in its methane content, as seen in Figure 23. In this context, the greater drop off in the methane content of the off-gas from MEC A may be related to the larger relative anode surface area. The larger anode may lead to the greater presence of acidogenic bacteria, in turn leading to more oxidation of the organic load into CO_2 and less reduction of organic acids and CO_2 into methane by the methanogenic bacteria on the cathode. MEC B (with a smaller anode) would favour the cathodic reaction, which accounts for its overall MPR being sustained at shorter HRTs even if the organic load was less completely converted (lower MCR).

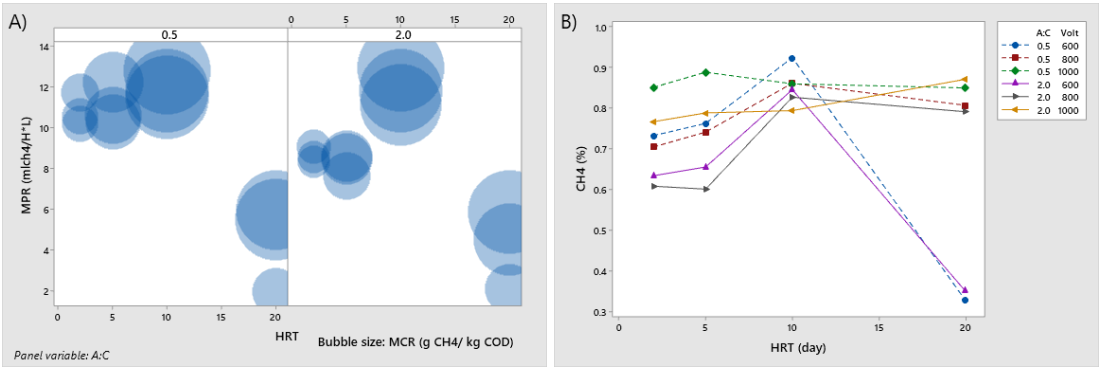

Figure 23: A) MPR (mL_{CH4} L^{-1} h^{-1}) at different HRT (days), with MCR (in g_{CH4} kg_{COD}^{-1}) as bubble size. B) Methane (in %) for both MECs at different voltages.

The higher current present when the voltage is increased affects the energy storage efficiency with respect to the voltage (Figure 23). As MEC B has a smaller anode to cathode ratio it led to systematically lower current densities despite similar performance. When 600 mV was applied no difference in MPR performance was noticed between the MECs, but the energy storage efficiency of MEC B was almost double as a consequence of the higher electric energy input of MEC A of 0.129 Wh versus just 0.003 Wh for MEC B. Increasing the potential from 600 to 800 and 1000 mV led to the energy storage efficiency increasing from 7.3% to 13.7% and 18% for MEC A, and from 12% to 37.3% and 33.2% for MEC B respectively. This trend is similar to that previously reported where a negligible effect of the cathode-to-anode ratio was noticeable at 0.5 V, but the difference increased when the applied voltages were closer to 0.9 V (Zhang et al., 2019).

This means that with 20 days HRT, MEC B achieves a maximum of 37% energy storage, while MEC A barely surpasses the 12% achieved by OCP runs (where no voltage was applied) despite them having similar MPRs. This indicates that the reduction of the oxidised organic matter into methane benefits from a greater cathode-to-anode ratio. This is similar to published results that indicate the increase in relative cathode surface area leads to improved energy storage through reduced energy loss (Sangeetha et al., 2020). There have been suggestions that this is dependent upon the applied voltage, with more pronounced effects at larger voltages, but no effect was observed here between 600-1000 mV (Guo et al., 2017). These results suggest that increasing the cathodic surface favours energy recovery from the organic substrates by reducing the current required as the level of COD removal remains similar regardless of the relative electrode surface areas.

6.3.3 The Effect of Hydraulic Retention Time (HRT)

The HRT was sequentially decreased from 20 to 2 days whilst maintaining a constant wastewater COD strength, resulting in an effective increase in the organic load. The effect of this variation is evaluated here for the two MECs with different anode-to-cathode relative surface areas under different voltages applied, as described in Table 15.

As shown in Table 10 (Chapter 5.3), an HRT of 10 days results in maximum MPR values of 12.8 and 12.9 $mL_{CH4}\,L^{-1}\,h^{-1}$ for MEC A and MEC B respectively. Shorter HRTs of 5 and 2 days had a detrimental effect on the MPR, especially for MEC A, where the overall performance dropped to between 8 to 10 $mL_{CH4}\,L^{-1}h^{-1}$ when 1000 mV was applied.

At extended HRTs, the off-gas showed high proportions of methane, with low levels of CO_2 and H_2. The changing composition of the off-gas can be attributed to the further reaction of the biogas under longer HRT conditions as it has been found that up to 10 different methanogenic reactions can occur after the biogas has been formed, leading to the production of additional methane (Mateos et al., 2020). Many of these pathways are interrelated. For example, the CO_2 of the biogas in the headspace is preferentially re-dissolved into the digestate (Krich et al., 2005), as CO_2 is about 400 times more soluble in water than CH_4. Consequently, the biogas becomes a secondary source of CO_2 for alternative methanogenic pathways. This is particularly relevant for MECs when voltage is applied, as the methanation of hydrogen and carbon dioxide is favoured (Villano et al., 2010), and the digestate acts as a CO_2 sink, altering the ultimate CO_2: CH_4 ratio.

Thus, HRT variations balance two competing effects. On the one hand, shorter HRT increases the organic load and volumetric biogas productivity, but extended HRT is beneficial for the re-dissolution of CO_2 and its contribution to methanation. As seen in Figure 24, 20 days HRT leads to a significantly lower MPR but a more efficient operation in terms of the conversion of organic matter (MCR) as shown by the bubble size in Figure 24. The energy storage efficiency drops when the HRT falls below 10 days, but the MPR remains at the same level. This suggests that at some point between 20 and 10 days, the effective organic load increases enough to supply organic matter without reaching the point where the methanogenic consortium starts to favour cellular growth over methane production. A similar case was previously reported (Shen et al., 2017), describing that operating within the evaluated range of 2-10 $g_{COD}\,L^{-1}\,d^{-1}$at 8 $g_{COD}\,L^{-1}\,d^{-1}$, rather than the extremes, achieved the best performance.

Reductions of the HRT under 10 days increase the organic load, but do not translate into higher MPR as would have been expected based on previous discussions of Chapter 5. A reduction of MCR is noticed when reducing HRT below 10 days, suggesting that the consortium is already producing methane at the maximum rate, and therefore additional organic load does not improve the overall performance. Longer HRTs would appear to induce nutrient limitations which reduce the MPR by virtue of approaching maximum methane conversion over the extended contact time.

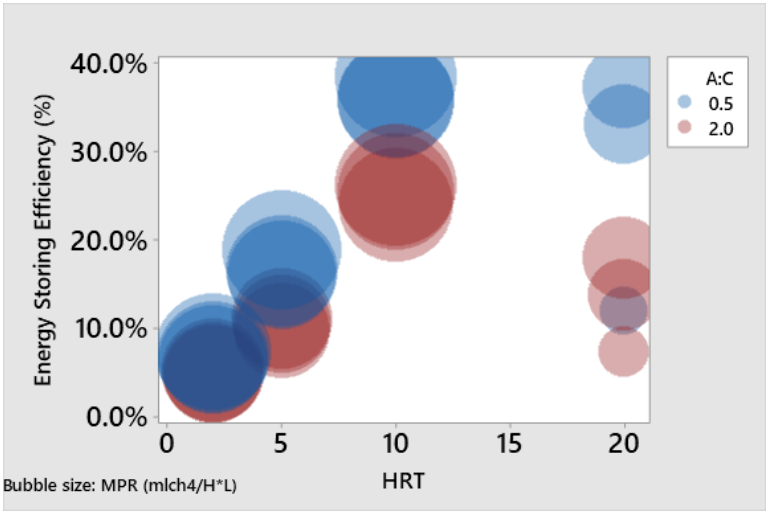

Figure 24: Energy storing efficiency (%) versus HRT (days) for both MECs represented by their anode-to-cathode ratio (MEC A=2; MEC B=0.5), where the size of the bubble represents the MCR (in g_{CH4} kg_{COD}^{-1}).

MECs operate based on the anaerobic digestion process that relies on the joint work of complex bacterial communities. These communities are responsive to a variety of different environmental conditions which leads to a close link between the dominant methanogenic pathway and the HRT (Li et al., 2016). It has been reported that shorter HRTs tend to produce more acidic digestate; more amenable for *hydrogenotrophic methanogens* that can tolerate pH < 6 rather than for *acetoclastic methanogens* (Ye et al., 2012). This is a potential explanation for the increased alkali consumption when HRT is reduced from 5 to 2 days.

An alternative explanation for the reduced MPR under the 2 days HRT conditions is that a washout of acetoclastic methanogenic bacteria has occurred, given their long duplication time of between 5-7 days (Zhang et al., 2019). This has been reported as a major concern (Baek et al., 2017) for anaerobic digester operation as it can lead to reaction imbalances. This imbalance is adverse for the overall performance, affecting, for instance, the off-gas composition, overall COD removal, and alkali consumption. Table 18 shows that reduced HRT increases alkali consumption, consistent with the formation of an acidic digestate. It has been proposed that a hydrogenophilic methanogenic enrichment of the consortium would improve the digestion performance at short HRT (Li et al., 2016), although this is not something actively investigated here. Hydrogenophilic methanogens, with a shorter doubling time, are favoured at temperatures greater than the 35 °C used here. Hence, the microbial consortium resulting of the operational conditions exhibits a slower growing rate (needing then an extended HRT), explaining the relatively poor results at short HRTs.

While the setup used in this study does not allow the direct calculation of the hydrogen production rate, the off-gas hydrogen content increased with a reduction in HRT and with increasing applied voltage (See Table 17). A similar trend has been reported previously (Sangeetha et al., 2020),

where the maximum hydrogen production rate was detected at 18 h HRT. The origin of the increase in hydrogen is probably the increase in the organic load. This translates into higher hydrogen production from organic matter, but as these conditions selectively wash out acetogenic methanogens, the methanation reaction is impaired. This leads to reduced methane formation alongside increased carbon dioxide and hydrogen production.

To evaluate whether the reduced performance of these systems is due to the washing out phenomenon, both MECs were returned to 10 days HRT and 800 mV applied following the 2 days HRT condition (Appendix E). After 20 days, MEC B had reached 10.3 mL_{CH4} L^{-1} h^{-1} of the previous 11.8 mL_{CH4} L^{-1} h^{-1} under those conditions, whereas MEC A only recovered to 7.8 mL_{CH4} L^{-1} h^{-1}. This suggests that 2 days HRT induced the washing out of the MECs, as MEC B, which was less affected by the shorter HRT, had recovered to almost 90% of the methane production in 2 HRTs, but MEC A only recovered to 67% of the activity, probably due to the characteristic slow-growing pace of methanogenic bacteria preferentially attached to the cathodic surface (more available in MEC B).

When examining the current density obtained under different applied voltages and HRT conditions (Figure 25), MEC A has a uniformly higher current density, most likely due to its total electrode surface being 4 times larger than for MEC B. Nevertheless, for both MECs, the current produced shows a negative correlation with the HRT. This is probably due to nutrients being supplied at a limiting rate, which would reduce the organic uptake of the electrode respiring microorganisms (Sangeetha et al., 2020) i.e.. microorganisms that directly interact with the electrodes. This is consistent with the significant change in the current density when the HRT is reduced from 20 to 10 days, compared to lesser reductions at 5 and 2 days HRTs.

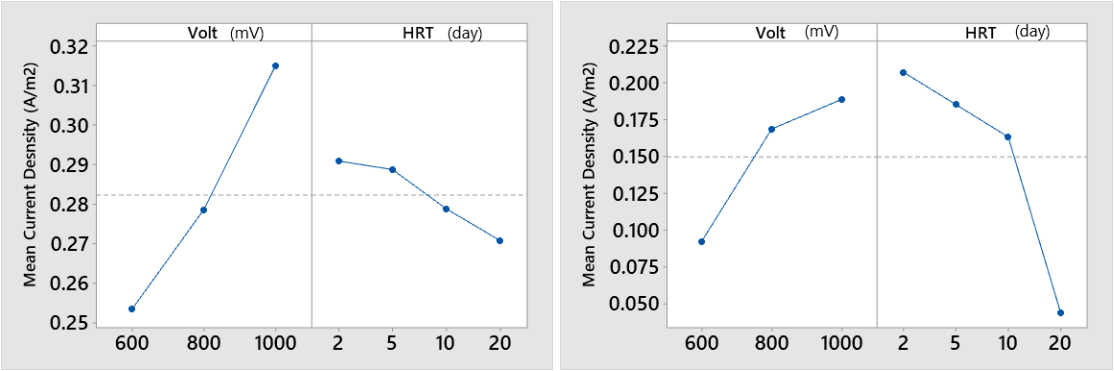

Figure 25: The mean values for each level of every factor is calculated to exhibit the effect on the current density. MEC A depicted on the left, MEC B on the right.

6.3.4 Applied voltage effect.

It has already been discussed in Section 5.2 that the electrodes by themselves are not sufficient for promoting optimal methanogenesis but need an applied voltage greater than 500 mV.

Nevertheless, MEC-OCP tests and AD are here also compared to experiments including increasing voltages to 600, 800, and 1000 mV. Table 18 and Figure 22 demonstrates that MEC-OCP tests and AD achieved a similar 12% energy storage efficiency to when 600 mV was applied. Increasing the voltage to 800 and 1000 mV raised the MPR from 1.9 mL_{CH4} L^{-1} h^{-1} as the combined average of MEC A and MEC B to 5.2 and 5.7 mL_{CH4} L^{-1} h^{-1} respectively at 20 days HRT, whereas the effect is negligible for other HRTs. Similar results have been reported by others (Guo et al., 2017), where the methane production rate was not affected by the anode-to-cathode ratio change when 500 mV was applied but increased as the applied voltage progressed to 0.7 and 0.9 V. A possible explanation is that, at elevated voltage the hydrolysis of organic matter may be assisted by micro-aerobic environments produced via water electrolysis (Liu et al., 2017; Zhang et al., 2019), allowing the faster metabolization of organic matter by facultative microbes at the external layers of the biofilm. A second possibility is that the voltage applied does not overcome the overpotential of the particular system due to poor electrodes performance, design, low electro-active bacteria population, or any of the factors presented in Section 2.8.3.

Table 18: Overall energy balance for MEC-OCP tests and AD at 20 days HRT.

Reactor	A:C	Voltage (mV)	COD (ppm)	Energy (Wh)			% Saved
				produced	chemical	Electrical	Total
MEC A	2	0	200	0.020	0.16	-	12.3%
MEC B	0.5	0	200	0.019	0.16	-	11.9%
AD	-	0	200	0.388	3.20	-	12.1%

It is worth noting that the single-chamber design used here allows any oxygen produced from water electrolysis to freely migrate to the cathode and promote parasitic reactions which reduce the current-to-methane efficiency. Increasing the voltage simultaneously increases the ohmic and Faradaic currents due to accelerated electrochemical processes such as hydrogen formation and recycling. It has been identified here an increase of the off-gas hydrogen content with increasing voltage (Table 17) which implies there are increasing side reactions such as water hydrolysis. As the efficiency of the MECs, measured by MPR or energy storage efficiency, was found to increase with increasing voltage up to 1000 mV it highlights that these apparent side reactions may be potentially implicated in the improved performance of the MECs. For applications where low levels of hydrogen are important, it highlights the need to fine-tune the level of voltage applied.

Regarding the MCR, there is a noticeable positive effect of increasing the voltage from 600 mV to 1000 mV for both MECs. However, the increase of 3-fold achieved by increasing the voltage at 20 days HRT reduces to less than 20% at 10 days HRT, even though the HRT reduction by itself increases the MCR almost 3 times. This implies that the advantage of the increased voltage is likely to be greatest in situations where the organic load is limited and residence times are long with more marginal effects under higher organic loads and short residence time conditions.

6.3.5 Overall efficiency

As the organic matter oxidation occurs at the anode and the methanogenesis at the cathode, the overall efficiency would be expected to be affected by the variation between the surface area of the electrodes (Sangeetha et al., 2020). In this study, there was little effect of the relative electrode size on the COD removal but a significant influence over the MPR. The rate-limiting step appears to be the methanogenesis rather than organic matter oxidation. This trend was noticed at various HRTs, which in turn affect the organic load. There is a clear independent effect of the voltage as the best performance was achieved when the cathodic area was favoured and the voltage was higher than 600 mV. Considering that favouring the cathodic surface area does not necessarily imply extra operational costs, this seems like a useful rule of thumb to assist with the design of MECs to maximise performance.

The MCR is highly affected by the HRT due to the change in the effective organic load being provided to the system. Optimisation of the HRT depends on ensuring there is sufficient time for the upgrading of the digestate to occur while avoiding lengthy HRTs that produce suboptimal MPRs due to the methanation reactions reaching completion. For the system used here, and other related MECs reported in the literature, this optimum appears to be an HRT of around 10 days, at least for systems operating at 35 °C when *acetoclastic methanogenesis* is the dominant pathway.

A key aim of this study is to understand the interaction between different parameters from an operational perspective with the energy storage efficiency being the key operational parameter to be optimised. The energy storage efficiency and overall energy balance for the MECs under the different operational conditions are summarised in Table 19.

In the literature 19 Wh L_{CH4}^{-1} (energy input per L methane produced) has been estimated (Geppert et al., 2016), much higher than values obtained here (between 1.6 and 7.2 Wh L_{CH4}^{-1}), suggesting a more efficient operation despite the lower methane production. This is probably due to a series of factors previously mentioned as the uncoupling effect of low strengths wastewater operation. It should be noted that directly comparing performance between different studies can be problematic due to the differences in reactor design and the operational mode employed. Certainly, some factors which would improve the Wh L_{CH4}^{-1} performance, such as double chamber designs or the use of metallic electrodes, would lead to significantly increased capital and operational costs which would need to be taken into account.

Table 19: Energy balance for both MEC A and MEC B.

HRT (d)	Voltage (mV)	MEC A - Energy (Wh)					MEC B - Energy (Wh)				
		Chem In	Elec In	Out	% saved	Wh L_{CH4}^{-1}	Chem In	Elec In	Out	% saved	Wh L_{CH4}^{-1}
20	600	0.16	0.13	0.021	7.3%	3.3	0.16	0.003	0.02	12.0%	6.3
20	800	0.16	0.17	0.045	13.7%	1.5	0.16	0.002	0.06	37.3%	2.3
20	1000	0.16	0.17	0.059	18.0%	1.2	0.16	0.008	0.056	33.2%	2.5
10	600	0.32	0.15	0.113	24.0%	1.2	0.32	0.005	0.117	35.9%	1.7
10	800	0.32	0.15	0.12	25.5%	1.2	0.32	0.013	0.12	36.0%	1.7
10	1000	0.32	0.18	0.131	26.2%	1.1	0.32	0.017	0.13	38.5%	1.6
5	600	0.64	0.15	0.087	11.0%	3.1	0.64	0.009	0.104	16.1%	3.2
5	800	0.64	0.16	0.077	9.7%	3.6	0.64	0.015	0.108	16.4%	3.1
5	1000	0.64	0.19	0.086	10.4%	3.2	0.64	0.016	0.124	18.9%	2.8
2	600	1.6	0.15	0.087	4.9%	7.9	1.6	0.01	0.107	6.6%	6.9
2	800	1.6	0.16	0.084	4.80%	8.1	1.6	0.02	0.103	6.4%	7.2
2	1000	1.6	0.19	0.092	5.10%	7.5	1.6	0.017	0.119	7.4%	6.4

The full factorial design used provides the information necessary to model the behaviour in response to changes in reaction conditions, allowing contour plots to be constructed that relate operational parameters to the system performance in terms of the energy storage efficiency. These relationships will contribute to the ability to deploy MEC technology. Figure 26 shows how the highest storage efficiency is obtained over 800 mV and between 10 and 15 days of HRT for both MECs. The efficiency would be expected to quickly drop if the HRT is less than 8 days, while the effect of voltage is much less pronounced. It is also clear that MEC B, which has a higher relative cathode surface area, leads to significantly greater energy storage efficiency. These plots provide an overview of how the three factors assessed in this study affect the overall energy storage performance.

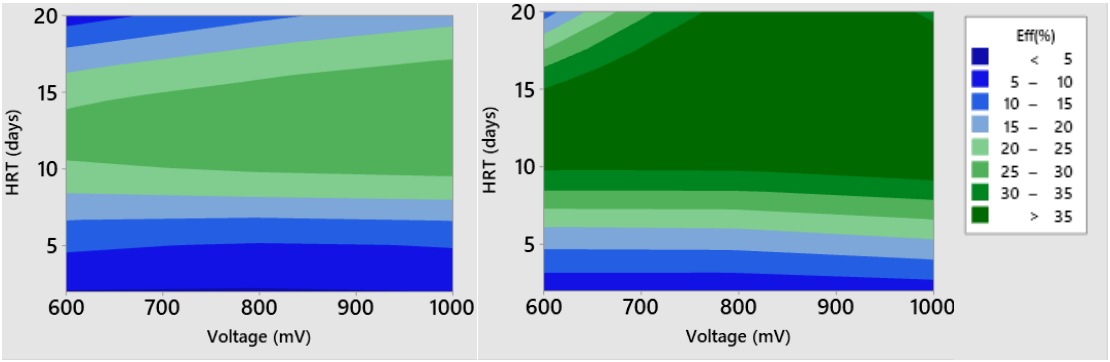

Figure 26: Contour plot of energy storing efficiency (in %) versus hydraulic retention time (HRT in day) and applied voltage (mV) for MEC A (left) and MEC B (right).

6.4. Conclusions

Efficient methane production was achieved in membraneless MECs with sandwich-like carbon felt electrodes. The highest methane production rate (12.9 ml_{CH4} L^{-1} h^{-1}) was obtained at 10 days HRT, 1000 mV applied, and the smaller anode area of the two otherwise identical systems. Favouring the cathodic surface area significantly improved the methane production efficiency and overall energy recovery from organic wastewater. The relevance of optimising HRT to provide sufficient organic load, avoiding washouts and incomplete organic matter conversion is highlighted. Over 600 mV should be applied to surpass the traditional anaerobic digestion energy storage capacity, increasing with higher potentials, albeit with limiting returns unless the MPR is increased sufficiently.

Chapter 7 MEC Deployment

7.1 Modelling the integration of MEC into a domestic and industrial scenario

7.1.1 Context and hypothesis

Accumulated knowledge regarding MEC operation and the underlying metabolic routes involved has led to several different possible integration strategies, such as MEC-AD that directly introduces the electrodes within a traditional AD system (Yu et al., 2018), or a two-stage system where the digestate from the first bioreactor feeds a hydrogenotrophic column which allows biogas containing 98% CH_4 to be formed (Kougias et al., 2017). However, fewer studies have explored the integration and potential contribution of MECs in terms of energy storage and reduction in CO_2 emissions from fossil fuels (Gajaraj et al., 2017) under full-scale conditions.

The primary aim of this section is to evaluate the practicality of MECs as a means of recovering energy from wastewater and storing energy from photovoltaics panels (PV) in a domestic setting, as well as the use of this technology to minimise CO_2 emissions from a power plant. These scenarios are explored in terms of energy flow, carbon balance, and their impact on overall CO_2 emissions to perform a preliminary examination of whether these integration modes prove to be viable at the current stage of technological development. The aim is to highlight areas that can lead to more effective resource use, to focus on future development efforts, and to inform how MECs could contribute towards a more sustainable energy matrix.

7.1.2 Materials and Methods

7.1.2.1 Process description and overview

The most common wastewater treatments are based on aerobic systems such as activated sludge (Arcadis et al., 2003). These include energy-intensive processes such as pumping and aeration, the main sources of CO_2 emissions. AD minimises these emissions as aeration is not needed, sludge production is reduced, and the methane produced can be utilised as a biofuel. This allows AD to be integrated within the energy generation network (Mayer et al., 2019).

Figure 27(A) depicts the independent operation of the power plant and wastewater treatment, where the MEC integrated configuration (Figure 27(B)) enables energy to be reclaimed from the wastewater in the form of biomethane coming from both the organic matter present in the waste stream and from recycling the CO_2 captured at the power plant. Therefore, the model considers the carbon inputs and methane contributions of both the AD and methane electrosynthesis.

From this integration, two cases have been examined. The first, referred to as the household scenario, corresponds to an “average” individual household, based on their energy needs and

wastewater generation. The second case corresponds to a small town hosting a power plant that feeds a bigger city, as per the case considered below where a 100 MW plant is hosted by Huntly near Auckland in New Zealand. While Auckland, New Zealand has been selected as a case study to enable real data to be used, it is expected that these results will broadly reflect scenarios commonly seen in many other countries.

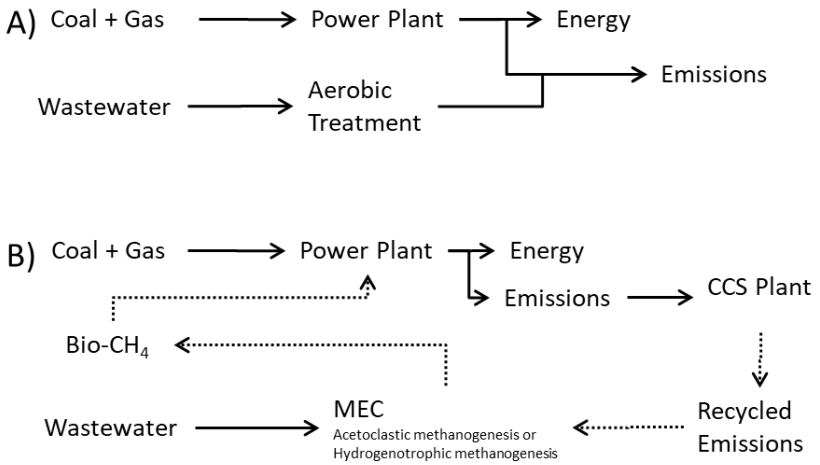

Figure 27: A) Typical decoupled wastewater treatment and power generation. B) Integration of power-to-gas technology for the low carbon operation of a power plant.

The household scenario considers a domestic grid-connected PV system as an energy source. The energy balance using batteries for storing excess energy from this PV is compared to that which would be incurred by a household MEC operation, accounting for the energy reclaimed from the wastewater treatment. The biogas produced by the MEC assumes a typical wastewater flow rate and organic load shown in Appendix C.

To assess the potential MEC contribution in this scenario without limits imposed by domestic wastewater supply, the required MEC performance and volume to store the totality of the surplus energy provided by the PV system was calculated by considering the MEC maximum current density reported (74 $A\ m^{-3}$ (Rader and Logan, 2010)), and daylight availability to estimate the average MPR (in $mL_{CH4}\ L^{-1}\ h^{-1}$).

The industrial scenario considers a power plant running on a constant proportion of natural gas and coal to avoid introducing factors outside the scope of this research. However, when possible, the natural gas is replaced by biomethane produced by the MEC. The MEC carbon inputs account for both the organic matter present in the wastewater and carbon present in the power plant emissions treated by a carbon capture and storage plant (CCS).

Three different referential MECs are used here, operated either at 35°C or 55°C to favour the *acetoclastic* or *hydrogenotrophic* methanogenic pathways respectively. The MPR used for MEC-35 is based on average values obtained from the literature for MECs operating at 35°C (see

Appendix C), whereas MEC-55 uses the values reported for an CSTR operated at 55°C as reference of the potential metabolic capacity achievable by the hydrogenotrophic methanogens (Luo and Angelidaki, 2012). Finally, MEC-reference corresponds to a low-tech device operated under similar conditions to those simulated here (synthetic domestic wastewater, 200ppm, 35°C) which reached a methane production rate of $7 mL\ CH_4 L^{-1} h^{-1}$, offering a baseline performance for a mesophilic MEC contribution. Section 4.3 details the operational parameters used in the simulations performed to assess the use of different MECs to offset the energetic burden of the CCS plant.

All simulations use the type of wastewater treatment (aerobic or anaerobic), population, energy demand, and fossil fuel used as inputs to the model. Mass and energy balances, taking into account efficiencies and other factors, are used to calculate the ultimate CO_2 emissions and necessary reaction rates.

7.1.2.2 Model description and calculations

Aerobic degradation requires energy-intensive aeration and sludge treatment, which results in CO_2 emissions and net energy consumption. Equation (7.1) gives the overall emissions of CO_2 from aerobic wastewater treatment. This includes emissions directly as consequence of breakdown of the organic matter and those related to the energy needed for operating the plant as function of the influent wastewater flow rate (Q_{WW}) (U.S. Environmental Protection Agency, 2011).

$$CO_{2,WW_{treatment}}\left(\frac{Kg_{CO_2}}{day}\right) = 0.26 * Q_{WW} \qquad (7.1)$$

Modelling the energy use of MECs requires the direct electrical energy input of the MEC to be determined, which is calculated using Equation (7.2).

$$Energy_{MEC}(Wh) = V * I_{density} * V_{MEC} * time \qquad (7.2)$$

In MECs the current density ($I_{density}$) is an important operational indicator, which can be related to the surplus energy to be stored ($Surplus_{energy}$) and operational parameters such as the applied voltage (V), working volume (V_{MEC}) and time of operation (time). When imposed the restriction that the energy involved in the reaction is the surplus energy over Equation (7.2), it can be expressed as Equation (7.3).

$$I_{density}\left(\frac{A}{m^3}\right) = \frac{Surplus_{energy}}{V * V_{MEC} * time} \qquad (7.3)$$

The direct electrical energy input is factored into the energy balance. However, other energy requirements arising from process considerations such as heating or pumping have not been taken into account, as these vary significantly depending on reactor design and other facility peculiarities.

The energy and mass balances of the MEC and anaerobic systems also must account for the production (in kg) of the main components of the biogas, methane (M_{CH4}) and carbon dioxide (M_{CO2}). These values are estimated from the influent wastewater using Equations (7.4) and (7.5) (U.S. Environmental Protection Agency, 2011).

$$M_{CO_2}\left(\frac{KgCO_2}{day}\right) = Q_{ww} * OD * CF_S * \left(1/\%C_{CO_2}\right) * \left(1 - MCF_{ww} * BG_{CH_4}\right) \quad (7.4)$$

$$M_{CH_4}\left(\frac{KgCH_4}{day}\right) = Q_{ww} * OD * CF_S * \left(1/\%C_{CH_4}\right) * \left(1 - MCF_{ww} * BG_{CH_4}\right) \quad (7.5)$$

The CO_2 emissions (in kg) from burning the methane produced as an energy source can be estimated using Equation (7.6), where MW corresponds to the molecular weight of the component.

$$Emissions_{CH_4}\left(\frac{KgCO_2}{day}\right) = DE * M_{CH_4} * \left(MW_{CO2}/MW_{CH4}\right) \quad (7.6)$$

When electrical energy is used to operate an MEC to produce a chemical energy carrier such as methane, that energy is effectively stored. Equation (7.7) relates the amount of methane needed to store a given amount of surplus energy available. By combining Equations (7.4) and (7.5), it is possible to relate the available surplus energy to the influent wastewater.

$$M_{CH_4}\left(\frac{gCH_4}{day}\right) = \frac{Surplus_{Energy}}{Specific_{Energy}} = \frac{kJ\,d^{-1}}{kJ\,g^{-1}} = g\,d^{-1} \quad (7.7)$$

From the energy demand and domestic wastewater production of each scenario, the CO_2 emissions are estimated, considering both chemical and electrical energy inputs. In the power plant scenario, there is also the consideration of the replacement of fossil-origin gas with MEC-produced methane with the total energy produced kept constant. These estimates were iterated until the level of CO_2 emissions converged.

The chemical energy input was estimated, as mentioned earlier, using the empirical factor of 16.1 kJ g_{COD}^{-1} (Dai et al., 2019), multiplied by the organic load (flowrate multiplied by the COD, in mg d^{-1}). The energy contained in the biogas is calculated by multiplying the mass of methane produced by its molar enthalpy of combustion (-890.5 kJ mol^{-1}) and dividing by its molar mass (16 g mol^{-1}) (Hao et al., 2019). Therefore, the chemical energy input of a wastewater flow of 160 L day^{-1} with 200 mg L^{-1} would be equivalent to 140 Wh day^{-1}.

7.1.3 Results and Discussion

7.1.3.1 Household

When solar PV generation exceeds the load, the surplus energy is stored if possible and any further excess is returned to the grid. When the generation is insufficient, energy is imported/bought from the grid (Museli et al., 2000). Here, the energy imported from the grid using a battery-based storage method is compared to what would be needed by a MEC that uses domestic wastewater as its sole carbon input. As part of this simulation, we have evaluated whether an MEC fed with domestic wastewater is sufficient to match the demands of this mode of energy storage.

Based on the average annual energy consumption in New Zealand of 1.13 x 10^7 $kJ\ y^{-1}\ person^{-1}$, it was estimated, using the System Advisor Model (SAM) (Laboratory, n.d.), that a 7 kW PV system is the appropriate rating for a household containing one individual. As seen in Table 20, the energy generation between October and March exceeds the load, generating surplus energy greater than the net energy deficit during the winter months (May to September), leading to a positive annual energy balance if the excess energy could be appropriately stored.

Domestic energy storage usually relies on batteries, which despite the latest improvements still offer primarily short-term storage (Schaaf et al., 2014), and have a limited number of charge-discharge cycles before needing to be replaced. A key parameter for battery use is the depth of discharge (DoD) which is the maximum % of charge taken from the battery up to its limiting practical discharged state. A lesser DoD extends the lifetime of batteries but reduces their total useful storage capacity, unlike chemical carrier-based storage capacity where the total is available. As batteries represent 50% to 60% of the initial investment of PV systems the DoD setting is an important consideration (Ardani et al., 2017).

A parametric simulation in SAM evaluating different battery pack capacities and the effect of the DoD is shown in Table 20. This highlights that a larger battery pack not only offers more energy storage, but also greater energy consumption as energy needs to be taken from the grid during winter to ensure the DoD limit is not exceeded. MECs operate on a different principle, as they require a direct electrical input estimated at 0.9 kWh per. Nonetheless, the methane that can be produced by the MEC contains about 37 kWh as chemical energy, which can be recovered as heat or electrical energy. As the efficiency of internal combustion engines is around 35% (Li et al., 2016), only 13 kWh per month is recoverable as electrical energy.

Considering the 160 L day^{-1} $person^{-1}$ wastewater flow rate and 20 days of HRT, a 3.2 m^3 household MEC could produce about 84.7 kg_{CH4} $month^{-1}$, based on the average 56 $mL\ CH_4\ L^{-1}h^{-1}$ MPR (calculated using values in the appendix D). However, the typical wastewater generated by an individual offers an organic load ($OL = Q_{ww} * OD * CF_S$) of only 17 g_{carbon} d^{-1}, enough to produce only 680 g_{CH4} $month^{-1}$. From Equation 32 it can be calculated that to utilise the full methanogenic potential of MECs, about 2000 g_{carbon} d^{-1} would be required,

therefore, at this scale the wastewater represents a carbon source limitation and a supplementary source is needed. It is assumed in a household scenario that there would be a negligible contribution from external CO_2, and therefore the contribution of the *hydrogenophilic methanogenesis* pathway, which enables the direct transformation of CO_2 and H_2 into CH_4, would be minimal and a mesophilic operation is recommended.

Table 20: Energy balance (in kWh) results of a simulated 7 kW PV system installed in Auckland New Zealand. The energy balance and energetic burden of a system without batteries, with 2, 4, 8 kWh battery packs, a theoretical MEC (without carbon limitation), and a MEC operating with domestic wastewater are compared.

System		No Energy Storing			Batteries Energetic burden - kWh imported from grid due to DoD			Current System (Wastewater carbon supply limitation)			
Parameter		PV generation (kWh Mo^{-1})	Load (kWh Mo^{-1})	Balance (kWh Mo^{-1})	2 kWh	4 kWh	8 kWh	Theoretical Energy in Methane (kWh)	Energy from Methane Combustion (kWh)	MEC energy used	Lost Energy
Month	Jan	972	375	597	29	20	19	37	13	0.9	559
	Feb	751	331	420	26	19	18	37	13	0.9	382
	Mar	576	334	242	25	23	21	37	13	0.9	204
	Apr	331	369	-38	19	48	38	37	13	0.9	-
	May	211	479	-268	9	51	78	37	13	0.9	-
	Jun	146	693	-547	18	70	126	37	13	0.9	-
	Jul	181	842	-661	12	54	137	37	13	0.9	-
	Aug	301	773	-472	5	31	111	37	13	0.9	-
	Sep	459	622	-163	3	31	76	37	13	0.9	-
	Oct	704	500	204	8	40	47	37	13	0.9	166
	Nov	863	325	538	27	22	21	37	13	0.9	500
	Dec	984	377	607	21	26	20	37	13	0.9	569
Year		6479	6020	459	200	433	711	446	156	11	2380

Comparing Equations (7.1) and (7.2) it can be noted that 41.6 $kg_{CO2}\,month^{-1}$ are produced when aerobically treating the wastewater, despite only 2 $kg_{CO2}\,month^{-1}$ being produced from the degradation of the organic matter itself. Hence, most of the CO_2 emissions come from the process energy demands, such as aeration and mixing. A traditional AD would produce CH_4 containing about 65% of the carbon obtained from direct emissions of CO_2, reducing the direct emissions of the waste treatment to about 0.7 $kg_{CO2}\,month^{-1}$. The integration of decentralised MECs with PV systems would reduce the energy-related emissions of the subsequent waste treatment. The MPR would be increased relative to AD, increasing the proportion of carbon used to produce methane rather than CO_2 (Taubner et al., 2015).

It is clear that the full MEC potential cannot be achieved in a domestic application solely from wastewater produced by the household. Nonetheless it is worthwhile determining the requirements for an MEC system unconstrained by household wastewater generation to identify

the viability of this technology in the presence of alternative sources of oxidisable carbon. The published current density values for MECs range from 0.001 A m^{-3} (Gajaraj et al., 2017), to 74 $A\ m^{-3}$ (Rader and Logan, 2010). The highest of these values has been used in Equation (7.6) to determine the operational conditions required to store all surplus energy as methane.

Based on these calculations, as seen in Table 21, there is a carbon source limitation, as would be expected from the earlier discussion. For example, around 29 kg_{carbon} $month^{-1}$ are needed in January to store the total surplus energy provided by the PV system, but only 0.5 kg_{carbon} $month^{-1}$ can be sourced from the wastewater.

The average MPR (in mL_{CH4} L^{-1} h^{-1}) required was calculated directly by dividing the methane produced to contain the equivalent energy to the total PV surplus energy by the time and MEC volume. However, as the electric input from PV is only present during the day, a maximal theoretical MPR of 192 mL_{CH4} L^{-1} h^{-1} is needed if 5 mL_{CH4} L^{-1} h^{-1} is assumed (similar to traditional AD systems) when no surplus energy is available. The maximum theoretical MPRs are well within the range of those that have been reported to achieve up to 330 mL_{CH4} L^{-1} h^{-1} (K. S. Choi et al., 2017).

Table 21 also details the wastewater flow rate that would be required to supply the carbon, assuming the same COD as household wastewater. It is clear that the required wastewater flow rate ranges between 3124 and 9165 L d^{-1} $person^{-1}$, well in excess of the average of 160 L d^{-1} $person^{-1}$, emphasising that here the main restriction on the integration of the MEC is carbon availability and not the rate of conversion. The volume estimated to maintain the desired current density ($I_{density}$) is approximately 1 m^3. This would require a short HRT of about 2 h at the flowrates required under the typical wastewater COD. This is relevant as anaerobic treatments are known for extended HRTs of up to 20 days, however, single-chamber MEC with carbon-based electrodes and HRT between 5 and 6 hours have been reported to achieve between 170 (Clauwaert and Verstraete, 2009) and 250 mL_{CH4} L^{-1} h^{-1} (Li et al., 2016). This reiterates that the MEC contribution is not limited by kinetics but carbon source limitations.

Increasing the COD of the organic load source used would reduce the required flowrate and enable the use of longer HRT, highlighting the importance of identifying alternative carbon sources for the integration of MECs. Moreover, despite the positive annual energy balance for PV generation, it is not until the third year of operation that an MEC with appropriate methane storage would allow for a sufficient energy supply without needing to buy from the grid.

These simulations are based on an intermittent electric input when surplus energy is available, which, as discussed in section 5.2, plays a significant role on the overall performance of MECs. Such systems have been proven to tolerate short- and long-term interruptions (Mateos et al., 2020). Furthermore, the overall performance of the process depends on the organic load which

affects the preferred metabolic pathways as well as playing an important role controlling the reaction rate (Garcia-Pena, 2015).

Table 21: Theoretical MEC methane production rate (MPR in mL CH4 L^{-1} H^{-1}) for full surplus energy storage without carbon source limitations.

System		Theoretical operation without carbon supply to store the total surplus energy						Estimated MPR for theoretical MEC	
Parameter		daylight (h day^{-1})	% daylight	Vol MEC (m^3)	CH_4 (kg)	ORL	(kg_{carbon} $month^{-1}$)	Qww (L d^{-1})	Average MPR	Average MPR daylight adjusted
Month	Jan	14	58%	0.72	39	29	9165	114	192
	Feb	13	54%	0.55	27	20	6443	106	191
	Mar	12	50%	0.34	16	12	3712	98	191
	Apr	11	-	-	-	-	-	-	-
	May	10	-	-	-	-	-	-	-
	Jun	9	-	-	-	-	-	-	-
	Jul	9	-	-	-	-	-	-	-
	Aug	10	-	-	-	-	-	-	-
	Sep	11	-	-	-	-	-	-	-
	Oct	12	50%	0.29	13	10	3134	98	191
	Nov	13	54%	0.7	35	26	8263	106	191
	Dec	14	58%	0.73	40	30	9327	114	192

For an increased organic load feedstock to be viable for energy storage, it must be low-cost and sourced from an abundant supply (Garcia-Pena, 2015). Hence, two possible options are agro-industrial waste or separating toilet flushed water from greywater, as that would provide a COD over 1000 mg L^{-1}, although it would not increase the carbon availability, the organic load would increase as the reduced wastewater volume reduction allows a smaller MEC. Other potential sources could come from the use of solid organic matter since in New Zealand over 320 kg $person^{-1}$ of plant matter and food scraps are sent annually to landfill (Ministry for the Environment of New Zeland, 2019). An alternative option is the use of external carbon sources such as CO_2 with renewably sourced hydrogen to promote hydrogenophilic methanogenesis pathways (see Figure 3) to enhance methane production (Villano et al., 2010), although very unlikely in a household scenario.

7.1.3.2 Power plant scenario

The integration of carbon capture and storage (CCS) within newly built power plants is an increasingly common approach to reduce CO_2 emissions. CCS can capture nearly 90% of CO_2 emissions (Leung et al., 2014), albeit with a substantial energy requirement of 375 kJ mol^{-1} CO_2 captured (8.5 kJ g_{CO2}^{-1}) (Leung et al., 2014; Watcher, 2017). The aim of this scenario is to examine whether the methane production of an MEC fed with the wastewater of the nearby town and the recycled CO_2 emissions from the power plant is sufficient to offset the energy consumption of the CCS plant. It is envisaged that fossil fuel-derived natural gas can be replaced by the biogas-derived methane produced from the MEC fed with CO_2 emissions.

The base scenario for the industrial case is an aerobic wastewater treatment that runs separately from the power plant fuelled by coal (40%), and gas (60%) with combustion efficiencies of 35% and 33% respectively (Bright Hub Engineering, 2019). The proportion of fuel inputs is kept constant in this simulation when replacing natural gas by biogas to avoid introducing artefacts from the reduced input of coal, the base case emissions reach 49 tonne CO_2 day^{-1} in an 8 h day^{-1} operation cycle, as the plant operates just when renewable energies are not available, hence most of the time runs on standby..

The studied case has a CO_2 emission rate of 0.137 g_{CO2} kJ^{-1}. If the supply chain emissions are included, the emission rate increases to 0.17 g_{CO2} kJ^{-1}. This highlights the role of the supply chain when it comes to overall emissions, which are avoided with an *in situ* low-carbon power-to-gas operation as discussed here.

Additionally, the sole use of an anaerobic wastewater treatment instead of an aerobic process reduces the emissions from wastewater treatment from 13.35 kg_{CO2} h^{-1} to 5.49 kg_{CO2} h^{-1}, although biological emissions are not normally counted as contributing to carbon footprint because it short-term circular While this is a significant reduction as a proportion of the initial wastewater treatment emission rate, it has a negligible impact on the total emissions, as the power plant generates almost 16 Ton_{CO2} h^{-1} when working at full capacity (100 MW).

To achieve the direct conversion of CO_2 under limited organic matter input requires the activation of both acetoclastic and hydrogenotrophic methanogenic pathways. According to (Luo and Angelidaki, 2012), when the MEC is operated at 55°C, the methane production rate has been reported to reach 5.3 L_{CH4} L^{-1} day^{-1} (200 mL_{CH4} L^{-1} h^{-1}) due to the full engagement of *hydrogenotrophic methanogenesis*. Whether this can occur under excess CO_2 conditions at the required rate is an area of critical importance to explore. The extra energy required for heating to 55 °C has not been considered in the model given the availability of waste heat from the power plant.

Table 22: Emissions saved by using anaerobic digestion and MECs integrating the wastewater treatment and powerplant operation, for each MEC simulated, whereMEC-35 represents an operation at 35 °C, MEC-55 an operation at 55 °C, and MEC-ref the results from previous chapter of this work

Parameter		Units	MEC-35	MEC-55	MEC-ref
Methane Production rate		**$mL_{CH4}L^{-1}$ h^{-1}**	56	200	7
Biogas production		**kg_{CH4} h^{-1}**	48	171	6
Emissions savings	**by Biogas**	**Kg_{CO2} h^{-1}**	227	810	28
	by wastewater treatment	**Kg_{CO2} h^{-1}**	7.86	7.86	7.86
	Total		235	818	36

Factoring the contribution of the MECs into the energy balance, the MEC integration becomes a net positive element which translates into the CO_2 emissions saving (in kg_{CO2} h^{-1}) depicted in

Table 22, corresponding to 3% and 10% of the natural gas related emissions for MEC-35 and MEC-55 respectively. These calculations were performed under the assumptions in Appendix C of a town containing 7700 persons with 160 L person^{-1} day^{-1} of wastewater for three different MEC cases, MEC-35, MEC-55 and MEC-reference, representing the average baseline performance of the MECs established in Section 4.3 at 35°C and 800 mV. This scenario models the Huntly power plant near Auckland as an example of a power plant located in a small town near a major city, as also occurs in Chile with Ventanas hosting most of the power generation for Santiago, or in the United Kingdom with Didcot supplying power for London.

MEC-35 and MEC-55 have methane production rates of 56 and 200 mL CH_4 L^{-1} h^{-1} respectively which would enable them to generate approximately 1000 and 4000 kg_{CH4} day^{-1} based on the wastewater organic load available. This is sufficient energy to offset the energy consumption of 340 and 1200 average New Zealanders respectively (Laboratory, n.d.), representing approximately 16% of the simulated population.

The emission rates of integration of both MECs are compared to the base case in Table 23. Both MEC-35 and MEC-55 result in a reduction in the emission rate arising from reduced combustion emissions and savings in the supply chain emissions. The overall impact on CO_2 emissions for the power plant is relatively modest, however, with only a 4 % improvement in the overall emission rate for the best-performing MEC-55 case. This is primarily limited by wastewater availability and the use of wastewater from a larger city (e.g., Auckland) could lead to a more substantial reduction in the emission rate.

Figure 29 depicts the fossil fuel dependency when a hypothetical MEC without any mass or kinetic limitations is simulated. The MEC would provide biomethane to replace fossil-origin natural gas, reducing the overall emissions. However, by reducing the emissions, less carbon is available for biomethane production, leading to an increase of the percentage of fossil fuel needed to offset this effect, subsequently increasing the biomethane production. These oscillations (see Figure 28) decrease after roughly 40 cycles before converging to the values used for the comparison between different recycling rates and conversion efficiencies.

As expected, a higher rate of CO_2 recycling achieves a greater reduction of the fossil fuel required to complement the biofuel for power generation, dropping to 6% (Figure 29(B)). Nevertheless, the overall emissions reduction also depends on the conversion efficiency of the MEC being sufficiently high to completely convert the 90% of CO_2 emissions captured by the CCS plant.

Table 23: Emission rate comparison among three different process configurations, for a power operation with coal and natural versus the operation eliminating coal completely.

Fuel	Case	Emissions (tonne CO_2 h^{-1})			Emission Rate (g_{CO_2} kJ^{-1})		Overall Improvement
		combustion	Supply	total	Combustion	Overall	
40% Coal - 60% Natural gas	Base	49.42	11.6	61.0	0.137	0.170	0%
	Mec-35	49.08	11.3	60.3	0.136	0.168	1%
	MEC-55	48.20	10.4	58.6	0.134	0.163	4%
Natural gas + Biogas	Base	32.69	7.7	40.4	0.091	0.11	34%
	MEC-35	32.35	7.3	39.7	0.090	0.110	35%
	MEC-55	31.47	6.5	37.9	0.088	0.105	38%

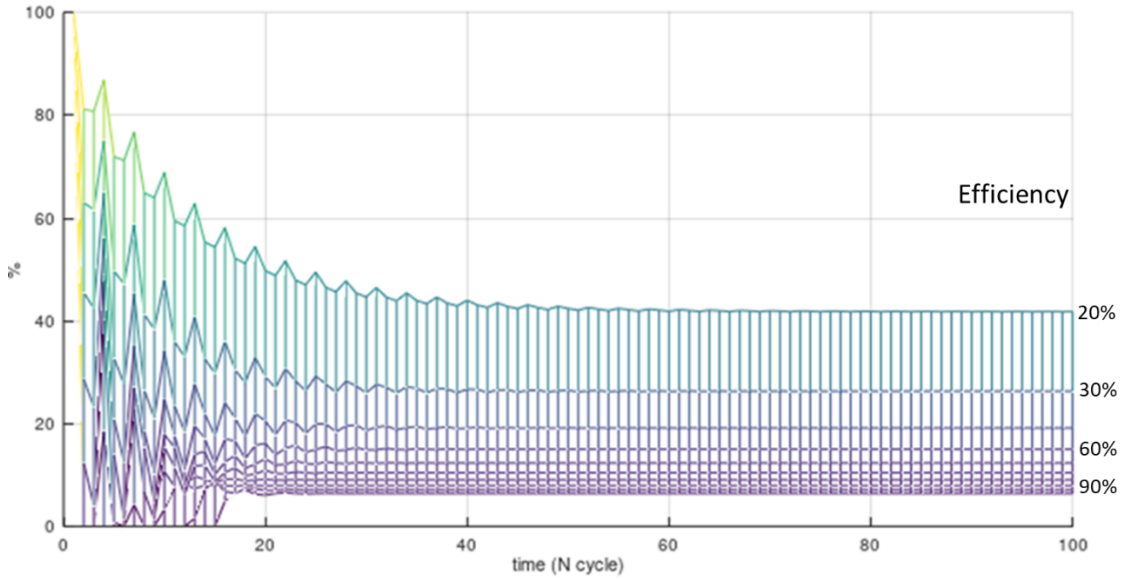

Figure 28: Percentage of fuel from fossil origin required for 90% recycling at multiple conversion efficiencies.

The composition of the fossil fuel used for operating the power plant has a significant effect over the total biomethane production as the fossil fuel emissions, hence, the carbon availability differs (International Energy Agency, 2017). As shown in Table 23, the contribution of MEC integration is maximised when methane (natural gas and biogas) is the sole fuel of the power plant. It is noteworthy here that the emission rate improves by replacing coal by natural gas, but the supply chain emissions of the natural gas used are also reduced by the local bioenergy production from the MECs.

Despite the direct calculation of the emission rate (dividing the emissions calculated by the power demand), these simulations consider only theoretical emission reductions that could be achieved at specific emission recycling and CO_2 conversion efficiencies. To achieve the desired conversion efficiency for 100% CO_2 conversion at the typical wastewater flow rate would require a methane

production rate of 6400 mL CH_4 $L^{-1}h^{-1}$, far in excess of the current technological average of 56 and 200 mL CH_4 L^{-1} h^{-1} for -operations at 35°C and 55 °C respectively. Methane production rates as high as 329 $mL\ CH_4 L^{-1} h^{-1}$ have been reported (K. S. Choi et al., 2017) indicating that complete conversion of the recycled CO_2 would require an increase in CO_2 conversion efficiencies by more than an order of magnitude.

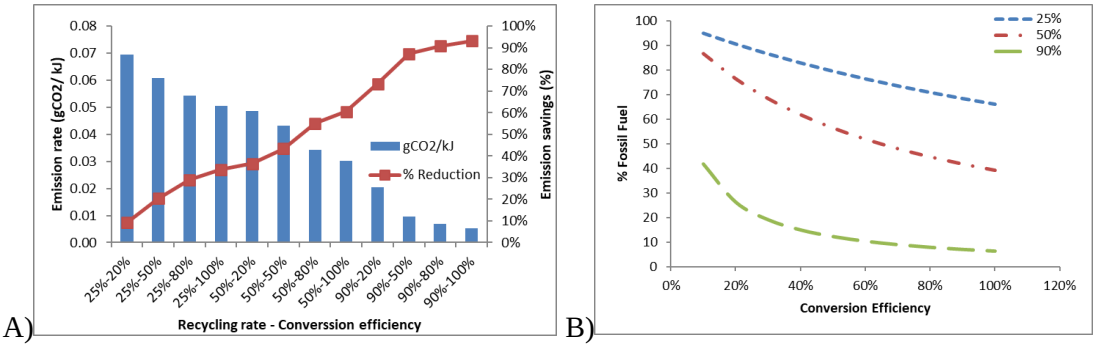

Figure 29. (A) Emission rate and emission saving comparison among different recycling rates (25%, 50%, 90%) and MEC conversion efficiency combinations (20%,50%,80%,100%). (B) . Fossil fuel requirement for different recycling rates at multiple conversion efficiencies.

This also overlooks the organic load limitations as the reduction of CO_2 to CH_4 at the cathode requires a corresponding amount of hydrogen and oxidation reaction arising from the COD of the wastewater. This can be partially overcome if external CO_2 effectively engages the *hydrogenophilic methanogenic* pathway, which is reported to be the dominant operation of MEC-55 °C. Nonetheless, the technology is still not able to make a significant direct contribution if implemented at the power plant level because the required reaction rate is orders of magnitude larger than the current technology allows.

There is substantially more carbon available from power plant emissions than from the domestic wastewater. Table 24 shows the amount of carbon contained in the methane produced by each MEC, it is also calculated the number of MECs that would be needed to produce enough methane to convert the whole 98 $tonne_{Carbon}$ d^{-1} contained in the fossil fuel feed of the base case.

Table 24: Carbon content of methane produced by MECs and how many unitary MECs would be needed to completely fulfil the powerplant fuel consumption.

	Units	MEC-35	MEC -55	MEC-reference
Carbon in Biogas	**tonne C / day**	0.86	3.07	0.11
MECs needed	**number**	115	32	918

Nevertheless, it is noted that the size of the unitary MECs is determined by the wastewater source, therefore, if a mix of carbon sources and wastes streams are used, the methane production rate and total methane production required will change.

7.1.4 Conclusions

The household-level simulations highlighted the possibility of using MECs to store surplus solar energy to counteract seasonal fluctuations. However, methane production is limited by the organic load of domestic wastewater illustrating the need to identify alternative sources of oxidizable organic matter.

By contrast, in the industrial powerplant scenario, the emission rate (in g_{CO2} kJ^{-1}) improves 4% against the base case with the use of MECs. Further improvements rely on increasing the methane production rate as the rate needed to convert all the available carbon is nearly two orders of magnitude above current technological feasibility. The ability to control *hydrogenotrophic methanogenesis* under high concentrations of externally fed CO_2 was highlighted as a particularly important area of future development. In general, the control and modulation of metabolic pathways to improve catalytic performance is a key challenge in MEC development.

7.2. Relevance of direct energy input versus heating and pumping

This section does not intend to present a detailed calculation of the energy demands of the pumping and heating operations, but to estimate them to understand how important they are compared to the energy balance directly implied to the MEC operation.

The industrial power plant scenario works as base, using Equations. (2.21), (2.22), and (2.23) for the estimations under thermophilic and mesophilic operation, and the parameters detailed below:

- 35 -55°C operational temperature
- 15°C ambient temperature
- 48 m^3 h^{-1} wastewater flow
- 1300 m^3 MEC volume
- MEC is a HDPE cylinder of 9 m diameter and 5 m high.

a) Pumping

The effect of temperature over the pump efficiency and viscosity of the fluid among other factors have been ignored, as the intention is to offer a reference of the order of magnitude of the energy demand, and not a detailed study of them. Hence, the following estimate is used for both cases.

$$\boldsymbol{P_h = \frac{q * SG * h}{367} \langle kW \rangle = \frac{48 {}^{m^3}/_{h} * 1 * 5\ m}{367} = 0.65 \langle kW \rangle} \quad (7.8)$$

b) MEC-55 operation (thermophilic)

Here the temperature of operation is assumed 55°C, and a MPR of 5.3 L_{CH4} L^{-1} d^1 (Luo and Angelidaki, 2012) is assumed.

Heat Losses

$$hl\langle kW\rangle = U * A * \Delta T = 0.45\,{}^{W}/_{m^2 * k} * 148m^2 * (328 - 288)\ \mathrm{k}$$

$$= 2.7\ kW$$

Feedstock heating

$$hf = C * Q * \Delta T = 4179.6\,{}^{J}/_{°C * kg} * 1300\,{}^{tonne}/_{h} * (55 - 15)°C$$

$$= 4.1796\,{}^{Mj}/_{°C * tonne} * 1300\,{}^{tonne}/_{h} * (55 - 15)°C$$

$$= 217.3\,{}^{MJ}/_{h} = 60.4kW$$

c) MEC-35 operation (mesophilic)

The mesophilic operation assumes the average MPR of 563 mL_{CH4} L^{-1} d^1, and an operational temperature of 35.

Heat Losses

$$hl\langle kW\rangle = U * A * \Delta T$$

$$= 0.45\,{}^{W}/_{m^2 * k} * 148m^2 * (308 - 288)\mathrm{k} = 0.07\ kW$$

Feedstock heating

$$hf = C * Q * \Delta T$$

$$= 4179.6\,{}^{J}/_{°C * kg} * 1300\,{}^{m^3}/_{h} * (35 - 15)°C$$

$$= 4.1796\,{}^{Mj}/_{°C * tonne} * 1300\,{}^{tonne}/_{h} * (35 - 15)°C = 108.7\,{}^{Mj}/_{h} = 30.4\ kW$$

As explained in Section 2.3, the literature suggests that full engagement of *hydrogenotrophic methanogenesis* would allow an MPR of 5.3 L_{CH4} L^{-1} d^{-1} to be reached (Luo and Angelidaki, 2012). Although it has not been confirmed that this is possible under excess CO_2 conditions, the reference has been used to estimate the equivalent energy recovered through the MEC-35 and MEC-55 operation. Assuming a net calorific value for wastewater of 9.3 kWh m^{-3} (Gil-Carrera et al., 2019) a total energy production of about 2670 kWh would be achieved.

Table 25 depicts the relative % of the energy used for pumping and heating for the operation of the simulated operation of MEC-35 and MEC-55. As expected, the higher temperature gradient

of MEC-55 increases significantly both the heat losses through the wall of the bioreactor and the feedstock heating requirements, which explains why the operation requires a bigger portion of the energy produced. Overall MEC-55, despite needing a higher energy input than MEC-35, as the total available energy after discounting the heating and pumping requirements is still greater for MEC-55. This emphasises the relevance of heating and pumping energy consumptions for MECs operation.

Table 25: Comparison of the energy magnitudes involved directly in the biogas production and secondary energy demands as heat losses and pumping.

Bioreactor	Temperature of operation	Energy demands (kW)				MEC reclaimed (kW)	% of MEC produced
		Pumping	Heat losses	Heating	Total		
MEC-35	35°C	0.65	0.07	30.4	31.12	748	4.2%
MEC-55	55°C	0.65	2.7	217.3	220.65	2670	8.3%

7.3. Perspectives and challenges

7.3.1 MEC Perspectives and future development

Events of excess energy generation from renewable energy plants are increasingly common. In this context, synthetic fuels offer a medium to transfer and store energy in a chemical reactor and convert it back to electricity. Hydrogen is one of the most promising synthetic fuels, although it has a major drawback due to its flammability and low energy density per unit volume, and which requires very expensive storage systems under elevated pressures and/or liquefaction, besides the need for special steels to avoid hydrogen embrittlement. Methane can also be produced from low-quality energy sources in an environmentally friendly manner (Dai et al., 2014).

Additionally, methane can be synthesised from hydrogen and CO_2 and it is a major fuel, with an established distribution network, that can be easily isolated and stored. Finally, MECs offer the possibility of creating a closed cycle where the CO_2 emissions are recycled and used for CH_4 production. However, it is clear that the organic matter oxidation reaction that produces CO_2, acetate and other organic acids is limiting, by quantity if not by rate, which suggests that the use of a sacrificial agent to provide the electrons, or further integration with external sources of hydrogen will be required to enable MEC integration to be feasible.

When it comes to the deployment of the technology, there are two main challenges. The first is finding an abundant and reliable feedstock to overcome the carbon input limitation that arises from using a low strength domestic wastewater. In this sense, the New Zealand biogas potential has been estimated to be almost 5 PJ, primarily from solid waste (2.5 PJ), followed by dairy shed waste (1.5 PJ), and other sources such as sewage biosolids (0.9 PJ), meat processing biosolids (0.6 PJ) and dairy processing biosolids (0.4 PJ) (Luo and Angelidaki, 2012).

Although it is not directly addressed by the simulations of Section 7.1, it is clear from the literature and results from Section 2.6 that, to increase the MEC performance, either the temperature or organic load may be increased within the tolerable range for the bacterial population (Ding et al., 2016). The addition of solid wastes (higher organic load) improves the biogas production, whereas temperature has a rather uncertain effect by itself but is significant when coordinated with solid wastes (Cheng et al., 2009; Kerroum et al., 2014; Xu et al., 2015).

When treating high organic loads, a traditional mesophilic AD (35°C) may suffer inhibition, whereas a thermophilic AD (55°C) would achieve higher digestion rates (Yu et al., 2018), although it would have a higher energy input requirement due to the increased temperature of operation. Therefore, a thermophilic operation may be recommended for industrial applications, whereas, at a household level, a mesophilic operation would be more appropriate as an easier and more reliable operation. Furthermore, the need to activate the *hydrogenophilic methanogenesis* pathway is reduced since no external CO_2 is being fed.

The second challenge is to engage all the available metabolic routes necessary. This highlights the importance of the MEC design and operation, particularly the electrode architecture, materials, and temperature used to develop the highly specialised electro-active microbial communities needed. Also, the time required for the consortium to adapt, especially when hydrogen is injected. The recommended strategy, followed by Villano *et al.*, is to start the bioreactor operation by imposing -850mV to encourage the electrodes' colonisation, changing later to the 200mV intended for the operation (Villano et al., 2016).

This change of imposed voltage during operation may appear trivial during the design process, but it directly influences the underlying biochemical process. As discussed in chapter 4, electrodes are more than a mere substrate; the electrode-microbe relationship can be noticed in the current density. The total current that the power supply must bear is the product of the current density (indicative of the biochemical activity) and the electrodes' surface area (a design feature).

Additionally, the electrode size, position, material, and overall design will affect performance including the mass transfer phenomena. Consequently, the overpotential will be affected, and hence, the maximum overall energy efficiency that the biocathode may attain. It would be interesting to optimise these parameters by modelling the mass transfer effect of electrodes and its effect on the key performance indicators. Park *et al.* investigated the simulation of different electrode separations for their system (Park et al., 2017), although they did not consider electrodes of different relative sizes. These simulations also did not account for changed electrode positions with respect to the feeding nor a sandwich-like electrode package, so there remains considerable additional work to be done.

As shown above, the integration of the MEC to convert the CO_2 recycled from the power plant emissions requires a reaction rate orders of magnitude above the current technological

development. However, an *ex-situ* methanation strategy would allow an anaerobic digestion reactor with a longer HRT as an initial stage (Voelklein et al., 2019), reducing the required reaction rate. In a second stage the biogas upgrading could occur at a faster rate due to optimised hydrogenophilic performance in the biocathode (Kadier et al., 2016a). Some detailed work has been done on this but always using an external hydrogen supply. Hence, integrating an MEC as a methanation stage of CO_2 directly vented from the generator without needing any cleaning nor hydrogen supplementation may result in the possibility to facilitate a carbon circular economy.

Similarly, hydrogen methanation could be performed by injecting externally produced hydrogen into an AD as has been done by (Tao et al., 2020), or into a MEC to increase the conversion rate which is usually controlled by the hydrogen production rate (Kadier et al., 2016a). This is also a possibility that needs further investigation, particularly as a means of storing hydrogen that utilises existing infrastructure, without needing high pressure or cryogenic conditions for long-term energy storage. The development of these processes will go towards solving the increasingly difficult task of matching supply and demand with a greater share of renewable energies in the energy matrix and build capacity to respond to peak demand.

To fully seize the decarbonising potential offered by biological upgrading technologies of biogas, the hydrogen needs to be produced by using renewable energy (Angelidaki et al., 2018). In this sense, when surplus energy is used, the integrated use of water electrolysers and methane electrosynthesis would serve the dual purpose of treating wastes and storing energy from fluctuating sources such as solar and windmills; effectively working as a power-to-gas system (Angelidaki et al., 2018).

This green hydrogen generation and methane electrosynthesis integration overcomes the inherent disadvantage of the low volumetric energy density of hydrogen (10.88 MJ m^{-3}) (Angelidaki et al., 2018). Therefore, this power-to-gas integration is very appealing as an approach to complement wind or solar energy technology with biogas technology.

Overall, such integration significantly reduces the investment costs, as it complements existing anaerobic digesters and other biogas plants already operating, using the biogas as a chemical energy carrier that can be stored in existing natural gas infrastructure with an energy density of about 36 MJ m^{-3}. In addition, it has been highlighted (Kougias et al., 2017) that decoupling the biogas production from biomass would be possible, which, as discussed in Section 7.1, represents the main limitation.

It seems then that an important adaptation of the microbial electrolysis cell technology, and of bio-electrochemical systems in general, will focus on biogas upgrading technologies, or some form of biofuel synthesis. This is due to the inherent advantage of converting CO_2 into a useful and valuable form, such as methane, at mild operating conditions. This is unquestionably a relevant contribution to a sustainable low emission economy.

7.3.2 Operational challenges

To effectively convert hydrogen and CO_2 into methane, the operation needs its parameters carefully monitored and controlled. In this sense, two of the most challenging to control are hydrogen dissolution and pH control.

7.3.2.1 Hydrogen dissolution

Before microorganisms can metabolise the hydrogen, it needs to reach the cells, which means crossing from the gaseous phase into the liquid. This mass transfer is inherently low and negatively affected by the liquid temperature, as shown in Table 1 in Chapter 2.3.

Here, the interaction between the bioreactor design and operational conditions again plays a crucial role. The material and type of hydrogen injector are important and can be complemented with gas recirculation, especially for *in-situ* biogas upgrading applications (Angelidaki et al., 2018).

Although results cannot be directly compared due to the differences in the designs and operational conditions, the operational mode also plays a relevant role. When the CO_2 content fell under 12%, a batch system was reported to diminish its hydrogen uptake rapidly. This would have limited the batch operation to a maximum of 89% methane content in the final off-gas (Agneessens et al., 2017), whereas continuously fed bioreactors with membrane reported 96% and 94% respectively (Luo et al., 2014; Luo and Angelidaki, 2013a). However, the cost of the membrane of the hollow fibre bioreactor presents a serious constraint to full-scale operation despite its more efficient design (Angelidaki et al., 2018).

The comparison between different works using an *ex-situ* upgrading approach highlights the high inflow gas capacity of such a design, getting to a gas retention time as low as 1 h, with off-gas reaching methane contents in the range 79-98% (Angelidaki et al., 2018). The major challenge here seems to be the mass transfer limitation previously mentioned. As seen in Equation (7.9), the H_2 transfer rate between gas and liquid (r_t in L $L^{-1}_{reactor}$ d^{-1}) directly depends on the hydrogen concentration in the gas and liquid phases (H_{2g} and H_{2L}, in mol L^{-1}), and the gas transfer coefficient (K_La in d^{-1}) that is characteristic of the system (diffusion system, reactor, etc) for the given operational conditions (temperature, recirculation rate, etc).

$$r_t = 22.4 * k_La * (H_{2g} - H_{2L}) \qquad (7.9)$$

A secondary issue arising from increasing H_2 concentration is the promotion of volatile fatty acid and alcohol formation. Whereas hydrogen partial pressure over 10 Pa tends to promote the accumulation of ethanol, propionate, and lactate (these work as electron sinks) due to the inhibition of the overall digestion process (Angelidaki et al., 2018). This imbalance can cause additional accumulation of volatile fatty acids. It has been reported that hydrogen injection greater

than the stoichiometric ratio led to the accumulation of acetate, attributable to the combined effect of diminished acetoclastic methanogenesis (inhibited at low pH) and increased homoacetogenic pathway (Agneessens et al., 2017).

7.3.2.2 pH Imbalance

A major concern for a stable operation of anaerobic processes is controlling the pH, so that it does not become inhibitory. However, the inhibitory threshold is not a constant value and varies according to the feedstock flow, nature, and microbial consortium composition (Tao et al., 2020).

Typically, the pH in anaerobic processes is controlled by the equilibrium between bicarbonate and ammonium ions (Alessi et al., 2020). Neutralisation is achieved when an equal molar concentration of NH_4^+ and HCO_3^- is achieved, derived from the dissociation of the metabolic products CO_2 and NH_3 respectively (Tao et al., 2020). Consequently, it can be assumed that the digestate's pH can be controlled by the CO_2 and total ammonia nitrogen concentrations.

The CO_2 present in the digestate produces bicarbonate following Equation (7.10). When the CO_2 is consumed, the amount of bicarbonate is therefore reduced and the pH tends to increase (Angelidaki et al., 2018), even surpassing the threshold of pH 8.5 that has been reported for both mesophilic and thermophilic consortia (Ilaria Bassani, Panagiotis G. Kougias, Laura Treu, 2015), as bicarbonate plays a crucial role as a buffer in biogas producing operations.

$$H_2O + CO_2 \leftrightarrow H^+ + HCO_3^- \qquad (7.10)$$

A main technical challenge that this technology faces is an increase of pH level to values above 8.5, leading to the inhibition of methanogenesis. This issue has been tackled by co-digesting manure and cheese whey to produce a more acidic digestate, which can also be produced by operating the system at shorter HRT (Ye et al., 2012), or directly controlling the pH (G. Luo and Angelidaki, 2013).

The *ex-situ* upgrading system uses a secondary reactor for the injection of both hydrogen and CO_2 produced externally, simplifying the process, and avoiding the organic substrate degradation that makes the biogas production susceptible to the instabilities explained above. In addition, this process is not dependent on biomass; hence it is more flexible and can handle high gas inflows (Angelidaki et al., 2018).

In the context of CO_2 methanation, the partial pressure of CO_2 in the headspace tends to diminish with a rise in pH. This information can be used to construct a pH versus P_{CO2} profile, to estimate the constant "a" for a given system, following Equation 7.11 (Tao et al., 2020). The authors

recommend estimating this constant prior to beginning the CO_2 methanation as it is highly dependent on the feedstock and the particular operating conditions (Tao et al., 2020).

$$a = \frac{\left(10^{-pH^0}\right)^2}{10^{-8.89}+10^{-pH^0}} \cdot \frac{1}{P^0_{CO2}} \qquad (7.11)$$

The constant "a"plays a fundamental role in the predictive model shown in Equation 7.12. This simple model was derived by (Tao et al., 2020) from the chemical equilibria and successfully predicted the pH variation from the CO_2 content in the off-gas, as shown in equation 7.12. Operationally this is relevant as it offers a quick method, easily implemented on an industrial scale, to predict the maximum achievable methane content in the off-gas while conserving a stable operation (Tao et al., 2020).

$$pH = -log_{10}\left(\frac{a \cdot P_{CO2}+\sqrt{a^2 \cdot {P_{CO2}}^2+4 \cdot 10^{-8.89} \cdot a \cdot P_{CO2}}}{2}\right) \qquad (7.12)$$

Further understanding of how the pH balance operates within the context of bio-electrochemical systems will address the architectural design requirements and optimise the operation. A good case in point are the specific adaptations of the MEC for waste-to-energy and the power-to-gas applications, with different functionalities and strengths, highlighting the versatility of MEC platform while indicating the gaps in the knowledge of the underlying molecular process of its operation.

7.3.2.3 Microbial community

Typically, the hydrogen used for methanogenesis is obtained from acetate oxidation in an endergonic reaction that needs the energetic compensation of *hydrogenotrophic methanogen* activity and which reduces the hydrogen content in the off-gas.

When hydrogen is injected, the typical microbial population dynamics are altered, promoting the growth of *hydrogenotrophic methanogens* and homoacetogens such as *Acetobacterium woodii*, *Moorella thermoacetica*, and Clostridium, that produce acetate from CO_2. The *hydrogenotrophic methanogens* are key for the hydrogen utilisation for methane production. This population can be augmented via the cultivation of pure cultures, but it is considered to be more practical to adapt a mixed culture under appropriate conditions, as these cultures tend to be more robust, and do not need sterile conditions thus avoiding additional operational costs (Angelidaki et al., 2018).

It has been suggested (Díaz et al., 2015) that in many cases the limitation for hydrogen uptake comes from mass transfer rather than metabolic capacity or insufficient microbial population, as

hydrogenotrophic bacteria such as *Methanobacterium*, *Methanoculleus*, *Methanomicrobium*, and *Methanothermobacter* are commonly found, whereas *acetoclastic methanogens* such as the *Methanosarcina* are less abundant (Agneessens et al., 2017; Ilaria Bassani, Panagiotis G. Kougias, Laura Treu, 2015).

Interestingly, when the injection of hydrogen leads to high H_2 partial pressures within the bioreactor, multiple effects have been reported. A relevant example is the reduction in the growth yield of the methanogen *M. thermoautotrophicum*, attributed by the authors to the transcription of methanogenesis-related genes in the presence of hydrogen (Angelidaki et al., 2018). Therefore, hydrogen injection does not just impact the species present within the consortium but directly promotes transcriptional activity.

Considering the case where the hydrogen uptake of an operation is limited by hydrogen availability instead of the metabolic rate, suggests a clear path for technological development in the design of the bioreactors and the need for incremental improvements to attain the required conditions for the desired reaction to occur. This strategy would move methanation and upgrading technologies toward pilot and industrial-scale tests.

7.3.2.4 Scaling up

A major challenge for MECs, and all bioelectrochemical systems (BES), is the scaling-up process. Scaling up bio-electrochemical systems is particularly complex as their performance relies on a series of factors such as the metabolic and physiological capacity of the culture, electrode architecture, feedstock, and the interaction between them (Sharma et al., 2014).This unique interplay between bacterial consortia, mass transfer, and reactor design as has been discussed previously, and its scaling up is not a task that can be directly implemented from general correlations without going through laboratory and pilot plant phases to determine the optimum operational conditions.

Scale translation has been extensively studied for inanimate matter, basing the approach on the correlation of the variables involved using a dimensional analysis that will feed through to the new conditions. Effectively, some variables will remain constant such as the temperature, pH, but the mixing, gas injection, heat losses, and other requirements will change significantly (Acevedo et al., 2002). At this point, BES and their characteristic bioelectrodes present several other variables, as they include a biofilm that will constantly interact and adapt to/with the environment in terms of its shape, size, constitution, and activity. As discussed in Section 2.7, due to this constant self-adaptation, the natural key performance indicator and scaling up criterion (current density) is hardly appropriate.

Nevertheless, some general relationships have been established. The literature recommends the use of porous electrodes and decreasing the distance between them to achieve higher current densities, which would translate into higher production rates, but lower energy efficiencies (Sharma et al., 2014). Identifying these rules and how different parameters interact is essential for the operationalisation of current knowledge to achieve efficient conversion of CO_2 into CH_4.

For BES in general, knowing how the different parameters affect and influence the microbiological component is central to harnessing the metabolic capacity of the bioelectrodes to transform energy between chemical and electrical forms by the exoelectrogens colonising the electrodes. (Xie et al., 2015).

The bacterial colonisation of electrodes provides another challenge for the scaling-up process, as special conditions may be needed to ensure a mature biofilm formation over the electrodes. Bacterial cell surfaces are usually negatively charged, hence, anodes are more likely to be colonised than cathodes (Guo et al., 2015), but both electrodes need to be colonised to maintain a balanced operation. Some researchers have used different conditions for the start-up phase, initially applying -850 mV vs. SHE to ensure the biofilm development and then changing to +500 mV vs. SHE (Villano et al., 2011). This strategy highlights the importance of the microbiological dynamics, where different bacteria fulfill different functions, where some work as anchors the solid electrode, others -electroactive bacteria- facilitate electrical interactions and produce electron shuttles or recycle cell lysis products, as mentioned in section 2.3 (Dykstra and Pavlostathis, 2017).

In this study instead, the relative size between anode and cathode has drawn an important share of the attention and has indeed an important effect on the overall performance, but the simple flat design of the electrodes used here is far from the maximum surface area that could be fitted in the bioreactors. The systematically tested concept of favouring the cathodic surface area combined with ample material testing and innovative electrode design such as the spiral wound electrode proposed by (Hou et al., 2015) would optimise the use of the space and resources when designing a MEC.

Chapter 8 Conclusions

This study aimed to operationalise the knowledge regarding MECs operation for biogas production. To achieve this, a series of controlled bio-electrochemical tests were run under specific environmental conditions, organised in statistical designs of experiments full factorial designs. It was proven here that efficient methane production in membraneless MECs, with sandwich-like carbon felt electrodes is possible and is more efficient than a traditional AD reactor.

The sensitivity to a series of individual and combined operational conditions was assessed, finding that MECs are more resilient and efficient at low organic loads than traditional AD operated under analogous conditions and having limited advantages at high organic loads despite the increased methane production. Additionally, *in-situ* hydrogen methanation was evaluated and compared to MEC-OCP tests, highlighting the necessary specificity of the operation targeting to recruit different metabolic pathways and the effect of these on the overall performance.

In this sense, organic load, applied voltage, and favouring the cathodic surface area have a positive correlation with methane production, although the MCR improves as the organic load decreases. When both bio-electrochemical systems are compared, MEC B consistently outperformed MEC A, regardless of the organic load, and in spite of its smaller electrode surface area. The difference is even clearer when the results are normalised to the surface area, highlighting that favouring the cathodic surface area significantly improves the methane production efficiency and overall energy recovery from synthetic municipal wastewater.

As expected, the applied voltage plays a key role in the MECs' performance, with a positive correlation for both MPR and MCR when the applied voltage surpasses 600 mV. However, applying an adequate voltage and favouring the cathodic reaction surface translates into a limited improvement unless sufficient carbon supply is available to increase the MPR. This restriction emphasises the relevance of optimising HRT to provide sufficient organic load while avoiding washouts and incomplete organic matter conversion. When the balance between the higher MPR obtained (high organic load) and a reasonable efficiency (characteristic of carbon source restriction) is achieved, the energy storage efficiency can be maximised. A 33% energy storage efficiency was achieved with MEC B when imposing 1000 mV and with 10 days' HRT, almost 3 times the 12% achieved in similar conditions by the traditional AD system.

The study of the correlation between performance and operational conditions organised as a full factorial design of experiments has been presented. A zone of best performance was proposed for each MEC as well as information regarding how performance would be affected as the operational parameters vary. These relationships are expected to contribute to the MEC technology deployment.

Two different case scenarios of MEC integration were simulated to assess the potential contribution of MECs towards a low emission economy. Household-level simulations highlighted the feasibility of surplus solar energy storage. However, the organic load available from typical domestic wastewater illustrates the need to identify alternative sources of oxidizable organic matter. On the other hand, simulations at the industrial scale showed that the MEC contribution is rate limited. Therefore, hydrogenotrophic methanogenesis engagement appears crucial to converting greater amounts of externally produced CO_2. Here, this methanogenic pathway has not been recruited at full capacity due to the operational conditions tested.

Overall, metabolic control and modulation is a key challenge in MECs' development and hence the role the technology will play going towards a low emission economy. The results obtained here suggest that modulation could be achievable by favouring one electrode surface area according to the targeted product. Thus, this study contributed to the MEC development with new insights regarding the overall performance sensitivity to both the operational conditions and some key feature designs, as the electrodes' relative size.

The relative electrodes surface area was proven to work as a rule of thumb to enhance the overall methane production, but a simple plain sheet design was used, which leaves space for a significant improvement in terms of potential performance improvement. Therefore, it is expected that this work will enrich the innovative electrode design to go beyond the physical challenge of maximising the available surface area, thus contributing to the technology development and successful deployment to decarbonise the energy matrix.

Chapter 9 Future Work

Microbial electrolysis cells are becoming a very versatile platform, where each new application brings challenges and opportunities. In the perspectives and challenges section above areas of interest for the waste-to-energy and the power-to-gas applications involved in this study have already been discussed, so here will be introduced what are considered the more relevant areas of work, pointing out what the most necessary topics are, and how they could be addressed to continuing bridging the knowledge for optimising performance and upscale the laboratory experience into the industrial environment.

Two different applications in the waste-to-energy context have been investigated here and the MEC-AD integration will play a relevant role in the deployment of the technology. Based on the improved performance of the MECs when compared to a traditional AD operated under similar conditions, the next step is to design a MEC that can be retrofitted into operational AD plants, with the design of electrodes being a key element for the bio-electrodes performance.

The term bio-electrodes emphasises the role of the microbial consortium, which with the solid-state electrode underneath, fulfils more functions than just conducting electricity. It also offers a channel to discharge the metabolic wastes of the biofilm, allows (or can hinder) the through flow of fluids and facilitates the overall mass transfer of nutrients to the microorganisms. Due to its overall architecture, it will affect the fluid dynamics within the MEC and affect the interaction between the biofilm macrostructure and the digestate flows. Therefore, it is relevant to work further on multiphysics designs of electrodes, including the knowledge gained from comprehensive material testing, and employ innovative designs to maximise the surface area, prioritising cathodic surface, and it needs also to consider mass transfer and fluid dynamics.

Initially, this design work could be performed with computer simulations to optimise resource usage and allow more innovative approaches. Nevertheless, this approach would simultaneously pave the path toward the scaling-up process, necessary to go from the laboratory to the industrial-scale. As it has been discussed, some peculiarities of the MECs make a direct geometrical scale-up process unlikely. The sole use of carbon felt for the electrodes, as in this study, makes it necessary to provide supports at a bigger scale due to their soft nature; this is just one example, as the particular application will impose many different constrictions and material needs.

MEC-AD operation is very different from a hydrogen methanation device, working at a different temperature range, relying on different microbial consortia, etc. Nevertheless, hydrogen methanation is a promising application of the technology, as the hydrogen economy is advancing fast and many countries have decided to invest important resources to develop it.

In a hydrogen economy context, MEC focused on methanation could have a pivotal role to play, allowing to simultaneously treat the CO_2 emissions from industrial processes and offer a more

economically viable alternative to high pressure or cryogenic hydrogen storage. In this sense, and beyond the technical design and feasibility, an important topic that has been left for future investigation, due to the early development stage of the technology, is cost modelling. Especially when aiming at energy storage, the MEC needs to be integrated into the energy matrix, and cost efficiency becomes one of the key performance indicators to drive the decision-making process.

References

Acevedo, F., Gentina, J., Illanes, A., 2002. Fundamentos de Ingenieria Bioquimica, Third. ed. Ediciones Universitarias de Valparaiso, Valparaiso.

Achinas, S., Jan, G., Euverink, W., 2016. Theoretical analysis of biogas potential prediction from agricultural waste. Resour. Technol. 2, 143–147. https://doi.org/10.1016/j.reffit.2016.08.001

Agneessens, L.M., Ottosen, L.D.M., Voigt, N.V., Nielsen, J.L., de Jonge, N., Fischer, C.H., Kofoed, M.V.W., 2017. In-situ biogas upgrading with pulse H2 additions: The relevance of methanogen adaption and inorganic carbon level. Bioresour. Technol. 233, 256–263. https://doi.org/10.1016/j.biortech.2017.02.016

Al Seadi, T., Rutz, D., Prassl, H., Kottner, M., Finsterwalder, T., Volk, S., Jansen, R., 2008. Biogas Handbook.

Alessi, A.M., Tao, B., Zhang, W., Zhang, Y., Heaven, S., Banks, C.J., Chong, J.P.J., 2020. A rapid, sensitive, low-cost assay for detecting hydrogenotrophic methanogens in anaerobic digesters using loop-mediated isothermal amplification. Microorganisms 8. https://doi.org/10.3390/microorganisms8050740

Angelidaki, I., Treu, L., Tsapekos, P., Luo, G., Campanaro, S., Wenzel, H., Kougias, P.G., 2018. Biogas upgrading and utilization: Current status and perspectives. Biotechnol. Adv. 36, 452–466. https://doi.org/10.1016/j.biotechadv.2018.01.011

Ardani, K., O'Shaughnessy, E., Fu, R., Mc Clurg, C., Huneycutt, J., Margolis, R., 2017. Installed Cost Benchmarks and Deployment Barriers for Residential Solar Photovoltaics with Energy Storage: Q1 2016. NREL Tech. Rep. 30.

Bachmann, N., 2015. Sustainable biogas production in municipal wastewater treatment plants, IEA Bioenergy.

Baek, G., Kim, J., Lee, S., Lee, C., 2017. Development of biocathode during repeated cycles of bioelectrochemical conversion of carbon dioxide to methane. Bioreasource Technol. 1201–1207.

Balcombe, P., Anderson, K., Speirs, J., Brandon, N., Hawkes, A., 2015. Methane and CO2 emissions from the natural gas supply chain: an evidence assessment.

Bensmann, A., Hanke-Rauschenbach, R., Heyer, R., Kohrs, F., Benndorf, D., Reichl, U., Sundmacher, K., 2014. Biological methanation of hydrogen within biogas plants: A model-based feasibility study. Appl. Energy 134, 413–425. https://doi.org/10.1016/j.apenergy.2014.08.047

Bodegom, P. Van, 2007. Microbial Maintenance: A Critical Review on Its Quantification 53, 513–523. https://doi.org/10.1007/s00248-006-9049-5

Bright Hub Engineering, 2019. The Efficiency of Power Plants of Different Types [WWW Document]. URL https://www.brighthubengineering.com/power-plants/72369-compare-the-efficiency-of-different-power-plants/

Burkhardt, M., Busch, G., 2013. Methanation of hydrogen and carbon dioxide. Appl. Energy 111, 74–79. https://doi.org/10.1016/j.apenergy.2013.04.080

Cai, W., Han, T., Guo, Z., Varrone, C., Wang, A., Liu, W., 2016. Methane production enhancement by an independent cathode in integrated anaerobic reactor with microbial electrolysis. Bioresour. Technol. 208, 13–18. https://doi.org/10.1016/j.biortech.2016.02.028

Cerrillo, M., Vinas, M., Bonmatí, A., 2017. Startup of Electromethanogenic Microbial Electrolysis Cells with Two Different Biomass Inocula for Biogas Upgrading. ACS

Sustain. Chem. Eng. 5, 8852–8859. https://doi.org/10.1021/acssuschemeng.7b01636

Cheng, S., Xing, D., Call, D.F., Logan, B.E., 2009. Direct biological conversion of electrical current into methane by electromethanogenesis. Environ. Sci. Technol. 43, 3953–3958. https://doi.org/10.1021/es803531g

Choi, K.-S., Kondaveeti, S., Min, B., 2017. Bioelectrochemical methane (CH4) production in anaerobic digestion at different supplemental voltages. Bioresour. Technol. 245, 826–832. https://doi.org/10.1016/j.biortech.2017.09.057

Choi, K.S., Kondaveeti, S., Min, B., 2017. Bioelectrochemical methane (CH4) production in anaerobic digestion at different supplemental voltages. Bioresour. Technol. 245, 826–832. https://doi.org/10.1016/j.biortech.2017.09.057

Clauwaert, P., Verstraete, W., 2009. Methanogenesis in membraneless microbial electrolysis cells. Appl. Microbiol. Biotechnol. 82, 829–836. https://doi.org/10.1007/s00253-008-1796-4

Dai, P., Chen, Z., Chen, S., 2014. Ignition of methane with hydrogen and dimethyl ether addition. FUEL 118, 1–8. https://doi.org/10.1016/j.fuel.2013.10.048

Dai, Z., Heidrich, E., Dolfing, J., Jarvis, A., 2019. Determination of the Relationship between the Energy Content of Municipal Wastewater and Its Chemical Oxygen Demand 396–400. https://doi.org/10.1021/acs.estlett.9b00253

Deutzmann, J.S., Sahin, M., Spormann, A.M., 2015. Extracellular Enzymes Facilitate Electron Uptake in Biocorrosion and Bioelectrosynthesis. MBio 6, 1–8. https://doi.org/10.1128/mBio.00496-15.Editor

Díaz, I., Pérez, C., Alfaro, N., Fdz-Polanco, F., 2015. A feasibility study on the bioconversion of CO2 and H2 to biomethane by gas sparging through polymeric membranes. Bioresour. Technol. 185, 246–253. https://doi.org/10.1016/j.biortech.2015.02.114

Ding, A., Yang, Y., Sun, G., Wu, D., 2016. Impact of applied voltage on methane generation and microbial activities in an anaerobic microbial electrolysis cell (MEC). Chem. Eng. J. 283, 260–265. https://doi.org/10.1016/j.cej.2015.07.054

Dou, Z., Dykstra, C.M., Pavlostathis, S.G., 2018. Bioelectrochemically assisted anaerobic digestion system for biogas upgrading and enhanced methane production. Sci. Total Environ. 633, 1012–1021. https://doi.org/10.1016/j.scitotenv.2018.03.255

Dykstra, C.M., Pavlostathis, S.G., 2017. Methanogenic Biocathode Microbial Community Development and the Role of Bacteria. Environ. Sci. Technol. 51, 5306–5316. https://doi.org/10.1021/acs.est.6b04112

EIA, 2014. Tables 1.3, 2.1--2.6, Primary Energy Consumption by Source and Sector, 2013. Energy Inf. Adm. 2012, 2014.

Escapa, A., Gómez, X., Tartakovsky, B., Morán, A., 2012. Estimating microbial electrolysis cell (MEC) investment costs in wastewater treatment plants: Case study. Int. J. Hydrogen Energy 37, 18641–18653. https://doi.org/10.1016/j.ijhydene.2012.09.157

Flores-Rodriguez, C., Min, B., 2020. Enrichment of specific microbial communities by optimum applied voltages for enhanced methane production by microbial electrosynthesis in anaerobic digestion. Bioresour. Technol. 300, 122624. https://doi.org/10.1016/j.biortech.2019.122624

Fradler, K.R., Kim, J.R., Shipley, G., Massanet-Nicolau, J., Dinsdale, R.M., Guwy, A.J., Premier, G.C., 2014. Operation of a bioelectrochemical system as a polishing stage for the effluent from a two-stage biohydrogen and biomethane production process. Biochem. Eng. J. 85, 125–131. https://doi.org/10.1016/j.bej.2014.02.008

Fu, Q., Kobayashi, H., Kawaguchi, H., Vilcaez, J., Sato, K., 2013. Identification of new microbial mediators for electromethanogenic reduction of geologically-stored carbon dioxide. Energy Procedia 37, 7006–7013. https://doi.org/10.1016/j.egypro.2013.06.635

Gajaraj, S., Huang, Y., Zheng, P., Hu, Z., 2017. Methane production improvement and associated methanogenic assemblages in bioelectrochemically assisted anaerobic digestion. Biochem. Eng. J. 117, 105–112. https://doi.org/10.1016/j.bej.2016.11.003

Garcia-Pena, J.G.-R.R.G.-G.I.C.L.T.E., 2015. Continuous two-staged co-digestion process for biohydrogen production from agro-industrial waste. Int. J. Energy Res. 40, 257–272.

Geetha, K., Raj, S.A., 2015. Biomass-electrochemical integrated system for distillery wastewater treatment with electricity generation using anaerobic mixed consortium in microbial fuel cells. Int. J. Environ. Waste Manag. 15, 217–234. https://doi.org/10.1504/IJEWM.2015.069131

Geppert, F., Liu, D., van Eerten-Jansen, M., Weidner, E., Buisman, C., ter Heijne, A., 2016. Bioelectrochemical Power-to-Gas: State of the Art and Future Perspectives. Trends Biotechnol. 34, 879–894. https://doi.org/10.1016/j.tibtech.2016.08.010

Gil-Carrera, L., Browne, J.D., Kilgallon, I., Murphy, J.D., 2019. Feasibility study of an off-grid biomethane mobile solution for agri-waste. Appl. Energy 239, 471–481. https://doi.org/10.1016/j.apenergy.2019.01.141

Gil-Carrera, L., Escapa, A., Carracedo, B., Morán, A., Gómez, X., 2013. Performance of a semi-pilot tubular microbial electrolysis cell (MEC) under several hydraulic retention times and applied voltages. Bioresour. Technol. 146, 63–69. https://doi.org/10.1016/j.biortech.2013.07.020

Gil-Carrera, L., Mehta, P., Escapa, A., Morán, A., García, V., Guiot, S.R., Tartakovsky, B., 2011. Optimizing the electrode size and arrangement in a microbial electrolysis cell. Bioresour. Technol. 102, 9593–9598. https://doi.org/10.1016/j.biortech.2011.08.026

Goh, C.-P., Lim, P.-E., 2008. Potassium Permanganate As Oxidant in the Cod Test for Saline Water Samples. ASEAN J. Sci. Technol. Dev. 25, 383–393. https://doi.org/10.29037/ajstd.269

Gondal, I.A., 2019. Hydrogen integration in power-to-gas networks. Int. J. Hydrogen Energy 44, 1803–1815. https://doi.org/10.1016/j.ijhydene.2018.11.164

Guangyin Zhen; Shaojuan Zheng, ; Xuequin Lu; Xuefeng Zhu; Juan Mei; Takuro Kobayashi; Kaiqin Xu; Yu-You Li; Youcai Zhao, 2018. A comprehensive comparison of five different carbon-based cathode materials in CO2 electromethanogenesis: Long-term performance, cell-electrode contact behaviors and extracellular electron transfer pathways 382–388.

Guo, K., Prévoteau, A., Patil, S.A., Rabaey, K., 2015. Engineering electrodes for microbial electrocatalysis. Curr. Opin. Biotechnol. 33, 149–156. https://doi.org/10.1016/j.copbio.2015.02.014

Guo, X., Liu, J., Xiao, B., 2013. Bioelectrochemical enhancement of hydrogen and methane production from the anaerobic digestion of sewage sludge in single-chamber membrane-free microbial electrolysis cells. Int. J. Hydrogen Energy 38, 1342–1347. https://doi.org/10.1016/j.ijhydene.2012.11.087

Guo, Z., Thangavel, S., Wang, L., He, Z., Cai, W., Wang, A., Liu, W., 2017. Efficient methane production from beer wastewater in a membraneless microbial electrolysis cell with a stacked cathode: The effect of the cathode/anode ratio on bioenergy recovery. Energy and Fuels 31, 615–620. https://doi.org/10.1021/acs.energyfuels.6b02375

Hao, X., Li, J., van Loosdrecht, M.C.M., Jiang, H., Liu, R., 2019. Energy recovery from wastewater: Heat over organics. Water Res. 161, 74–77. https://doi.org/10.1016/j.watres.2019.05.106

Hara, M., Onaka, Y., Kobayashi, H., Fu, Q., Kawaguchi, H., Vilcaez, J., Sato, K., 2013. Mechanism of electromethanogenic reduction of CO2 by a thermophilic methanogen. Energy Procedia 37, 7021–7028. https://doi.org/10.1016/j.egypro.2013.06.637

Heidrich, E.S., Curtis, T.P., Dolfing, J., 2010. Additional information on the data calculated for use in the study . 3–5.

Hiranga Energy, n.d. How Hydrogen Will Play a Key Role in Our New Energy Future.

Hou, Y., Zhang, R., Luo, H., Liu, G., Kim, Y., Yu, S., Zeng, J., 2015. Microbial electrolysis cell with spiral wound electrode for wastewater treatment and methane production. Process Biochem. 50, 1103–1109. https://doi.org/10.1016/j.procbio.2015.04.001

Hu, Z., Grasso, D., 2005. Encyclopedia of Analytical Science. https://doi.org/10.1016/B0-12-369397-7/00663-4

Huong Le, T.X., Bechelany, M., Cretin, M., 2017. Carbon felt based-electrodes for energy and environmental applications: A review. Carbon N. Y. 122, 564–591. https://doi.org/10.1016/j.carbon.2017.06.078

Ilaria Bassani, Panagiotis G. Kougias, Laura Treu, and I.A., 2015. Biogas Upgrading via Hydrogenotrophic Methanogenesis in Two-Stage Continuous Stirred Tank Reactors at Mesophilic and Thermophilic Conditions. Environ. Sci. Technol. 49, 12585–12593.

International Energy Agency, 2017. CO2 emissions from fuel combustion: Highlights.

Jang, H.M., Kim, M.S., Ha, J.H., Park, J.M., 2015. Reactor performance and methanogenic archaea species in thermophilic anaerobic co-digestion of waste activated sludge mixed with food wastewater. Chem. Eng. J. 276, 20–28. https://doi.org/10.1016/j.cej.2015.04.072

Jung, S., Lee, J., Park, Y.K., Kwon, E.E., 2020. Bioelectrochemical systems for a circular bioeconomy. Bioresour. Technol. 300. https://doi.org/10.1016/j.biortech.2020.122748

Kadier, A., Simay, Y., Abdeshahian, P., Azman, N., Chandrasekhar, K., Kalil, M., 2016a. A comprehensive review of microbial electrolysis cells (MEC) reactor designs and configurations for sustainable hydrogen gas production. Alexandria Eng. J. 55, 427–443. https://doi.org/10.1016/j.aej.2015.10.008

Kadier, A., Simay, Y., Abdeshahian, P., Azman, N., Chandrasekhar, K., Kalil, M., 2016b. A comprehensive review of microbial electrolysis cells (MEC) reactor designs and configurations for sustainable hydrogen gas production. Alexandria Eng. J. 55, 427–443. https://doi.org/10.1017/CBO9781107415324.004

Kaneco, S., Hiei, N.H., Xing, Y., Katsumata, H., Ohnishi, H., Suzuki, T., Ohta, K., 2002. Electrochemical conversion of carbon dioxide to methane in aqueous NaHCO3 solution at less than 273 K. Electrochim. Acta 48, 51–55. https://doi.org/10.1016/S0013-4686(02)00550-9

Katuri, K.P., Ali, M., Saikaly, P.E., 2019. The role of microbial electrolysis cell in urban wastewater treatment: integration options, challenges, and prospects. Curr. Opin. Biotechnol. 57, 101–110. https://doi.org/10.1016/j.copbio.2019.03.007

Kerroum, D., Mossaab, B., Hassen, A., 2014. Production of bio-energy from organic waste: effect of temperature and substrate composition. Int. J. energy 38, 270–276.

Kougias, P., Treu, L., Peñailillo, D., Boe, K., Campanaro, S., Angelidaki, I., 2017. Ex-situ biogas upgrading and enhancement in different reactor systems. Bioresour. Technol. https://doi.org/10.1016/j.biortech.2016.11.124

Krich, K.K., Augenstein, D., Batmale, J., Benemann, J., Rutledge, B., Salour, D., 2005. Stoichiometry of the Anaerobic Digestion Process. Biomethane from Dairy Waste A Sourceb. Prod. Use Renew. Nat. Gas Calif.

Kumar, M., Sundaram, S., Gnansounou, E., Larroche, C., Thakur, I.S., 2018. Carbon dioxide capture, storage and production of biofuel and biomaterials by bacteria: A review. Bioresour. Technol. 247, 1059–1068. https://doi.org/10.1016/j.biortech.2017.09.050

Kuramochi, Y., Fu, Q., Kobayashi, H., Ikarashi, M., Wakayama, T., Kawaguchi, H., Vilcaez, J., Maeda, H., Sato, K., 2013. Electromethanogenic CO2 conversion by subsurface-reservoir microorganisms. Energy Procedia 37, 7014–7020. https://doi.org/10.1016/j.egypro.2013.06.636

Laboratory, N.R.E., n.d. System Advisor Model.

Lecker, B., Illi, L., Lemmer, A., Oechsner, H., 2017. Biological hydrogen methanation – A review. Bioresour. Technol. 245, 1220–1228. https://doi.org/10.1016/j.biortech.2017.08.176

Leung, D.Y.C., Caramanna, G., Maroto-Valer, M.M., 2014. An overview of current status of carbon dioxide capture and storage technologies. Renew. Sustain. Energy Rev. 39, 426–443. https://doi.org/10.1016/j.rser.2014.07.093

Li, W.W., Yu, H.Q., Rittmann, B.E., 2015. Chemistry: Reuse water pollutants. Nature 528, 29–31. https://doi.org/10.1038/528029a

Li, X., Zeng, C., Lu, Y., Liu, G., Luo, H., Zhang, R., 2019. Development of methanogens within cathodic biofilm in the single-chamber microbial electrolysis cell. Bioresour. Technol. https://doi.org/10.1016/j.biortech.2018.12.002

Li, Y., Zhang, Y., Liu, Y., Zhao, Zhiqiang, Zhao, Zisheng, Liu, S., Zhao, H., Quan, X., 2016. Enhancement of anaerobic methanogenesis at a short hydraulic retention time via bioelectrochemical enrichment of hydrogenotrophic methanogens. Bioresour. Technol. 218, 505–511. https://doi.org/10.1016/j.biortech.2016.06.112

Liu, D., Zhang, L., Chen, S., Buisman, C., Ter Heijne, A., 2016. Bioelectrochemical enhancement of methane production in low temperature anaerobic digestion at 10 °C. Water Res. 99, 281–287. https://doi.org/10.1016/j.watres.2016.04.020

Liu, H., Grot, S., Logan, B., 2005. Electrochemically Assisted Microbial Production of Hydrogen from Acetate 39, 4317–4320.

Liu, S.Y., Charles, W., Ho, G., Cord-Ruwisch, R., Cheng, K.Y., 2017. Bioelectrochemical enhancement of anaerobic digestion: Comparing single- and two-chamber reactor configurations at thermophilic conditions. Bioresour. Technol. 245, 1168–1175. https://doi.org/10.1016/j.biortech.2017.08.095

Liu, W., Cai, W., Guo, Z., Wang, L., Yang, C., Varrone, C., Wang, A., 2016. Microbial electrolysis contribution to anaerobic digestion of waste activated sludge, leading to accelerated methane production. Renew. Energy 91, 334–339. https://doi.org/10.1016/j.renene.2016.01.082

Liu, W., Wang, L., Gao, L., Wang, A.J., 2018. Hydrogen and methane production in bioelectrochemical system:: Biocathode structure and material upgrading, Biomass, Biofuels, Biochemicals: Microbial Electrochemical Technology: Sustainable Platform for Fuels, Chemicals and Remediation. Elsevier B.V. https://doi.org/10.1016/B978-0-444-64052-9.00038-8

Logan, B.E., Wallack, M.J., Kim, K.Y., He, W., Feng, Y., Saikaly, P.E., 2015. Assessment of Microbial Fuel Cell Configurations and Power Densities. Environ. Sci. Technol. Lett. 2, 206–214. https://doi.org/10.1021/acs.estlett.5b00180

Luo, Gang, Angelidaki, I., 2013. Hollow fiber membrane based H2 diffusion for efficient in situ biogas upgrading in an anaerobic reactor. Appl. Microbiol. Biotechnol. 97, 3739–3744. https://doi.org/10.1007/s00253-013-4811-3

Luo, G., Angelidaki, I., 2013. Co-digestion of manure and whey for in situ biogas upgrading by the addition of H2: Process performance and microbial insights. Appl. Microbiol. Biotechnol. 97, 1373–1381. https://doi.org/10.1007/s00253-012-4547-5

Luo, G., Angelidaki, I., 2012. Integrated biogas upgrading and hydrogen utilization in an anaerobic reactor containing enriched hydrogenotrophic methanogenic culture. Biotechnol. Bioeng. 109, 2729–2736. https://doi.org/10.1002/bit.24557

Luo, G., Wang, W., Angelidaki, I., 2014. A new degassing membrane coupled upflow anaerobic sludge blanket (UASB) reactor to achieve in-situ biogas upgrading and recovery of dissolved CH4 from the anaerobic effluent. Appl. Energy 132, 536–542. https://doi.org/10.1016/j.apenergy.2014.07.059

Manjusha, C., Beevi, S., 2016. Mathematical Modeling and Simulation of Anaerobic Digestion

of Solid Waste. Procedia Technol. 24, 654–660. https://doi.org/10.1016/j.protcy.2016.05.174

Mateos, R., Escapa, A., San-Martín, M.I., De Wever, H., Sotres, A., Pant, D., 2020. Long-term open circuit microbial electrosynthesis system promotes methanogenesis. J. Energy Chem. https://doi.org/10.1016/j.jechem.2019.04.020

Mayer, F., Enzmann, F., Lopez, A.M., Holtmann, D., 2019. Performance of different methanogenic species for the microbial electrosynthesis of methane from carbon dioxide. Bioresour. Technol. https://doi.org/10.1016/j.biortech.2019.121706

McCarty, S., Jones, E., Finnegan, S., Woods, E., Cochrane, C., Percival, S., 2014. Chapter Eighteen - Wound Infection and Biofilms, in: Press, A. (Ed.), Biofims in Infection Prevention and Control. pp. 339–358. https://doi.org/10.1016/B978-0-12-397043-5.00018-9

Ministry for the Environment, 2018. Sustainable Wastewater Management: A handbook for smaller communities [WWW Document]. URL http://www.mfe.govt.nz/publications/waste/wastewater-mgmt-jun03/html/appendices.html#appen3

Ministry for the Environment of New Zeland, 2019. Waste generation and disposal in New Zealand [WWW Document]. URL https://www.mfe.govt.nz/publications/environmental-reporting/waste-generation-and-disposal-new-zealand

Moreno, R., Martínez, E.J., Escapa, A., Martínez, O., Díez-Antolínez, R., Gómez, X., 2018. Mitigation of volatile fatty acid build-up by the use of soft carbon felt electrodes: Evaluation of anaerobic digestion in acidic conditions. Fermentation 4. https://doi.org/10.3390/fermentation4010002

Moreno, R., San-Martín, M.I., Escapa, A., Morán, A., 2016. Domestic wastewater treatment in parallel with methane production in a microbial electrolysis cell. Renew. Energy 93, 442–448. https://doi.org/10.1016/j.renene.2016.02.083

Muñoz-Aguilar, R.S., Molognoni, D., Bosch-Jimenez, P., Borràs, E., Della Pirriera, M., Luna, Á., 2018. Design, operation, modeling and grid integration of power-to-gas bioelectrochemical systems. Energies 11, 1–15. https://doi.org/10.3390/en11081947

Muselli, M., Notton, G., Poggi, P., Louche, A., 2000. PV-hybrid power systems sizing incorporating battery storage: An analysis via simulation calculations. Renew. Energy 20, 1–7. https://doi.org/10.1016/S0960-1481(99)00094-4

Najafpour, G., 2007. Biochemical Engineering and Biotechnology, Elsevier.

Nam, J., Kim, H., Lim, K., Shin, H., 2010. Effects of organic loading rates on the continuous electricity generation from fermented wastewater using a single-chamber microbial fuel cell. Bioresour. Technol. 101, S33–S37. https://doi.org/10.1016/j.biortech.2009.03.062

Navarro, S.S., Cimpoia, R., Bruant, G., Guiot, S.R., 2016. Biomethanation of syngas using anaerobic sludge: Shift in the catabolic routes with the CO partial pressure increase. Front. Microbiol. 7, 1–13. https://doi.org/10.3389/fmicb.2016.01188

Park, J.G., Lee, B., Shi, P., Kim, Y., Jun, H.B., 2017. Effects of electrode distance and mixing velocity on current density and methane production in an anaerobic digester equipped with a microbial methanogenesis cell. Int. J. Hydrogen Energy. https://doi.org/10.1016/j.ijhydene.2017.07.025

Park, J.H., Kang, H.J., Park, K.H., Park, H.D., 2018. Direct interspecies electron transfer via conductive materials: A perspective for anaerobic digestion applications. Bioresour. Technol. https://doi.org/10.1016/j.biortech.2018.01.095

Perez, D., Lie, T.T., Weber, C.C., 2020. Relative electrode size and organic load effects on the energy storage efficiency of microbial electrolysis cells. Bioresour. Technol. Reports 11, 100518. https://doi.org/10.1016/j.biteb.2020.100518

Perez, D., Weber, C., Lie, T., 2021. Operationalization of a microbial electrolysis cell : The interaction of the primary factors for energy storage efficiency. Bioresour. Technol. 326, 1–10. https://doi.org/10.1016/j.biortech.2021.124788

Perry, R.H., Green, D.W., 1997. Perry's Engineers' Handbook, Perry's Engineers' Handbook.

Persson, M., Jonsson, O., Wellinger, A., 2006. Biogas Upgrading to Vehicle Fuel Standards and Grid Injection.

Premier, G.C., Kim, J.R., Michie, I., Dinsdale, R.M., Guwy, A.J., 2011. Automatic control of load increases power and efficiency in a microbial fuel cell. J. Power Sources 196, 2013–2019. https://doi.org/10.1016/j.jpowsour.2010.09.071

Rader, G.K., Logan, B.E., 2010. Multi-electrode continuous flow microbial electrolysis cell for biogas production from acetate. Int. J. Hydrogen Energy 35, 8848–8854. https://doi.org/10.1016/j.ijhydene.2010.06.033

Rajendran, M., Dane, E., Conley, J., Tantama, M., 2016. Imaging Adenosine Triphosphate (ATP). Biol. Bull. 23, 73–84. https://doi.org/10.1016/j.physbeh.2017.03.040

Ran, Z., Gefu, Z., Kumar, J.A., Chaoxiang, L., Xu, H., Lin, L., 2014. Hydrogen and methane production in a bio-electrochemical system assisted anaerobic baffled reactor. Int. J. Hydrogen Energy 39, 13498–13504. https://doi.org/10.1016/j.ijhydene.2014.02.086

Reith, J., Wijffels, R., Barten, H., 2003. Bio-methane & Bio-hydrogen. Dutch Biological Hydrogen Foundation on behalf of the contributing authors, The Hague.

Rozendal, R.A., Hamelers, H.V.M., Euverink, G.J.W., Metz, S.J., Buisman, C.J.N., 2006. Principle and perspectives of hydrogen production through biocatalyzed electrolysis 31, 1632–1640. https://doi.org/10.1016/j.ijhydene.2005.12.006

Samora, I., Manso, P., Rossi, L., Heller, P., Schleiss, A.J., 2017. Assessment of hydropower potential in wastewater systems and application to Switzerland 113, 64–73. https://doi.org/10.1016/j.renene.2017.05.062

Sangeetha, T., Guo, Z., Liu, W., Cui, M., Yang, C., Wang, L., Wang, A., 2016. Cathode material as an influencing factor on beer wastewater treatment and methane production in a novel integrated upflow microbial electrolysis cell (Upflow-MEC). Int. J. Hydrogen Energy 41, 2189–2196. https://doi.org/10.1016/j.ijhydene.2015.11.111

Sangeetha, T., Rajneesh, C.P., Yan, W.-M., 2020. Integration of microbial electrolysis cells with anaerobic digestion to treat beer industry wastewater, Integrated Microbial Fuel Cells for Wastewater Treatment. INC. https://doi.org/10.1016/b978-0-12-817493-7.00015-1

Sasaki, D., Sasaki, K., Watanabe, A., Morita, M., Matsumoto, N., Igarashi, Y., Ohmura, N., 2013. Operation of a cylindrical bioelectrochemical reactor containing carbon fiber fabric for efficient methane fermentation from thickened sewage sludge. Bioresour. Technol. 129, 366–373. https://doi.org/10.1016/j.biortech.2012.11.048

Schaaf, T., Grünig, J., Schuster, M.R., Rothenfluh, T., Orth, A., 2014. Methanation of CO2 - storage of renewable energy in a gas distribution system. Energy. Sustain. Soc. 4, 1–14. https://doi.org/10.1186/s13705-014-0029-1

Schembecker, K.B.G., 2015. Production Rate - Dependent Key Performance Indicators for a Systematic Design of Biochemical Downstream Processes. Chem. Eng. Technol. 39.

Schildhauer, T.; Biollas, S., 2016. Synthetic Natural Gas from Coal, Dry biomass and Power-to-gas Applications. John Willey & Sons, Canada.

Schröder, U., 2007. Anodic electron transfer mechanisms in microbial fuel cells and their energy efficiency. Phys. Chem. Chem. Phys. 9, 2619–2629. https://doi.org/10.1039/b703627m

Sharma, M., Bajracharya, S., Gildemyn, S., Patil, S.A., Alvarez-Gallego, Y., Pant, D., Rabaey, K., Dominguez-Benetton, X., 2014. A critical revisit of the key parameters used to describe microbial electrochemical systems. Electrochim. Acta 140, 191–208.

https://doi.org/10.1016/j.electacta.2014.02.111

Shen, R.X., Lu, J.W., Zhu, Z.B., Duan, N., Lu, H.F., Zhang, Y.H., Liu, Z.D., 2017. Effects of organic strength on performance of microbial electrolysis cell fed with hydrothermal liquefied wastewater. Int. J. Agric. Biol. Eng. 10, 206–217. https://doi.org/10.3965/j.ijabe.20171003.2879

Siegert, M., Li, X.F., Yates, M.D., Logan, B.E., 2014a. The presence of hydrogenotrophic methanogens in the inoculum improves methane gas production in microbial electrolysis cells. Front. Microbiol. 5, 1–12. https://doi.org/10.3389/fmicb.2014.00778

Siegert, M., Yates, M.D., Call, D.F., Zhu, X., Spormann, A., Logan, B.E., 2014b. Comparison of Nonprecious metal cathode materials for methane production by electromethanogenesis. ACS Sustain. Chem. Eng. 2, 910–917. https://doi.org/10.1021/sc400520x

Smith, R., Davies, T., Baynes, N., Nichols, R., 2015. The electrochemical characterisation of graphite felts. J. Electroanal. Chem. 29–38.

Steed, J., Hashimoto, A., 1995. Methane emissions from typical manure management systems. Bioresour. Technol. 50, 123–130.

Tao, B., Zhang, Y., Heaven, S., Banks, C.J., 2020. Predicting pH rise as a control measure for integration of CO2 biomethanisation with anaerobic digestion. Appl. Energy. https://doi.org/10.1016/j.apenergy.2020.115535

Taubner, R.S., Schleper, C., Firneis, M.G., Rittmann, S.K.M.R., 2015. Assessing the ecophysiology of methanogens in the context of recent astrobiological and planetological studies. Life 5, 1652–1686. https://doi.org/10.3390/life5041652

Ter-Gazarian, A., 1994. Energy Storage for power Systems. Institution of Electrical Engineers, Lodon.

U.S. Environmental Protection Agency, 2011. Greenhouse Gas Emissions Estimation Methodologies for Biogenic Emissions from Selected Source Categories: Solid Waste Disposal Wastewater Treatment Ethanol Fermentation.

Urrutia, H., Vidal, R., Baeza, M., Reyes, J.E., Aspe, E., 1997. Growth of methylaminotrophic, acetotrophic and hydrogenotrophic methanogenic bacteria on artificial supports. Microbiologia 13, 209–214.

Van Eerten-Jansen, M., Ter Heijne, A., Buisman, C., Hamelers, H., 2012. Microbial electrolysis cells for production of methane from CO 2: Long-term performance and perspectives. Int. J. Energy Res. 36, 809–819. https://doi.org/10.1002/er.1954

Villano, M., Aulenta, F., Ciucci, C., Ferri, T., Giuliano, A., Majone, M., 2010. Bioelectrochemical reduction of CO2 to CH4 via direct and indirect extracellular electron transfer by a hydrogenophilic methanogenic culture. Bioresour. Technol. 101, 3085–3090. https://doi.org/10.1016/j.biortech.2009.12.077

Villano, M., Monaco, G., Aulenta, F., Majone, M., 2011. Electrochemically assisted methane production in a biofilm reactor. J. Power Sources 196, 9467–9472. https://doi.org/10.1016/j.jpowsour.2011.07.016

Villano, M., Ralo, C., Zeppell, M., Aulenta, F., Majone, M., 2016. Influence of the set anode potential on the performance and internal energy losses of a methane-producing microbial electrolysis cell. Bioelectrochemistry 107, 1–6.

Voelklein, M.A., Rusmanis, D., Murphy, J.D., 2019. Biological methanation: Strategies for in-situ and ex-situ upgrading in anaerobic digestion. Appl. Energy 235, 1061–1071. https://doi.org/10.1016/j.apenergy.2018.11.006

Wang, W., Wei, X., Choi, D., Lu, X., Yang, G., Sun, C., 2015. Electrochemical cells for medium-and large-scale energy storage: Fundamentals. Adv. Batter. Mediu. Large-Scale Energy Storage Types Appl. 3–28. https://doi.org/10.1016/B978-1-78242-013-2.00001-7

Watcher, C.P., 2017. Efficiency parameter of CCS [WWW Document]. URL

ttps://www.climate-policy-watcher.org/energy-consumption/efficiency-parameters-of-ccs.html

Xie, X., Criddle, C., Cui, Y., 2015. Design and fabrication of bioelectrodes for microbial bioelectrochemical systems. Energy Environ. Sci. 8, 3418–3441. https://doi.org/10.1039/c5ee01862e

Xu, H., Gong, S., Sun, Y., Ma, H., Zheng, M., Wang, K., 2015. High-rate hydrogenotrophic methanogenesis for biogas upgrading: The role of anaerobic granules. Environ. Technol. 36, 529–537. https://doi.org/10.1080/09593330.2014.979886

Yang, H.Y., Bao, B.L., Liu, J., Qin, Y., Wang, Y.-R., Su, K.-Z., Han, J.-C., Mu, Y., 2018. Temperature dependence of bioelectrochemical CO2 conversion and methane production with a mixed-culture biocathode. Bioelectrochemistry 119, 180–188. https://doi.org/10.1016/j.bioelechem.2017.10.002

Ye, R., Jin, Q., Bohannan, B., Keller, J.K., McAllister, S.A., Bridgham, S.D., 2012. PH controls over anaerobic carbon mineralization, the efficiency of methane production, and methanogenic pathways in peatlands across an ombrotrophic-minerotrophic gradient. Soil Biol. Biochem. 54, 36–47. https://doi.org/10.1016/j.soilbio.2012.05.015

Yin, Q., Zhu, X., Zhan, G., Bo, T., Yang, Y., Tao, Y., He, X., Li, D., Yan, Z., 2016. Enhanced methane production in an anaerobic digestion and microbial electrolysis cell coupled system with co-cultivation of Geobacter and Methanosarcina. J. Environ. Sci. (China) 42, 210–214. https://doi.org/10.1016/j.jes.2015.07.006

Yu, Z., Leng, X., Zhao, S., Ji, J., Zhou, T., Khan, A., Kakde, A., Liu, P., Li, X., 2018. A review on the applications of microbial electrolysis cells in anaerobic digestion. Bioresour. Technol. 255, 340–348. https://doi.org/10.1016/j.biortech.2018.02.003

Zeppilli, M., Agnese, L., Villano, M., Majone, M., 2016. Anion vs cation exchange membrane strongly affect mechanisms and yield of CO2 fixation in a microbial electrolysis cell. Chem. Eng. J. 304, 10–19. https://doi.org/10.1016/j.cej.2016.06.020

Zeppilli, M., Simoni, M., Paiano, P., Majone, M., 2019. Two-side cathode microbial electrolysis cell for nutrients recovery and biogas upgrading. Chem. Eng. J. 370, 466–476. https://doi.org/10.1016/j.cej.2019.03.119

Zhang, Y., Angelidaki, I., 2014. Microbial electrolysis cells turning to be versatile technology: Recent advances and future challenges. Water Res. 56, 11–25. https://doi.org/10.1016/j.watres.2014.02.031

Zhang, Z., Song, Y., Zheng, S., Zhen, G., Lu, X., Takuro, K., Xu, K., Bakonyi, P., 2019. Electro-conversion of carbon dioxide (CO2) to low-carbon methane by bioelectromethanogenesis process in microbial electrolysis cells: The current status and future perspective. Bioresour. Technol. 279, 339–349. https://doi.org/10.1016/j.biortech.2019.01.145

Zhen, G., Kobayashi, T., Lu, X., Xu, K., 2015. Understanding methane bioelectrosynthesis from carbon dioxide in a two-chamber microbial electrolysis cells (MECs) containing a carbon biocathode. Bioresour. Technol. 186, 141–148. https://doi.org/10.1016/j.biortech.2015.03.064

Zhen, G., Lu, X., Kobayashi, T., Kumar, G., Xu, K., 2016. Promoted electromethanosynthesis in a two-chamber microbial electrolysis cells (MECs) containing a hybrid biocathode covered with graphite felt (GF). Chem. Eng. J. 284, 1146–1155. https://doi.org/10.1016/j.cej.2015.09.071

Zoski, C., 2007. Handbook of Electrochemistry.

Appendix A ANOVA for Electrode Relative Size between MEC A and MEC B

a) MEC A vs MEC B at 200 ppm

Anova: Single Factor (Methane Production Rate)

SUMMARY

Groups	*Count*	*Sum*	*Average*	*Variance*
MEC A 200	11	49.54406	4.504005	0.418275
MEC B 200	11	61.19083	5.562803	0.565793

ANOVA

Source of Variation	*SS*	*df*	*MS*	*F*	*P-value*	*F crit*
Between Groups	6.165786	1	6.165786	12.53122	0.002056	4.351244
Within Groups	9.840678	20	0.492034			
Total	16.00646	21				

Anova: Single Factor (Methane Conversion Rate)

SUMMARY

Groups	*Count*	*Sum*	*Average*	*Variance*
MEC A 200	12	85.58631	7.132193	1.411553
MEC B 200	12	105.4307	8.785889	1.916106

ANOVA

Source of Variation	*SS*	*df*	*MS*	*F*	*P-value*	*F crit*
Between Groups	16.40826	1	16.40826	9.861743	0.004754	4.30095
Within Groups	36.60425	22	1.663829			
Total	53.01251	23				

b) MEC A vs MEC B at 4000 ppm

Anova: Single Factor (Methane Production Rate)

SUMMARY

Groups	*Count*	*Sum*	*Average*	*Variance*
MEC A 4000	11	65.3697	5.9427	1.277754
MEC B 4000	11	69.80261	6.345692	2.245515

ANOVA

Source of Variation	*SS*	*df*	*MS*	*F*	*P-value*	*F crit*
Between Groups	0.893215	1	0.893215	0.507038	0.484648	4.351244
Within Groups	35.23269	20	1.761634			
Total	36.1259	21				

Anova: Single Factor (Methane Conversion Rate)

SUMMARY

Groups	*Count*	*Sum*	*Average*	*Variance*
MEC A 4000	12	5.672214	0.472684	0.007248
MEC B 4000	12	6.113531	0.509461	0.012845

ANOVA

Source of Variation	*SS*	*df*	*MS*	*F*	*P-value*	*F crit*
Between Groups	0.008115	1	0.008115	0.807749	0.378518	4.30095
Within Groups	0.221022	22	0.010046			
Total	0.229137	23				

Appendix B ANOVA for Organic load effect (200ppm vs 4000ppm) over the performance of AD, MEC A and MEC B

a) AD 200 ppm vs AD 4000 ppm

Anova: Single Factor (Methane Production Rate)

SUMMARY

Groups	*Count*	*Sum*	*Average*	*Variance*
AD 200	11	22.16563	2.015057	0.053263
AD 4000	11	80.21316	7.292105	2.058714

ANOVA

Source of Variation	*SS*	*df*	*MS*	*F*	*P-value*	*F crit*
Between Groups	153.1598	1	153.1598	145.0393	1.28E-10	4.351244
Within Groups	21.11977	20	1.055989			
Total	174.2796	21				

b) MEC A 200 ppm vs MEC A 4000 ppm

Anova: Single Factor (Methane Production Rate)

SUMMARY

Groups	*Count*	*Sum*	*Average*	*Variance*
MEC A 200	11	49.54406	4.504005	0.418275
MEC A 4000	11	65.15086	5.922806	1.279995

ANOVA

Source of Variation	*SS*	*df*	*MS*	*F*	*P-value*	*F crit*
Between Groups	11.07147	1	11.07147	13.03853	0.001744	4.351244
Within Groups	16.9827	20	0.849135			
Total	28.05417	21				

c) MEC B 200 ppm vs MEC B 4000ppm

Anova: Single Factor (Methane Production Rate)

SUMMARY

Groups	*Count*	*Sum*	*Average*	*Variance*
MEC B 200	11	61.19083	5.562803	0.565793
MEC B 4000	11	69.80261	6.345692	2.245515

ANOVA

Source of Variation	*SS*	*df*	*MS*	*F*	*P-value*	*F crit*
Between Groups	3.371034	1	3.371034	2.398197	0.137154	4.351244
Within Groups	28.11308	20	1.405654			
Total	31.48411	21				

d) AD 200 ppm vs AD 4000 ppm

Anova: Single Factor (Methane Conversion Rate)

SUMMARY

Groups	*Count*	*Sum*	*Average*	*Variance*
AD 200	12	37.52291	3.126909	0.15091
AD 4000	12	6.537697	0.544808	0.010521

ANOVA

Source of Variation	*SS*	*df*	*MS*	*F*	*P-value*	*F crit*
Between Groups	40.00348	1	40.00348	495.6097	1.4E-16	4.30095
Within Groups	1.775745	22	0.080716			
Total	41.77923	23				

e) MEC A 200 ppm vs MEC A 4000 ppm

Anova: Single Factor (Methane Conversion Rate)

SUMMARY

Groups	*Count*	*Sum*	*Average*	*Variance*
MEC A 200	12	85.58631	7.132193	1.411553
MEC A 4000	12	5.672214	0.472684	0.007248

ANOVA

Source of Variation	*SS*	*df*	*MS*	*F*	*P-value*	*F crit*
Between Groups	266.0943	1	266.0943	375.0975	2.61E-15	4.30095
Within Groups	15.60681	22	0.7094			
Total	281.7011	23				

f) MEC B 200 ppm vs MEC B 4000ppm

Anova: Single Factor (Methane Conversion Rate)

SUMMARY

Groups	*Count*	*Sum*	*Average*	*Variance*
MEC B 4000	12	6.113531	0.509461	0.012845
MEC B 200	12	105.4307	8.785889	1.916106

ANOVA

Source of Variation	*SS*	*df*	*MS*	*F*	*P-value*	*F crit*
Between Groups	410.9955	1	410.9955	426.1337	6.87E-16	4.30095
Within Groups	21.21846	22	0.964476			
Total	432.214	23				

Appendix C: References and assumptions used for the simulation of MEC integration.

Parameter	Symbol	Units	Value	Reference
Household energy consumption		kJ	$1.1*10^8$	(Laboratory, n.d.)
Household population		person	1	-
Industrial energy consumption		kJ	$2.1*10^{13}$	(Hiranga Energy, n.d.),(EIA, 2014)
Industrial wastewater population		persons	7700	-
% Coal in fossil fuel		%	40	(International Energy Agency, 2017)
% Gas in Fossil fuel		%	60	(International Energy Agency, 2017)
Treatment efficiency	Eff_{ww}		0.85	(International Energy Agency, 2017),(Ministry for the Environment, 2018)
Flow rate	Q_{ww}	$L\ day^{-1}$	160	(International Energy Agency, 2017),(Ministry for the Environment, 2018)
Oxygen demand	OD	$mg_{COD}\ L^{-1}$	200	(International Energy Agency, 2017),(Ministry for the Environment, 2018)
Cell Yield	CFs	$gC\ g\ Cell^{-1}$	0.53	(International Energy Agency, 2017),(Ministry for the Environment, 2018)
Correction factor	MCF_{ww}	% s to CH_4	0.8	(International Energy Agency, 2017)
% CH_4 in biogas	BG ch4	$\%CH_4$	0.65	[26]
Yield CO_2/x	CF_{CO2}	$g\ CO_2\ g^{-1}$ OD	1.375	(International Energy Agency, 2017)
Yield CH_4/x	CF_{CH4}	$g\ CH_4\ g^{-1}$ OD	0.5	(International Energy Agency, 2017)
Yield x/s	I	Yx/S	0.1	(International Energy Agency, 2017)
%C in Biomass	CF_S	gC/g_{Cell}	0.53	(International Energy Agency, 2017)
Hydraulic Retention Time	HRT	Hour	24	-
Current density	$I_{density}$	$A\ m^{-3}$	-	-
Voltage	V	V	0.8	(Gajaraj et al., 2017), (Sangeetha et al., 2020)
Specific energy methane		$kJ\ g^{-1}$	55.3	
Specific energy coal		$kJ\ g^{-1}$	31.4	
Destruction efficiency coal		%	37	
Destruction efficiency gas		%	35	
Emission rate gas		$gCO_2\ kJ^{-1}$	0.13	(Balcombe et al., 2015)
Emission rate coal		$gCO_2\ kJ^{-1}$	0.09	
Emission rate bio-gas		$gCO_2\ kJ^{-1}$	0.05	
Supply emission rate gas		$gCO_2\ kJ^{-1}$	0.03	
Supply emission rate coal		$gCO_2\ kJ^{-1}$	0.27	

Appendix D: Reported operational conditions and KPI on selected studies

Reference	Chambers	Vol (ml)	Operation	HRT (H)	OL gCOD/L*D)	Temp ©	applied mV	Control method	Anode	Cathode	Methane production	
(Moreno et al., 2016)	1	3000	Batch vs continuous	24	300 mg_{COD} L^{-1}		1000	cell	Carbon felt	stainless steel	0.012	lCh4/ L d
(Gajaraj et al., 2017)	1	800	Batch	720	3 g_{COD} L^{-1} D^{-1}	35	600	cell	Reticulated vitrous carbon	Reticulated vitrous carbon	0.02	LHC4/ L*d
(Hou et al., 2015)	1	500	Fed-batch	120	1 g_{COD} L^{-1} D^{-1}	25	950	cell	Carbon cloth	Niquel foam	0.03	m3/ m3 *d
(Clauwaert and Verstraete, 2009)	1	256	Fed-batch	5.3	4.13 kg_{COD} m^{-3} d^{-1}	22	-800	cell	graphite granules	graphite rod	0.75	LCH4/ L MEC
(Hara et al., 2013)	1	10	Batch	140	0.2 $g_{yest\_extract}L^{-1}$	65	1000	cell	Carbon paper	Carbon paper	20	mmol CH4 m2
(Li et al., 2016)	1	130	batch	58	1 g_{COD} L^{-1} D^{-1}	30	800	cell	graphite brush	carbon cloth	93	l/m3*day
(Sangeetha et al., 2016)	1	600	continuous	24	2 g_{COD} L^{-1} D^{-1}	35	800	cell	Graphite felt	Graphite felt	142.8	mL/ g COD
(Guo et al., 2015)	1	300	Batch	720	11750 mg L^{-1}		1800	cell	Ti/Ru		160	acc mlCH4
(Park et al., 2017)	1	785	semi-continuous	480	2 kg_{COD} m^{-3} d^{-1}	35	300	cell	graphite carbon coated with Ni	graphite carbon coated with Cu	160	mL/ L day
(Li et al., 2016)	1	1000	continuous	6	-		1000	cell	Graphite	Graphite	248.5	ml/H
(Yin et al., 2016)	1	250	Batch	72	10 g L^{-1}	25	1000	cell	Carbon felt	stainless steel*	360	mL/ g_{COD}
(K. S. Choi et al., 2017)	1	330	Batch	144	2 g_{COD} L^{-1} D^{-1}	35	-835	cathode	Carbon fiber brush	Carbon fiber brush	408	mL_{CH4}/ g_{COD}
(Nelabhotla and Dinamarca, 2019)	1	3000	Fed-batch	24	7 g_{NaHCO3} L^{-1}	35	-800	cathodic	graphite rod	carbon felt	9	mmol/$L_{reactor}$ *d
(Mieke C. A., 2012)	2	560	continuous	93	5 g_{NaHCO3} L^{-1}	30	-700	cathode	Platinum	Graphite felt	0.006	m^3/m^3 d

(Rader and Logan, 2010)	2	2500	continuous	24	1 g_{COD} L^{-1} D^{-1}	30	900	cell	Graphite fiber	stainless steel	0.118	L_{biogas} $L^{-1}d^{-1}$
(Cerrillo et al., 2017)	2	500	continuous	6.8	7.83 kg_{COD} m^{-3} d^{-1}	23	-800	cathode	Graphite granules	Graphite granules	0.23	L_{CH4} m^{-3} d^{-1}
(Cai et al., 2016)	2	700	semi-continuous	48	2 g_{COD} L^{-1} D^{-1}	35	800	cell	Carbon brush	stainless steel	0.247	ml_{CH4} ml^{-1} day^{-1}
(Siegert et al., 2014a)	2	5	Batch	50	2.5 g_{COD} L^{-1} D^{-1}	30	700	cathode	Graphite plates	Graphite plates	0.27	$mLml^{-1}$ * cm^{-2}
(Liu et al., 2017)	2	500	Fed-batch	720	150 mM $NaHCO_3$	55	800	cathode	graphite felt	carbon felt	1.2	L_{biogas} $L^{-1}d^{-1}$
(Yang et al., 2018)	2	1200	batch	100	5 g $_{NaHCO3}$ L^{-1}	50	-900	cathode	carbon felt	carbon felt	2.06	mmol / L * h
(Sasaki et al., 2013)	2	4000	continous	96	-	55	-800	cathodic	carbon bar	carbon plate	3.57	L_{biogas} $L^{-1}d^{-1}$
(Villano et al., 2011)	2	867	Batch	480	10 $mM_{acetate}$	25	500	anode	Graphite plates	Graphite plates	15	meq $_{CH4}L^{-1}$ d^{-1}
(Gil-Carrera et al., 2011)	2	150	continuous	72	55.2 $g_{acetate}$ L^{-1}	30	1200	cell	carbon felt	Niquel foam	23.4	mLd^{-1}
(Ding et al., 2016)	2	800	Batch	72	3 g_{COD} L^{-1} D^{-1}	35	800	cell	Granular graphite	SS, Ni, Cu	60	Total ml_{CH4}
(Zhen et al., 2016)	2	400	Batch	24	0.5 g L^{-1}	35	-1200	cathode	Platinum	Carbon stick coated GF	78	ml^{CH4} $L^{-1}d^{-1}$
(Cerrillo et al., 2017a)	2	500	continuous	32	3.92 kg_{COD} $m^{-3}day^{-1}$	55	-800	cathode	carbon felt	carbon felt	79	L m^{-3} d^{-1}
(Zhen et al., 2016)	2	800	Batch	24	0.5 $g_{yest\_extract}L^{-1}$ yeast		-1400	cathode	Carbon stick	Carbon stick	80.9	mL L^{-1}
(Zeppilli; et al., 2016)	2	860	continuous	8.35	1 g_{COD} L^{-1} D^{-1}	25	-200	anode	Graphite granules	Graphite granules	83	meq L^{-1} d^{-1}
(Baek et al., 2017)	2	200	Batch	200	-	35	-700	cathode	Graphite felt	Graphite felt	384.3	mmol m^{-2} d^{-1}
(Cheng et al., 2009)	2	300	Fed-batch		1 $g_{acetate}$ L^{-1}	30	-1000		graphite fibre brush	carbon cloth	656	mmol d^{-1} m^{-2}
(Siegert et al., 2014b)	2	100	Batch	672	2.5 g_{NaHCO3} L^{-1}	30	600	cathode	carbon fiber brush	Pt on carbon black	259 =-90	mmol cm^{-3} d^{-1}

(Zeppilli et al., 2020)	2	12000	continuous	12.6	**	25	-2.25	anodic	Graphite granules	Graphite granules	449+ -32	meq d^{-1}
(Zeppilli et al., 2019)	3	2580	continuous	14	200 mg L^{-1}	25	200	Anode	graphite granules	graphite granules	14	Mmol d^{-1}
(Jang et al., 2015)	-	5000	semi-continuous	60	108 g L^{-1}	55	-				1422.5	ml_{CH4} L^{-1} * d^{-1}
(Kerroum et al., 2014)	NA	500 (L)	continuous	552	1.3 kg $m^{-3}d^{-1}$	35	-	-	-	-	0.39	m3 m^{-3} d^{-1}
(Kerroum et al., 2014)	NA	500 (L)	continuous	552	1.3 kg $m^{-3}d^{-1}$	55	-	-	-	-	0.96	m3 m^{-3} d^{-1}

* anode feeding (in g L^{-1}) 0.41 peptone, 0.5 yest extract, 0.19 acetate, 0.94 glucose; cathode fed 30%CO_2, 70% N_2

Appendix E: Washing out Recovery

a) Context and hypothesis

The design of experiments of chapter 6 consists of a series of sequential HRT reductions and voltages screening for each HRT. Going from 20 days to 10 days of HRT led to an important improvement of the performance in both MECs. However, further reductions of HRT led to a detrimental performance of MEC A, whereas MEC B showed a steady energy efficiency but a negatively affected MCR under 5 days of HRT.

Considering that the methanogenic capacity of the system comes mostly from Acetoclastic methanogens with a duplication time of between 5-7 days, whereas hydrogenotrophic methanogens range 4-8 hrs (Zhang et al., 2019), it is possible that going below this value produced a washing out of the planktonic methanogens, reducing its population to those contained on the biofilm on the electrodes. In such a case, the recovery of the performance should be noticed if the conditions are restored to allow the regrowth of the bacterial consortium.

b) Material and method

After finishing the work detailed in Chapter 6, including the design with a short HRT of 2days, the MPR and energy storage efficiency have dropped, especially for MEC A. As the washing out hypothesis seemed plausible, both MECs were returned to the operation regime where the maximum energy efficiency was achieved (10 days HRT – 800 mV), maintaining a steady operation and monitoring as usual.

c) Results

When the HRT was extended, a lower organic load (in g d^{-1}) is fed into the MECs, but it is expected to provide sufficient time to allow the acetoclastic methanogenic population to recover, hence an improvement on the overall performance is expected.

Figure 30 exhibit how both the MPR and MCR quickly tend to the previously measured performance level under those conditions. This is mostly led by an increase of the volumetric production, although the methane content (see Figure 31) of the off-gas shows a lag phase on MEC A that almost does not exist on MEC B. This difference can be explained by the fact that MEC A performance had dropped earlier in the HRT reduction process, meaning that a heavier washout consequence was suffered, whereas MEC B showed higher resilience.

The simultaneous presence of both planktonic cells in the bulk of the digestate and biofilm attached to the electrodes has been previously denominated as a hybrid consortium (Dou et al., 2018).The quick recovery of the overall performance suggests that the detrimental effect of HRT under 5 days is related to the washing out of just the planktonic cells, but that it did not affect the

biofilm on the electrodes. Nevertheless, this can only be theorized here and appropriate analysis that includes biofilm sampling should be done to confirm.

The combination of these results with the hypothesis of Gil-Carrera (Gil-Carrera et al., 2011) claiming that the main effect of MEC is based on providing a substrate for biofilm formation rather than the voltage imposition, suggest that the resilience of the system could benefit from including both electrodes and non-conductive substrates for bacteria to colonize in order to increase the cellular residence time. This would maintain a higher methanogenic population, hence methanogenic capacity under shorter HRT or other significant system disruption.

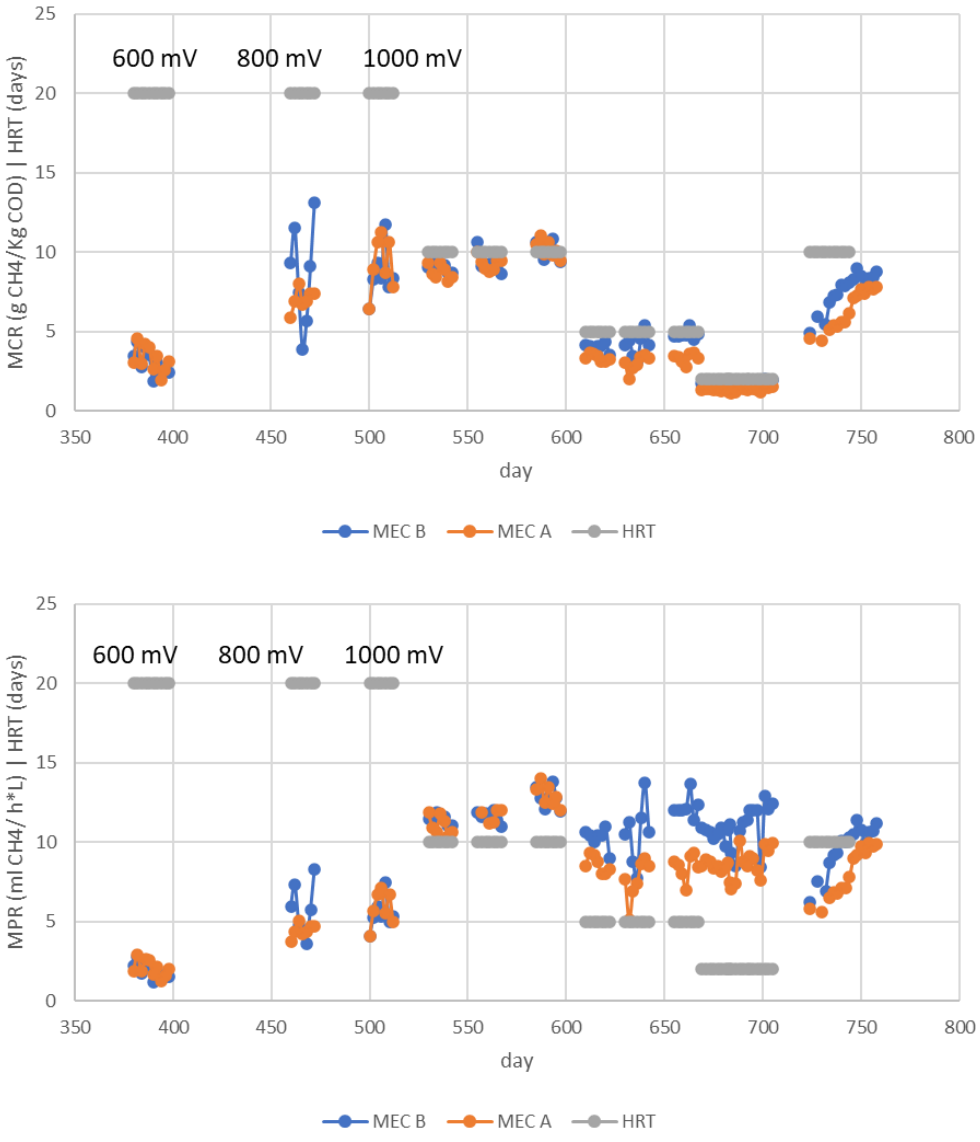

Figure 30: MECs performance as MPR and MCR, showing the HRT reductions and voltage screening detailed in Chapter 6, including the recovery to 10 days & 800mV operation.

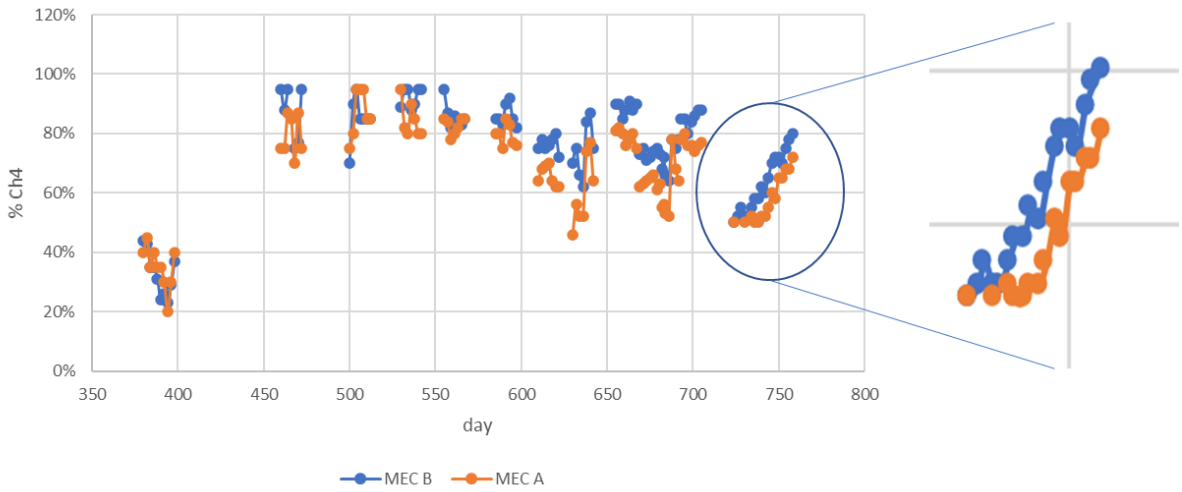

Figure 31: Off-gas methane content for both MECs as the HRT is reduced, and voltage screened between 600 to 1000V, zooming the recovery operation (10 days & 800mV).

Appendix F: Costs mathematical Modelling

To have an estimated cost of the energy storage system, beyond the direct operation of the MECs, all three components of the system (CS, PTS and CDCS) must be accounted for.

Energy storage is part of a power system and therefore the power capacity (PS) and energy storage (ES) have to satisfy the special system requirements. To define these requirements, it is necessary to formulate a power system mathematical model in which the energy storage model will be included.

Nevertheless, as the CS does not produce energy but only stores it in a given quantity and releases it at a designed speed, the stored energy (Es) is a function of construction parameters (CP_i, constant for the given device), variable parameters (VP_i, dependant on the current regime of the storage), and time (t).

Therefore, $E_S = f_{CS}(CP_i, VP_i, t)$. Considering the power is the first derivative of energy respect to time, the Eq. 39 describes the power flow from CS

$$P_{CS} = \frac{dE_S}{dt} = \frac{df_{CS}(CP_i, VP_i, t)}{dt} \qquad \text{EQUATION 1}$$

The capital cost of the energy storage is the sum of two parts. One is related to the storable energy; the other depends on the peak power that the storage must deliver and is controlled by the CDCS according to the demand requirements. So, logically, the capital cost C depends on the cost of CS, PTS and CDCS, as seen in Eq. 40, partly proportional to installed power capacity and in part to storable energy capacity:

$$C = C_{CS} + C_{PTS} + C_{CDCS} \qquad \text{EQUATION 2}$$

Ter-Gazarian recommends the use of specific cost per unit of storable energy capacity and installed power capacity, hence the capital costs for the storage components are given by Eq. 41 and Eq. 42 (Ter-Gazarian, 1994).

$$C_{CS} = +C_e^* * E_S \qquad \text{EQUATION 3}$$

$$C_{PTS} + C_{CDCS} = C_P^* * P_S \qquad \text{EQUATION 4}$$

Where C_e*=specific cost for the CS, C_P*=joint specific cost for PTS and CDCS, all in $/kWh

Hence the capital cost of energy storage is a function of the two main storage characteristics and may be written as shown in Eq 43.

$$C_S = C_e^* * E_S + C_P^* * P_S \qquad \text{EQUATION 5}$$

If reference is made to the specific cost per unit of generating capacity which is widely used in a power system design analysis, this cost may be given as follows, where P_d is the discharge or generating capacity as previously described, k_u is the restoring ratio, and t_d the rated discharge time.

$$\frac{C_S}{P_d} = C_e^* * E_S + C_P^* * P_S \rightarrow C_S^* = C_e^* * t_d + C_P^* * k_{\mu} \qquad \text{EQUATION 6}$$

The annual cost of a storage facility, Z_S, when operational cost comprises capital repayments, interest charges, operating and maintenance costs plus the cost of energy losses, may be given as shown in Eq 45.

$$Z_S = R * C_S + \eta_C * C_U * \delta E_S \qquad \text{EQUATION 7}$$

Where R represents the fix annual costs, comprising capital cost-capital repayments, interest charges, operational and maintenance cost, η_C is the number of charge-discharge cycles during a year and C_u is the specific cost of energy used for charging the storage. The cost of annual energy losses is a variable part of the annual cost.

The econometric model of an energy storage facility can thus be given in the form of annual cost of the facility

$$Z_S = R(C_e * E_S + C_P) + \eta_C * C_U * E_S * {}^{(1-\xi_S)}\Big/_{\xi_C} \qquad \text{EQUATION 8}$$

This allows us to optimise key parameters, the installed capacity and stored energy, or to use this model as a part of the power system econometric model, including the storing and charge efficiencies (ξ_S and ξ_C respectively).

Given the system specificity of this approach this has been considered out of scope for this study, nevertheless, it is a topic that needs to be explored further, as it would contribute generating an optimisable model for minimising cost with respect to energy production.

Appendix G: Recovering methanogenesis activity

a) Context and hypothesis

To assess the hydrogen impact on the MECs performance, hydrogen gas was injected into the vessel via using a peristaltic pump. A sudden and significant drop of the off-gas methane content from 45% to barely 10% was noticed. A crack along the pump hose was noted, suggesting that air was effectively injected, affecting the sensitive methanogenic consortium.

Having the diagnosis that the air affected the methanogenic bacteria, as they are very sensitive to oxygen, the hypothesis was that the MEC operation can be restored by re-inoculation to reinforce the remnant methanogenic capacity.

b) Material and method

In order to re-establish the methanogenic consortium, a re-inoculation program was used where 500 mL (half of the working volume) is removed from the MEC and replaced by liquor from an AD operating on a 40 days HRT but otherwise identical operation. The HRT of the MECs was also increased from 20 to 30 days to avoid washout of the new bacteria added to the bioreactors, facilitating the attachment and the re-colonization of the electrodes.

The MECs were initially inoculated from an AD vessel operating under analogous conditions (except for the voltage imposition). The AD bioreactor methanogenic activity was considered appropriate to work as source of the inoculum for the re-inoculation program as it achieved an 80% of methane content in the off-gas.

c) Results

As shown in Figure 32 after the first re-inoculation (day 2) the MPR changes to a gently positive trend, accelerated by the second re-inoculation and the extension of the HRT (day 5). The recovery of methane content on the off gas to the baseline levels was the main factor of recovery the MPR, reaching up to 50%.

The oxygen injection induced by a failed hydrogen injection probably inactivated the planktonic methanogens, but not the biofilms colonizing the electrodes. About 6 days were necessary to change the downward trend of MPR for both MECs, whereas the start-up operation of the MECs took about 30 days. This faster recovery suggests that the loss of methanogenic activity was partial, despite the low methane production. Biofilms are a macrostructure used by microorganisms as a mechanism that allows them to protect themselves from the environment, by creating a more appropriate micro-environment (Li et al., 2019). It seems then, planktonic cells, that do not account with such protection mechanisms, were directly affected by the accidental oxygen injection, hence inactivated as methanogens are strict anaerobic cells (Kumar et al., 2018). Contrarily, the biofilms developed over the electrodes would have protected the more sensitive methanogens, allowing a faster recovery when suitable conditions were given in the MECs. In

this sense, the re-inoculation would have helped to re-establish the planktonic population, but the apparent robustness of the MEC system was what allowed the fast methanogenic activity recovery.

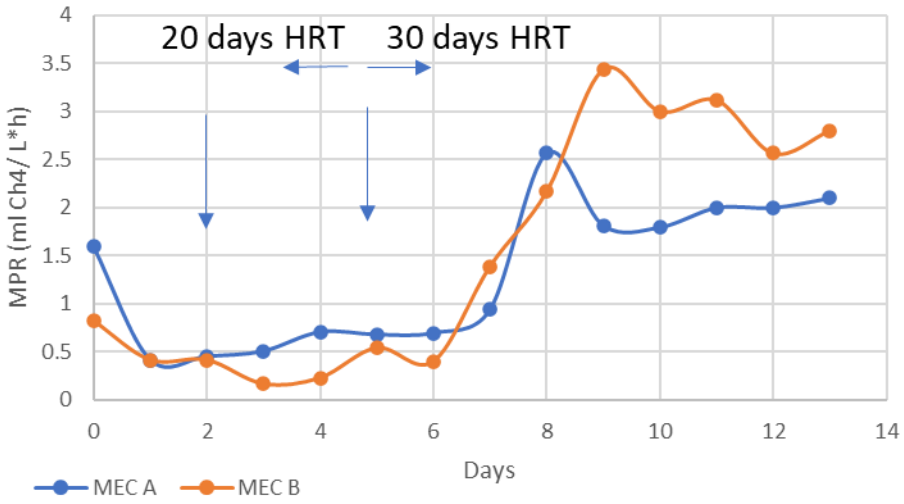

Figure 32: Methane production rate (in mL_{CH4} $L^{-1}h^{-1}$) after re-inoculation in both MECs, vertical arrows indicate the re-inoculation dates, horizontal arrows highlight the HRT used.

Additionally, the HRT was extended to contribute to the development of more appropriate conditions for the planktonic methanogenic population recovery. As the MECs are continuously operated, if the methanogenic-bacteria growing speed is slower than the dilution rate ($Vessel_{Working\ volume} / Feeding_{Flow\ rate}$), they would be effectively displaced by sterile medium and thus reduce to planktonic population, possibly reaching 0 cell/mL. An easy way to avoid this scenario is to increase the HRT (reducing the dilution rate below the bacterial growing rate), offering the more suitable conditions for bacterial attachment over the electrodes and enhancing the biofilm maturation required to recover a healthy operation of the system. Although the HRT extension was performed simultaneously to the re-inoculation of the MECs, it is possible to notice that combined re-inoculation and HRT extension has a greater positive impact in the MPR recovery compared to the sole first inoculation by itself, noticed in the positive slope of the MPR.

Therefore, the success of the methanogenic recovery in such a short timeframe is possible due to the combined action of the inherent MEC resilience given by the biofilms, and the planktonic population recovery due to the re-inoculation and HRT extension.

Appendix H: Statistical Analysis

All the statistical analysis provided here was performed with Minitab 19

ANOVA MPR versus ORL and Reactor

Factor Information

Factor	Type	Levels	Values
ORL	Fixed	2	200, 4000
Reactor	Fixed	3	AD, MEC A, MEC B

Analysis of Variance for ml CH4/L * H

Source	DF	SS	MS	F	P
ORL	1	40.058	40.058	31.82	0.000
Reactor	2	9.212	4.606	3.66	0.031
Error	62	78.055	1.259		
Total	65	127.325			

Model Summary

S	R-sq	R-sq(adj)
1.12203	38.70%	35.73%

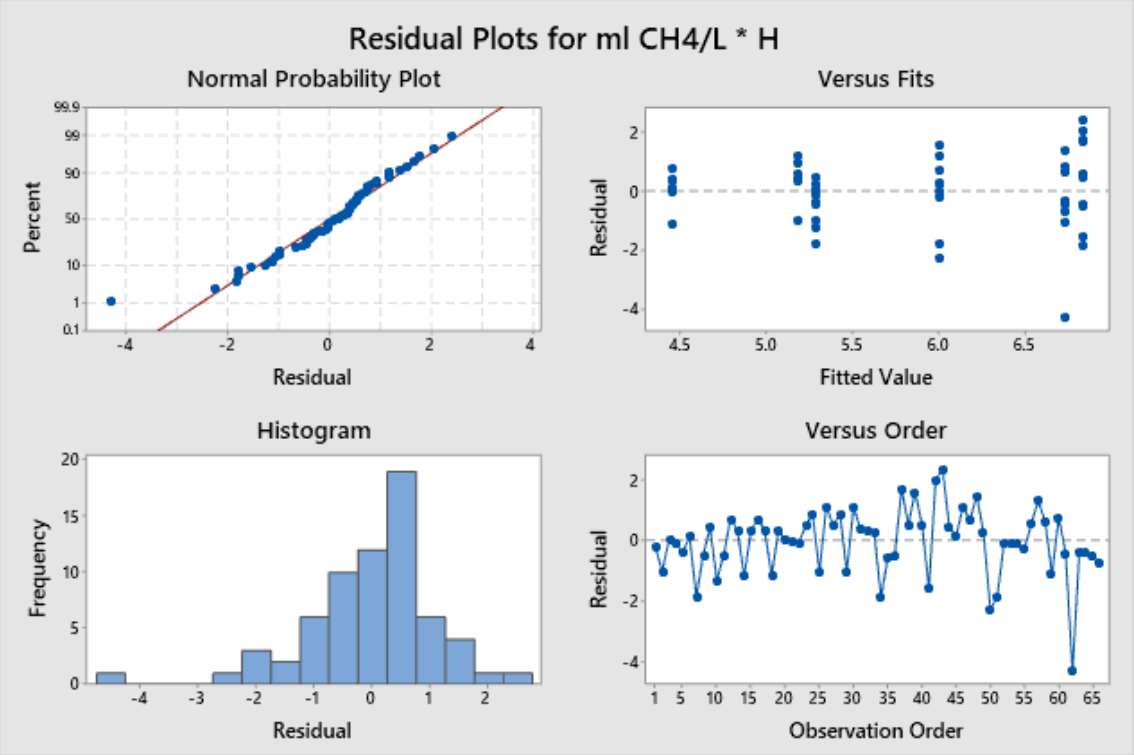

ANOVA MPR versus ORL

Method

Null hypothesis	All means are equal
Alternative hypothesis	Not all means are equal
Significance level	α = 0.05

Equal variances were assumed for the analysis.

Factor Information

Factor	Levels	Values
ORL	2	200, 4000

Analysis of Variance

Source	DF	Adj SS	Adj MS	F-Value	P-Value
ORL	1	40.06	40.058	29.38	0.000
Error	64	87.27	1.364		
Total	65	127.32			

Model Summary

S	R-sq	R-sq(adj)	R-sq(pred)
1.16771	31.46%	30.39%	27.11%

Means

ORL	N	Mean	StDev	95% CI
200	33	4.969	0.808	(4.563, 5.375)
4000	33	6.527	1.440	(6.121, 6.933)

Pooled StDev = 1.16771

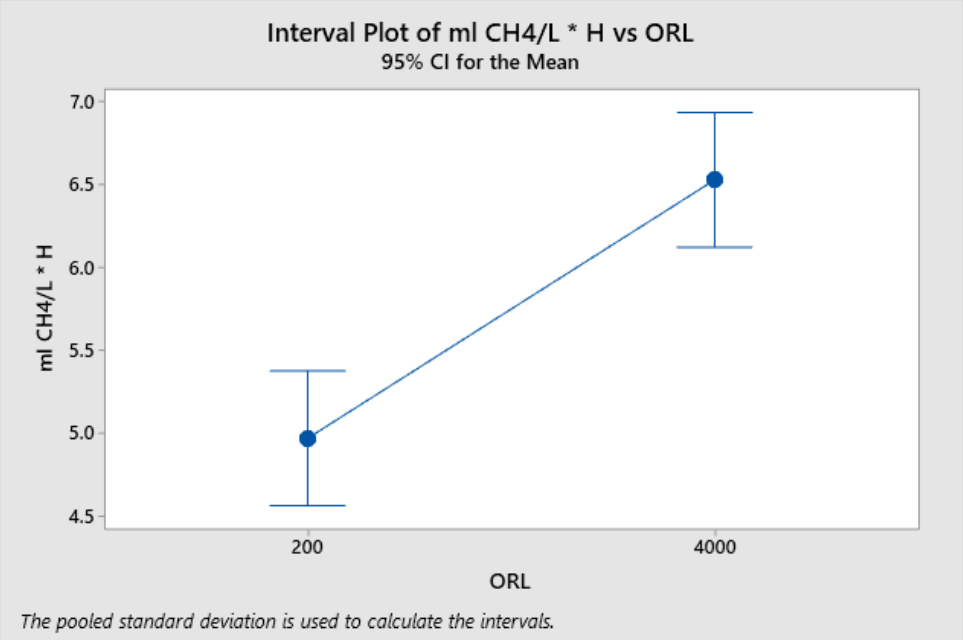

The pooled standard deviation is used to calculate the intervals.

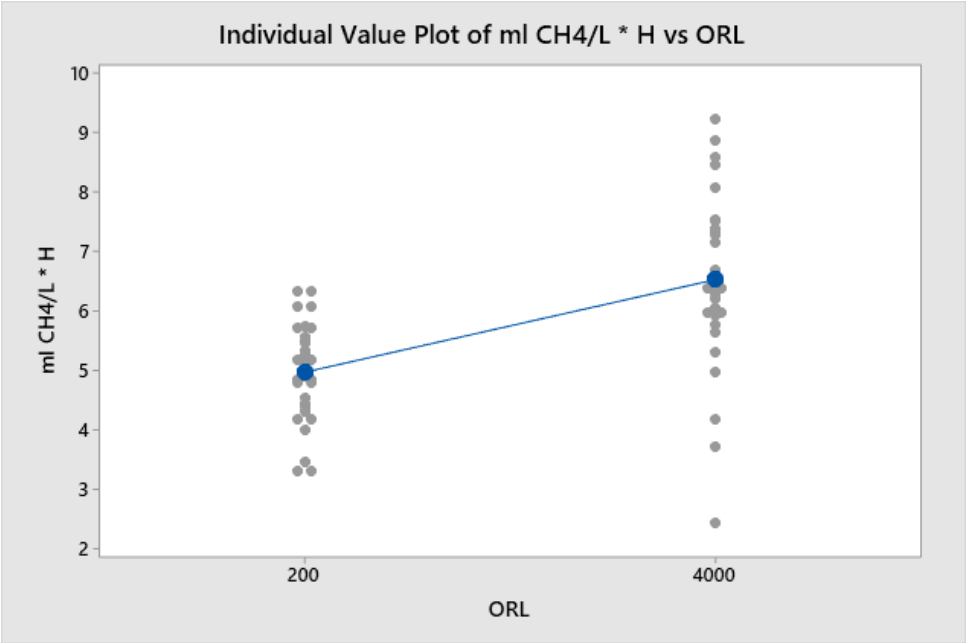
Individual Value Plot of ml CH4/L * H vs ORL
ml CH4/L * H
10
9
8
7
6
5
4
3
2
200
4000
ORL

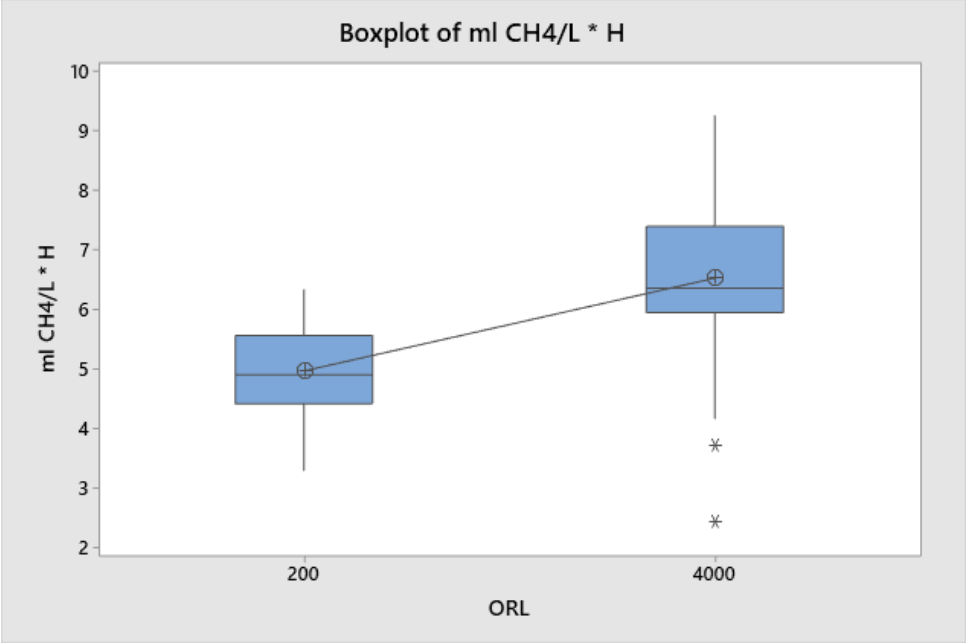
Boxplot of ml CH4/L * H
ml CH4/L * H
10
9
8
7
6
5
4
3
2
200
4000
ORL

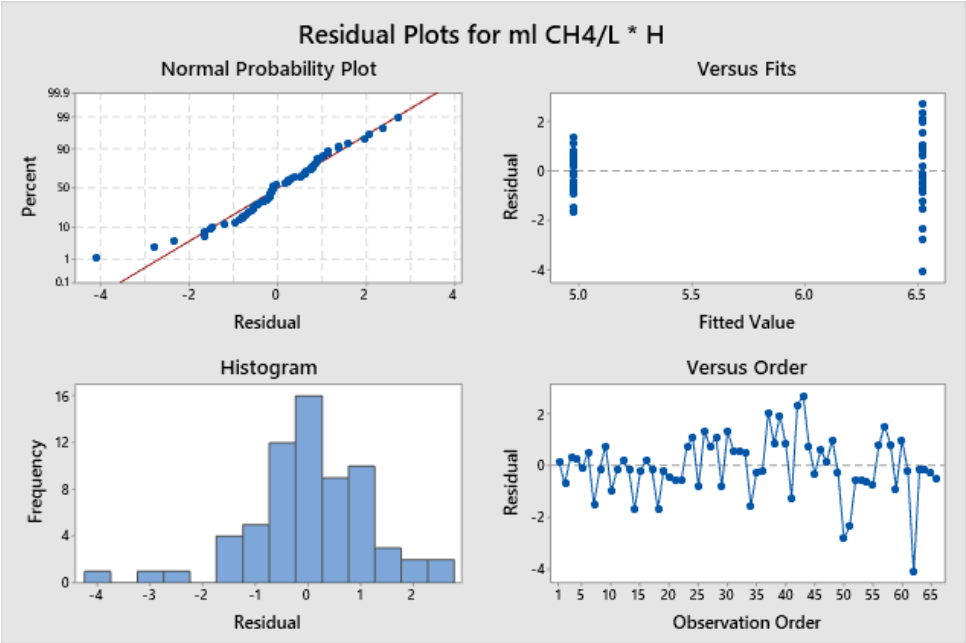
Residual Plots for ml CH4/L * H
Normal Probability Plot
Percent
Residual
Versus Fits
Residual
Fitted Value
Histogram
Frequency
Residual
Versus Order
Residual
Observation Order

ANOVA MPR versus Reactor

Method

Null hypothesis	All means are equal
Alternative hypothesis	Not all means are equal
Significance level	α = 0.05

Equal variances were assumed for the analysis.

Factor Information

Factor	Levels	Values
Reactor	3	AD, MEC A, MEC B

Analysis of Variance

Source	DF	Adj SS	Adj MS	F-Value	P-Value
Reactor	2	9.212	4.606	2.46	0.094
Error	63	118.113	1.875		
Total	65	127.325			

Model Summary

S	R-sq	R-sq(adj)	R-sq(pred)
1.36923	7.24%	4.29%	0.00%

Means

Reactor	N	Mean	StDev	95% CI
AD	22	6.066	1.666	(5.482, 6.649)
MEC A	22	5.223	1.162	(4.640, 5.807)
MEC B	22	5.954	1.224	(5.371, 6.538)

Pooled StDev = 1.36923

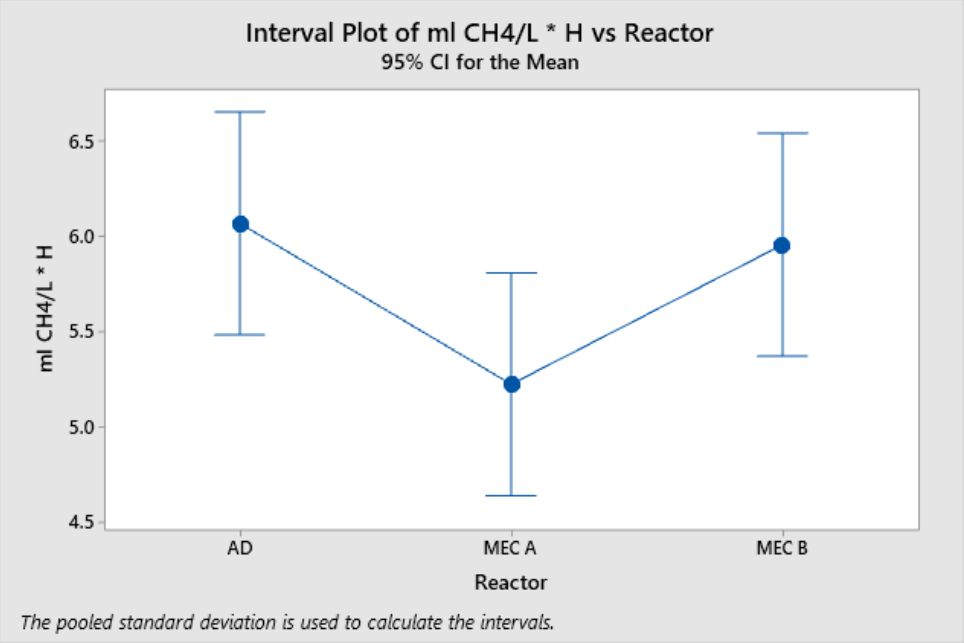

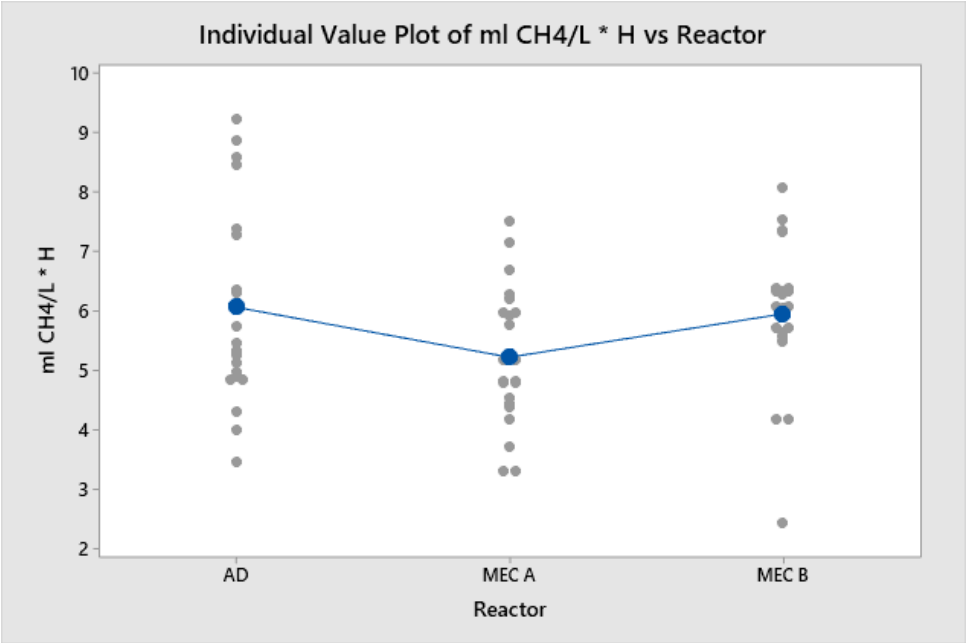
Individual Value Plot of ml CH4/L * H vs Reactor
ml CH4/L * H
10
9
8
7
6
5
4
3
2
AD
MEC A
MEC B
Reactor

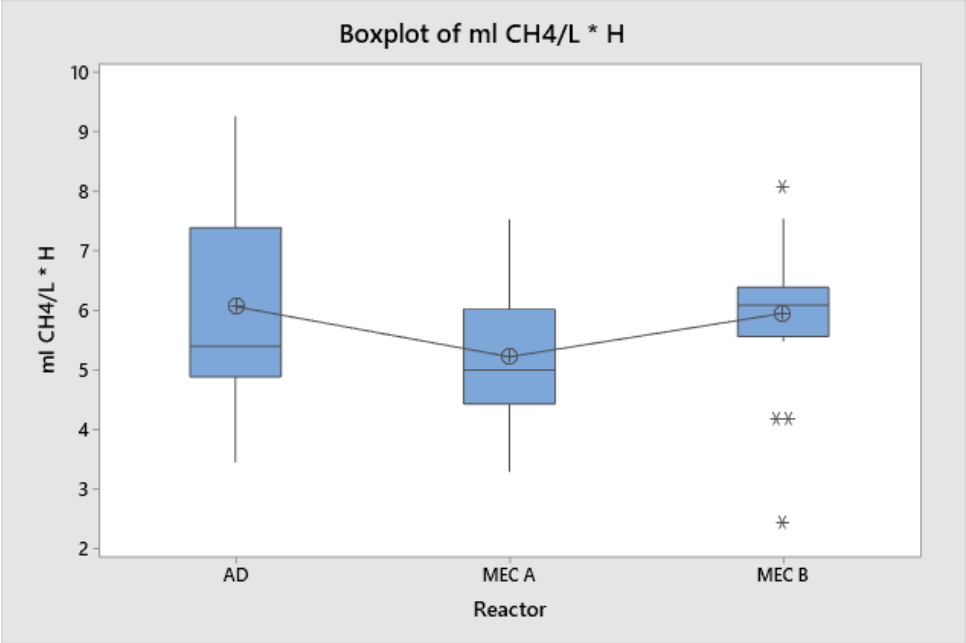
Boxplot of ml CH4/L * H
ml CH4/L * H
10
9
8
7
6
5
4
3
2
AD
MEC A
MEC B
Reactor

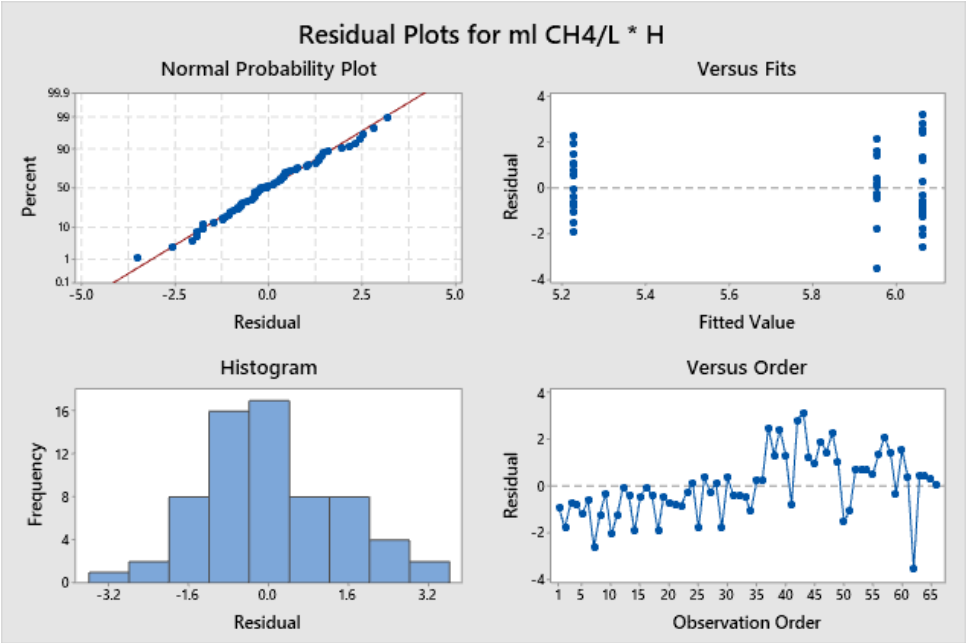
Residual Plots for ml CH4/L * H
Normal Probability Plot
Percent
Residual
Versus Fits
Residual
Fitted Value
Histogram
Frequency
Residual
Versus Order
Residual
Observation Order

Appendix I: Trace Elements Solution

All components of the trace element are given in mg L-1, using 1 mL L-1 of the trace solution for synthetic medium preparation

$MgCl_2 \cdot 6H_2O$	(410)
$MnCl_2 \cdot 4H_2O$	(50)
$FeCl_2 \cdot 4H_2O$	(50)
$NiCl_2 \cdot 4H_2O$	(12)
$ZnSO_4 \cdot 7H_2O$	(10)
$CoCl_2$	(7.7)
$CaCl_2 \cdot 2H_2O$	(30)
$Al(NO_3)_3 \cdot 9H_2O$	(29.4)
Na_2SeO_4	(8.7)
$Na_2MoO_4 \cdot 2H_2O$	(2)
$CuSO_4 \cdot 5H_2O$	(1)
H_3BO_3	(2)
$NaWO_4 \cdot 2H_2O$	(1)